Challenges and perspectives in modelling biosphere-atmosphere exchange of ammonia

Schrader, F.

2019

document version
Publisher's PDF, also known as Version of record

VRIJE UNIVERSITEIT

CHALLENGES AND PERSPECTIVES IN MODELLING BIOSPHERE-ATMOSPHERE EXCHANGE OF AMMONIA

ACADEMISCH PROEFSCHRIFT

ter verkrijging van de graad Doctor aan
de Vrije Universiteit Amsterdam,
op gezag van de rector magnificus
prof.dr. V. Subramaniam,
in het openbaar te verdedigen
ten overstaan van de promotiecommissie
van de Faculteit der Bètawetenschappen
op woensdag 3 juli 2019 om 11.45 uur
in de aula van de universiteit,
De Boelelaan 1105

door

Frederik Schrader

geboren te Peine, Duitsland

promotor: prof.dr.ing. J.W. Erisman
copromotor: dr. C. Brümmer

promotion committee: prof.dr. K. Butterbach-Bahl
prof.dr. A.J. Dolman
prof.dr. D. Fowler
prof.dr.ir. S. Houweling
prof.dr.ir. W. de Vries
prof.dr.ir. G.J.M. Velders

To Freya

In memory of Hans-Herbert Schrader
1957 – 2011

Praise the bridge that carried you over.

— George Colman the Younger

ACKNOWLEDGEMENTS

I have had the privilege of meeting a countless number of fellow researchers, students, technicians, and other great people during this early stage of my academic career, and I have learned a thing or two from each and everyone of them, which I am very thankful for.

Words cannot express the gratitude I feel for the chances and opportunities my supervisors have given me. They have set an example for how to be a great teacher, by patiently letting me explore my own ideas under their guidance, helping me learn from my failures, respecting my opinions, and always treating me like a peer.

Special thanks to: Christian, for being the most patient, understanding, and down-to-earth mentor I could have asked for; Jan Willem, for accepting me as a student, and always leaving me with a feeling of enlightenment and inspiration; Jean-Pierre, Jeremy, Undine, Pascal, and Miriam, for tirelessly collecting the invaluable data without which this thesis would not exist, and for being great colleagues on top of that; Antje and Toby, for sharing my views on scientific integrity, honesty, and rigour; Chris, for spending hours upon hours teaching a complete stranger; Wolfgang and Sascha, for encouraging me to pursue a career in science; Werner, for giving me a chance; my parents, for never doubting my decisions; and Sarah, for her sacrifices.

I greatly acknowledge financial support by the German Federal Ministry of Education and Research (BMBF) within the Junior Research Group NITROSPHERE, as well as the German Environmental Protection Agency (UBA). Many thanks to the Thünen Institute of Climate-Smart Agriculture for providing me with a stimulating work environment, and for its commitment to the promotion of young scientists.

CONTENTS

LIST OF FIGURES

LIST OF TABLES

LISTINGS

1 GENERAL INTRODUCTION

The irony would be that we know what we are doing.

— Kurt Vonnegut

1.1 AMMONIA IN THE ENVIRONMENT

In October 1908, the German chemist Fritz Haber filed a patent (Haber, 1908) for the catalytic formation of ammonia (NH_3) from hydrogen (H_2) and atmospheric nitrogen (N_2) under high pressure and temperature ($N_2 + 3\,H_2 \longleftrightarrow 2\,NH_3$), a process that was later upscaled for commercial use by Carl Bosch and is nowadays known as the *Haber-Bosch process*. Haber was awarded the 1918 Nobel Prize for Chemistry for his discovery, followed by Bosch in 1931 – jointly with Friedrich Bergius – for his contributions to high-pressure chemistry. The importance of this achievement for global food security can hardly be overstated, as up until then the world had been one of *fossil nitrogen* – and without a doubt an unsustainable one (Sutton et al., 2011; Sutton et al., 2008). This milestone for the industrial production of fertilisers solved the *nitrogen problem* of Haber's and Bosch's time, that is, feeding an ever-growing population in light of limited nutrient availability (Erisman et al., 2008; Galloway et al., 2013; von Liebig, 1840). However, it is doubtful that they envisioned laying the foundation for a new *nitrogen problem* at the very same time (Erisman et al., 2013). Today, global emissions of NH_3 range from 46–85 $Tg\,N\,yr^{-1}$, likely more than half of which originate from agricultural production (Sutton et al., 2013), and with additional sources including, but not limited to biomass burning, industrial processes, and vehicular emissions (Erisman et al., 2013; Erisman et al., 2008; Hertel et al., 2012; Sutton et al., 2011).

Emissions of reactive nitrogen (N_r) from these sources can have cascading effects in ecosystems (Figure 1.1), i.e., a single reactive N atom can undergo a multitude of chemical transformations, with each of these compounds affecting sensitive ecosystems in

different ways (Galloway et al., 2003). Adverse environmental impacts of NH_3, such as soil acidification and eutrophication leading to shifts in biodiversity, have only been recognised by the scientific community almost half a century after the invention of the Haber-Bosch process (Heil and Diemont, 1983; Sutton et al., 2008; van Breemen et al., 1982), and the dominant role of reduced nitrogen (NH_x) deposition with regard to negative impacts on sensitive habitats compared to nitrogen oxides (NO_y) even later (Sutton et al., 2008). In addition, atmospheric N_r can have detrimental effects on human health, especially in the form of respiratory disorders (Erisman et al., 2013). Finally, atmospheric deposition of reactive nitrogen has a number of direct and indirect climate change related effects: Directly, through enhanced nitrous oxide (N_2O) emissions at different stages along the nitrogen cascade (e.g., from fertilisation, industrial production, and microbial processes) and the formation of tropospheric ozone (O_3) from NO_x – both greenhouse gases – as well as a net cooling effect from aerosol formation. Indirect effects include the alteration of carbon dioxide (CO_2) and methane (CH_4) fluxes in terrestrial ecosytems, and secondary (e.g., phytotoxic) effects of increased O_3 production. Overall, it is assumed that the net climatic effect of N_r deposition is a slightly negative radiative forcing, albeit with considerable uncertainty (Erisman et al., 2011).

Sinks for NH_3 are a large variety of reactions with other compounds in the ambient air, as well as wet and dry deposition to the surface. Arguably the most important reactions in terms of their environmental impact are the formation of ammonium (NH_4^+) aerosols in the presence of sulphuric acid (H_2SO_4), nitric acid (HNO_3), and hydrogen chloride (HCl). A comprehensive review of the numerous different potential reactions involving atmospheric NH_3 can be found in Behera et al. (2013).

Wet deposition is an effective removal process for atmospheric NH_3 due to its very large solubility in water and strongly contributes to its low atmospheric lifetime (Hertel et al., 2012). It can directly be measured by collecting precipitation, either with bulk, or wet only samplers (Staelens et al., 2005), or estimated from precipitation rates using scavenging coefficients (Behera et al., 2013). Cloud droplet or *occult* deposition is relatively unim-

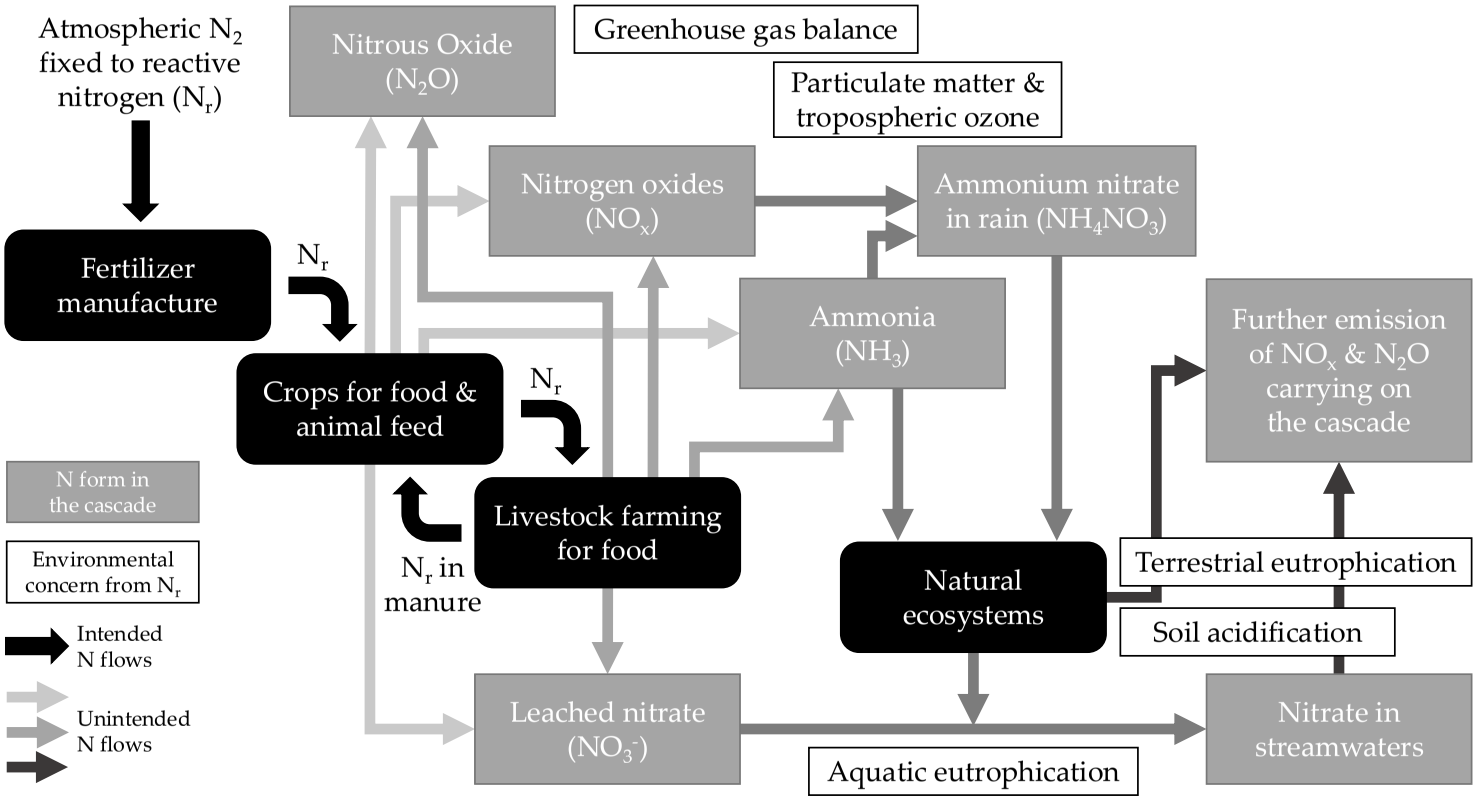

Figure 1.1: Simplified view of the nitrogen cascade, highlighting the synthesis of reactive nitrogen (N_r) from atmospheric dinitrogen (N_2) in the Haber-Bosch process. Grey boxes are the main pollutant forms of N_r; white boxes five primary environmental concerns from N_r. Adapted and redrawn from Sutton et al. (2011).

portant in flat areas, but can be very significant in mountainous regions (Hertel et al., 2011; Lovett et al., 1982).

Dry deposition is the process of removal of atmospheric NH_3 by surface uptake, e.g. through exchange with vegetated surface, the soil, or bodies of water. This is fundamentally a bidirectional pathway, i.e., NH_3 can be re-emitted or dry deposition can be limited due to a non-zero near-surface air concentration of NH_3 that originates from equilibrium reactions with NH_3 stored in the vegetation or the ground (Flechard et al., 2013). This thesis focuses on modelling these processes, and they will therefore be discussed in much greater detail later.

1.2 QUANTIFYING DRY DEPOSITION OF ATMOSPHERIC NH_3 AT THE FIELD SCALE

1.2.1 *Measurement techniques*

A large variety of methods for the measurement of NH_3 biosphere-atmosphere exchange is known, from chamber methods (e.g., Farquhar et al., 1980), over throughfall measurements (e.g., Beudert and Gietl, 2015), to biomonitoring approaches (e.g., Russow and Böhme, 2005). The de-facto standard for micrometeorological measurements of NH_3 biosphere-atmosphere exchange has for a long time been the *aerodynamic gradient method* (AGM), in which the total flux F_t ($\mu g\, m^{-2}\, s^{-1}$) (negative when directed to the surface) is estimated in analogy to Fick's law as the product of a turbulent diffusion coefficient K ($m^2\, s^{-1}$) and the vertical gradient of the air NH_3 concentration χ_a ($\mu g\, m^{-3}$):

$$F_t = -K\frac{\partial \chi_a}{\partial z}. \tag{1.1}$$

$\frac{\partial \chi_a}{\partial z}$ is usually calculated from concentration measurements with wet denuders at two or more heights, and K is derived from accompanying micrometeorological measurements based on flux-gradient theory (Businger et al., 1971; Dyer and Hicks, 1970). This technique has found widespread use in the NH_3 flux measurement community (e.g., Baek et al., 2006; Biswas et al., 2005; Erisman and Wyers, 1993; Flechard and Fowler, 1998b; Hayashi et al., 2012; Horvath et al., 2005; Milford et al., 2001a, 2009, 2001b;

Myles et al., 2011; Neirynck and Ceulemans, 2008; Neirynck et al., 2005, 2007; Nemitz et al., 2004; Phillips et al., 2004; Sutton et al., 2009; Wolff et al., 2010; Wyers and Erisman, 1998; Wyers et al., 1992, and many more), but it is relatively labour-intensive and requires uncertain empirical stability corrections in the estimation of K.

An alternative requiring only one measurement height is the so-called *relaxed eddy accumulation* (REA) technique (Businger and Oncley, 1990). The idea is based on conditional sampling, i.e., up- and downdraft fluxes are sampled into separate reservoirs. In this method, the flux is given as:

$$F_t = \beta \cdot \sigma_w \cdot \left(\chi_{a\uparrow} - \chi_{a\downarrow}\right), \tag{1.2}$$

where $\chi_{a\uparrow}$ ($\mu g\, m^{-3}$) and $\chi_{a\downarrow}$ ($\mu g\, m^{-3}$) are the average up- and downdraft concentrations in the sampling interval, respectively, σ_w ($m\, s^{-1}$) is the standard deviation of fast-response measurements of the the vertical wind velocity w ($m\, s^{-1}$), and β ($-$) is an empirical parameter. The REA technique has the fundamental advantage of requiring measurements at only one height, thus avoiding issues with a variable flux footprint across different levels and potentially allowing for the assessment of vertical flux divergence; only using one empirical parameter that can be estimated from parallel measurements instead of uncertain stability corrections; and at the same time avoiding the need for the high sampling frequency that would be required for the eddy-covariance technique outlined below (Hensen et al., 2009). This method has seen widespread application for NH_3 (e.g., Hansen et al., 2017, 2015, 2013; Hensen et al., 2009; Meyers et al., 2006; Myles et al., 2007), but far less than AGM thus far.

Latest developments in measuring biosphere-atmosphere exchange of NH_3 involve the use of fast-response optical systems, e.g. using line-integrated *differential optical absorption spectroscopy* (DOAS; e.g., Volten et al., 2012) or point-measurements by *quantum cascade laser* spectroscopy (QCL; e.g., Zöll et al., 2016). The former currently requires the use of multiple measurement locations or dispersion modelling (Bell et al., 2017; Häni et al., 2018; Sintermann et al., 2016; Voglmeier et al., 2018). QCL-based instruments, however, in principle allow using the eddy-covariance technique – which is considered the gold-standard

for measuring carbon dioxide (CO_2) fluxes nowadays, and yields direct measurements of turbulent fluxes without the empirical corrections and labour-intensive wet chemistry necessary for AGM or REA. Given all assumptions are justified and the temporal resolution is large enough to cover most of the turbulence spectrum, the flux is directly calculated from the covariance of high-frequency (10–20 Hz) measurements of the vertical wind velocity and the air NH_3 concentration:

$$F_t = \overline{w'\chi'_a}, \tag{1.3}$$

following the Reynolds decomposition of a turbulent variable x into its time average $\bar{x}$ and fluctuating x' parts; $x = \bar{x} + x'$ (Baldocchi, 2003). Using this technique for the measurement of turbulent NH_3 exchange was long limited by the low temporal resolution and / or precision of existing measurement devices, as well as a lack of suitable solutions for the problem of NH_3 adsorption to the inlet of closed- or enclosed-path instruments. However, recent developments have largely overcome these issues, e.g. through the use of specialised inlet designs that minimise surface adsorption and particle contamination of the measurement cell, and by improving the time-response through large effective path lengths and carefully balancing cell pressure (e.g., Ellis et al., 2010). First studies successfully measuring NH_3 fluxes with an eddy-covariance setup have emerged in the literature since then (e.g., Famulari et al., 2004; Sintermann et al., 2011; von Bobrutzki et al., 2010; Whitehead et al., 2008; Zöll et al., 2016). At present, robust long-term monitoring using QCL-based eddy-covariance setups is still somewhat challenging, as these systems require a lot of fine-tuning to operate especially at sites with very low NH_3 concentrations. Nevertheless, with reduced costs and increasing commercial availability, successful demonstrations of long-term monitoring campaigns, future developments in open-path spectroscopy for NH_3, and proven solutions for spectral correction and gap-filling, these pioneering studies may soon be regarded as cornerstones of a new era in NH_3 flux monitoring using optical techniques.

1.2.2 *Modelling techniques*

Early approaches of modelling biosphere-atmosphere exchange of NH_3 involved the use of a so-called *deposition velocity* v_d ($cm\,s^{-1}$). The idea behind it is to infer an NH_3 deposition flux from ambient concentrations by multiplying them with a surface-dependent scaling factor, that can be interpreted in terms of a conductance, i.e.,

$$F_t = v_d \cdot \chi_a. \tag{1.4}$$

This concept is useful for conservative back-of-the-envelope estimates of long-term average fluxes, but fundamentally limited in terms of its temporal resolution (when working with constant values per ecosystem type) and its informative value about site-specific conditions.

In research contexts, surface-atmosphere exchange of NH_3 (and many other trace gases) is usually modelled using an electrical analogy. In its simplest form, the flux is treated unidirectionally and it is only limited by three resistances in series:

$$F_t = -\frac{\chi_a}{R_a + R_b + R_c}, \tag{1.5}$$

where R_a ($s\,m^{-1}$) is the aerodynamic resistance at the reference height, R_b ($s\,m^{-1}$) is the quasi-laminar boundary layer resistance, and R_c ($s\,m^{-1}$) the canopy resistance (Erisman and Wyers, 1993; Wesely, 1989). In terms of the aforementioned electrical analogy, a reference potential of zero is assumed in this simple approach, i.e. the numerator is representative of the potential difference $\chi_a - 0$. Note that $v_d = (R_a + R_b + R_c)^{-1}$. R_a and R_b are dependent on micrometeorological conditions, surface roughness, and chemical properties of NH_3, whereas R_c integrates specific properties of the receptor surface (i.e., usually vegetation and / or the soil).

In order to futher discern between different exchange pathways, R_c can be split into multiple sub-components (Erisman et al., 1994), the most common nowadays being simply a stomatal and a non-stomatal exchange pathway, and, when it can be distinguished from the other components to a reasonable degree of certainty, a ground-layer pathway (Nemitz et al., 2001). The total flux is then given as the sum of all component fluxes:

$$F_t = F_s + F_w + F_g, \tag{1.6}$$

where F_s, F_w, and F_g (all in $\mu g\,m^{-2}\,s^{-1}$) are the fluxes to and from the stomata, external leaf surfaces, and the ground-layer, respectively. Note that F_w is sometimes also called the *cuticular* or *non-stomatal* flux. Modern implementations, in addition, usually employ the concept of a *canopy compensation point* (Farquhar et al., 1980; Sutton et al., 1998) that integrates the effects of exchange with all leaf-layer pathways into an effective air NH_3 concentration in equilibrium with the surface as the central model parameter (Massad et al., 2010a; Nemitz et al., 2001; van Zanten et al., 2010; Wichink Kruit et al., 2010; Zhang et al., 2010). This allows for modelling bidirectional exchange (i.e., both deposition and emission) while at the same time explicitly modelling the exchange with different pathways (e.g. stomata and cuticula) separately (Sutton et al., 1998), yielding important information about the underlying drivers. Specific implementations of models describing the exchange with these pathways are discussed in great detail in Chapters 3 and 4 of this thesis.

A plethora of models with different purposes and varying degrees of complexity has been developed in the past, from multi-layer models (Nemitz et al., 2000), over dynamic leaf-chemistry approaches (Flechard et al., 1999), to those explicitly resolving in-canopy air-column chemistry (Kramm and Dlugi, 1994). I will here focus on model parameterisations that have found wide application both on the field-scale and within large-scale chemistry transport models (CTMs). These are nowadays primarily based on the two-layer (ground- and leaf-layer) canopy compensation point model of Nemitz et al. (2001), which has been noted as perhaps being the optimal compromise between accuracy and simplicity for these applications (Flechard et al., 2013). Variants of it have been used for predicting deposition fluxes (e.g., Flechard et al., 2011), interpreting (e.g., Hansen et al., 2017; Schrader et al., in preparation; Zöll et al., 2016) and gap-filling measurements (Brümmer et al., in press; Lucas-Moffat et al., in preparation), as well as regional modelling (e.g., Wichink Kruit et al., 2012),

1.3 AIMS OF THIS THESIS

The research forming the foundation of this thesis was carried out at the Thünen Institute, a German Federal Research Institute

under the auspices of the German Ministry of Food and Agriculture. Part of its mission statement is to supply policy with scientifically-based decision making tools, and to carry out own independent research for this purpose. I have always held these goals to a high standard, and made a point of working towards solutions that can readily be implemented in existing workflows, as well as towards improving the tools that are being used to support political action right now.

In the context of modelling biosphere-atmosphere exchange of NH_3, these tools are the simple, yet effective parameterisations of one- and two-layer canopy compensation point models outlined in the preceeding section. The overarching aim of this thesis was to analyse the challenges associated with parameterising and using these models, to find suitable modifications to these schemes with respect to recent developments in our knowledge about ammonia exchange processes, to identify the key issues and uncertainties that need to be addressed by the scientific community, and to give recommendations on how to do so. In doing so, I have adhered to a philosophy of *practical model development*, i.e., working at the interface between fundamental research on NH_3 biosphere-atmosphere exchange processes on the one hand, and users of these models and their results on the other hand. My fundamental goal is to make a contribution towards strengthening confidence in these tools that we need to identify key areas that need to be in the focus of environmental protection efforts, and to find sustainable solutions for one of the greatest challenges of the 21st century: Mitigating the impact of excessive reactive nitrogen emissions.

This PhD thesis consists of a collection of four separate academic articles, three of which have been published in peer-reviewed international journals, and one of which is to be submitted shortly. In particular, these articles are:

- Schrader, F. & Brümmer, C. (2014). Land use specific ammonia deposition velocities: A review of recent studies (2004–2013). *Water, Air, and Soil Pollution*, *225*(10), 2114
  - in which I present results from a literature review on recent measurements and modelled estimates of the NH_3 deposition velocity.

- Schrader, F., Brümmer, C., Flechard, C. R., Wichink Kruit, R. J., van Zanten, M. C., Zöll, U., Hensen, A. & Erisman, J. W. (2016). Non-stomatal exchange in ammonia dry deposition models: Comparison of two state-of-the-art approaches. *Atmospheric Chemistry and Physics*, *16*(21), 13417–13430
  - in which I analyse problems in the parameterisations of two state-of-the-art approaches to modelling non-stomatal NH_3 exchange, by comparison with measurements and theoretical considerations.
- Schrader, F., Erisman, J. W. & Brümmer, C. (in preparation). Towards a coupled paradigm of NH_3-CO_2 biosphere-atmosphere exchange modelling
  - in which I make an argument for estimating the stomatal conductance for the use in NH_3 biosphere-atmosphere exchange models from measured or modelled fluxes of CO_2, and highlight issues with the widespread use of empirical approaches.
- Schrader, F., Schaap, M., Zöll, U., Kranenburg, R. & Brümmer, C. (2018). The hidden cost of using low-resolution concentration data in the estimation of NH_3 dry deposition fluxes. *Scientific Reports*, *8*(1), 969
  - in which I formally derive and quantify the error associated with applying models with concentrations sampled at low temporal resolution, and propose a solution to correct for these errors in the future.

These articles are reproduced in Chapters 2–5, respectively. No modifications have been made to the text or the contents of the articles, i.e. they appear in the same way they were originally published, apart from minor language editing, typesetting, and redrawing the figures to a common format. In Chapter 6, the key findings are summarised, and discussed in terms of their implications for users of these models and the associated uncertainties. Finally, I propose some recommendations for future research in the context of further model development.

Further contributions to the field of NH_3 biosphere-atmosphere exchange research that are not part of this thesis are co-authorships on the works of Zöll et al. (2016), in which we present

eddy-covariance measurements and modelled estimates of NH_3 fluxes over an ombrotrophic bog; Zöll et al. (under review), in which we analyse common micrometeorological drivers of CO_2 and NH_3 exchange using artificial neural networks; and Lucas-Moffat et al. (in preparation), in which we will present practical solutions for gap-filling eddy-covariance flux measurements of arbitrary trace gases, with NH_3 as a prominent example without an established gap-filling solution thus far.

2

DEPOSITION VELOCITIES

All models are wrong,
but some are useful.

— George E. P. Box

This chapter is published as: *Schrader, F. & Brümmer, C. (2014). Land use specific ammonia deposition velocities: A review of recent studies (2004–2013). Water, Air, and Soil Pollution, 225(10), 2114.*

ABSTRACT

Land-use specific deposition velocities of atmospheric trace gases and aerosols – particularly of reactive nitrogen compounds – are a fundamental input variable for a variety of deposition models. Although the concept is known to have shortcomings – especially with regard to bidirectional exchange – the often limited availability of concentration data and meteorological input variables make it a valuable simplification for regional modelling of deposition fluxes. In order to meet the demand for an up-to-date overview of recent publications on measurements and modelling studies, we compiled a database of ammonia (NH_3) deposition velocities published from 2004 to 2013. Observations from a total of 42 individual studies were averaged using an objective weighting scheme and classified into seven land-use categories. Weighted average and median deposition velocities are 2.2 and 2.1 $cm\,s^{-1}$ for coniferous forests, 1.5 and 1.2 $cm\,s^{-1}$ for mixed forests, 1.1 and 0.9 $cm\,s^{-1}$ for deciduous forests, 0.9 and 0.7 $cm\,s^{-1}$ for semi-natural sites, 0.7 and 0.8 $cm\,s^{-1}$ for urban sites, 0.7 and 0.6 $cm\,s^{-1}$ for water surfaces, and 1.0 and 0.4 $cm\,s^{-1}$ for agricultural sites, respectively. Thus, values presented in this compilation were considerably lower than those found in former studies (e.g., VDI, 2006). Reasons for the mismatch were likely due to different land-use classification, different averaging methods, choices of measurement locations, and improvements in measurement and in modelling techniques. Both data and code used for processing are made available as supplementary material to this article.

2.1 INTRODUCTION

Atmospheric ammonia (NH_3) has long been recognised as a major airborne pollutant. It can act as a precursor for aerosols and its deposition has a significant impact on soil acidification, ecosystem eutrophication and, consequently, changes in species composition and biodiversity (Sutton et al., 2011). In order to assess the impact of ammonia emissions and transport, mainly caused by livestock and fertilisation (Bouwman et al., 1997) some air quality models (e.g., the AUSTAL2000 model of Janicke, 2002) use a so called inferential method; that is, the deposition flux F ($\mu g\,m^{-2}\,s^{-1}$) is calculated as the product of the concentration of a compound at a certain reference height, χ_a ($\mu g\,m^{-3}$), and a proportionality constant, the deposition velocity v_d ($cm\,s^{-1}$) (Wesely and Hicks, 2000). In addition, land-use specific average deposition velocities may be used for quick estimates of N deposition to an ecosystem, or to verify plausibility of flux measurements and model results.

Conceptually, using tabulated deposition velocities for a certain land-use category is based on strongly simplified assumptions about the relationship between near-ground NH_3 concentrations and the respective deposition flux; however, for now, this simplification is still often necessary once we leave the single plot scale. The deposition of NH_3 involves a large number of complex processes, especially due to the high reactivity of the compound, strong water solubility, formation of particulate matter in the form of ammonium nitrate (NH_4NO_3) in the presence of nitric acid (HNO_3), bidirectional transport paths and canopy-dependent compensation points, non-stomatal uptake, co-deposition of NH_3 and SO_2, and other factors (Flechard et al., 2013; Sutton et al., 2011, 2007). In practice, it is not always possible to resolve these processes in regional models, primarily due to limited availability of spatial input data. In the recent past, many formulations for bidirectional, compensation point based dry deposition models have arisen in the literature (Bajwa et al., 2008; Massad et al., 2010a; Neirynck and Ceulemans, 2008; Personne et al., 2009; Zhang et al., 2010).

However, necessary input parameters for these models may not always be available for larger areas. Therefore, many of

these processes and characteristics are sometimes aggregated in a single reference value of the deposition velocity per land-use type. For example, in Germany, a set of three reference values compiled by the Association of German Engineers (Verein Deutscher Ingenieure, VDI) based on data from 10 years ago and earlier (VDI, 2006) is commonly used in regional model applications.

The ongoing intensification of agricultural practices, as well as increasing traffic volume and industrial processes, calls for a periodic update of these land-use specific values. Furthermore, flux measurement and modelling techniques have greatly improved, and a number of large monitoring studies were carried out in the last few years. Measurements covered by this literature study were carried out using a number of different methods, including the aerodynamic gradient technique (Phillips et al., 2004), relaxed eddy accumulation (Meyers et al., 2006), chamber methods (Jones et al., 2007a) and N deposition estimation using biomonitoring (Russow and Böhme, 2005; Russow and Weigel, 2000; Sommer et al., 2009; Tauchnitz et al., 2010; Weigel et al., 2000) or synthetic surrogate surfaces (Anatolaki and Tsitouridou, 2007). Additionally, inferential (Hicks et al., 1987; Wesely and Hicks, 2000) and chemical transport models (Builtjes et al., 2011) were used to simulate deposition fluxes. The aim of this study is to incorporate these new measurement and model approaches into an up-to-date database of ammonia deposition velocities published in the preceding decade. These are presented in a generalised form as weighted annual averages and median values for different land-use types. Both the data and IPython code that was used for the calculation of these new reference numbers are published as supplementary material of this article for re-use and modification by other researchers.

2.2 MATERIALS AND METHODS

2.2.1 *Literature survey*

We performed an iterative, snowball-type literature research: In a first step, the citation indexing service *Thomson Reuters Web of Science* (formerly *ISI Web of Knowledge*), was queried using

they keywords *ammonia + deposition + veloc**. Search results were limited to the period from 2004 to 2013. The query yielded a total of 90 international publications, which were then screened for obviously unrelated articles, e.g. such articles that only deal with the deposition velocity of other trace gases in detail. We only used sources in our further analysis that either directly report measured, modelled or otherwise researched deposition velocities, or that include measurements of deposition fluxes and corresponding NH_3 concentrations that could be used to calculate deposition velocities. Consequently, studies that only discuss the concept of deposition velocities in general were disregarded. All sources were reviewed for (i) measurement method, (ii) NH_3 deposition velocities (directly reported, or calculated by the authors of this article), (iii) reference height, (iv) NH_3 concentrations at the reference height, (v) descriptions of the measurement site and land-use and (vi) temporal coverage (how many seasons do the measurements cover and how long did the authors measure during these respective seasons). In a second step, the references cited in the results from the initial database query were screened for further potentially useful articles published in the time frame of interest. These were then again treated as described above and likewise screened for further relevant studies. This process was repeated until no additional literature could be obtained. In the end, this approach led to a collection of 42 suitable sources that were used for statistical analysis and classification into different land-use types.

2.2.2 *Data processing*

Most of the studies cited here report their findings on NH_3 deposition velocities either directly in the text or as tabulated values. If in the studies cited NH_3 deposition velocity values were not directly reported in the text or in tables, we determined v_d from deposition fluxes and concentrations at the reference height. In a few studies, v_d could only be visually estimated from figures. In those cases when only a range of measured deposition velocities was reported, the center of this range was taken as an estimate for the average deposition velocity for the respective site. When multiple values of v_d were reported, e.g. as a result of data

syntheses, modelling studies or literature surveys, these were grouped by land-use class, arithmetically averaged and used as a single study in the further analysis.

The results were categorised into seven land-use classes: deciduous-, coniferous- and mixed forests, semi-natural sites (e.g., grasslands or peatlands), urban sites, agricultural sites and water surfaces. Studies were classified as unspecified when the site description was unclear (e.g., *remote site*) or when deposition velocities were reported as one for multiple land-use categories. Two statistics were calculated as a means of aggregation: The median, as a robust estimator for the central tendency, and a weighted average of the respective groups.

The former was calculated as

$$\widetilde{v_{\mathrm{d}}} = \begin{cases} v_{\mathrm{d},\frac{n+1}{2}}, & \text{if } n \text{ is odd,} \\ \frac{1}{2}\left(v_{\mathrm{d},\frac{n}{2}} + v_{\mathrm{d},\frac{n}{2}+1}\right), & \text{if } n \text{ is even,} \end{cases} \tag{2.1}$$

where $\widetilde{v_{\mathrm{d}}}$ ($\mathrm{cm\,s^{-1}}$) is the median deposition velocity of one land-use class and $v_{\mathrm{d},i}$ ($\mathrm{cm\,s^{-1}}$) is the deposition velocity at the i^{th} position of a sorted array of v_{d} for the respective category.

Weights for the latter were derived from the temporal coverage of the corresponding studies: For each season (i.e., spring, summer, fall, and winter) of the year where the measurements were conducted (regardless of the number of years) a study was assigned 1 *point*, as well as additional points for the measurement duration during these seasons (i.e. zero to three weeks of a season: 1 point; three to six weeks: 2 points, six to nine weeks: 3 points, nine weeks and more: 4 points). Consequently, each study would be weighted with a minimum of 2 points (one day to three weeks of measurement during one season) and a maximum of 8 points (average of nine weeks of measurements or more for each of four seasons). The weighted average deposition velocity for one land-use class $\overline{v_{\mathrm{d}}}$ ($\mathrm{cm\,s^{-1}}$) was then calculated by multiplication of the individual studies' $v_{\mathrm{d},i}$ with the weights for the number of seasons $w_{\mathrm{s},i}$ $(-)$ and the coverage of these seasons $w_{\mathrm{c},i}$ $(-)$, and division by the total sum of weights assigned for all $v_{\mathrm{d},i}$ of one land-use class:

$$\overline{v_{\mathrm{d}}} = \frac{\sum_{i=1}^{n}\left(v_{\mathrm{d},i}\cdot w_{\mathrm{c},i} + v_{\mathrm{d},i}\cdot w_{\mathrm{s},i}\right)}{\sum_{i=1}^{n}\left(w_{\mathrm{c},i} + w_{\mathrm{s},i}\right)}. \tag{2.2}$$

2.3 RESULTS

A total of 42 studies were deemed relevant and reliable and were, except for two duplicate values (Neirynck and Ceulemans, 2008; Neirynck et al., 2005, 2007), consequently used in the calculation of average and median v_d for the seven land-use classes. Since a subset of these studies were compilations of results from large measurement campaigns, or literature studies themselves, a higher number (61) of individual values for the ammonia deposition velocity could be extracted. Only one value per land-use class (if based on the same measurement technique) of an individual study was used in the averaging process; some studies, such as Flechard et al. (2011), are actually based on data syntheses from more than 50 sites. Broken down into land-use classes, we were able to use 6, 4, 4, 19, 5, 3, 18 and 2 individual values for coniferous forests, mixed forests, deciduous forests, semi-natural sites, urban sites, water surfaces, agricultural sites and unspecified sites, respectively (Table 2.1). Studies conducted at semi-natural and agricultural sites were clearly found to be dominant.

Median deposition velocities were highest for coniferous forests and lowest for agricultural sites. Weighted averages show a slightly different order, with the highest values again from coniferous forest sites, but the lowest for urban sites and water surfaces (Figure 2.1).

While many studies (75 %) covered all four seasons, 18 % of all studies only measured during one season. Two thirds of v_d values are based on continuous measurements; however, 21 % and 11 % of all studies only covered up to three or up to six weeks per season, respectively.

2.4 DISCUSSION AND CONCLUDING REMARKS

We presented a compilation of ammonia deposition velocities (Table A.1 in the Appendix) as a function of land-use based on measurements, modelling studies and literature survey results from the period 2004–2013. In total, 61 individual v_d values (not including duplicates) were extracted from 42 studies. Two studies were omitted because they appeared to be reanalysis studies of

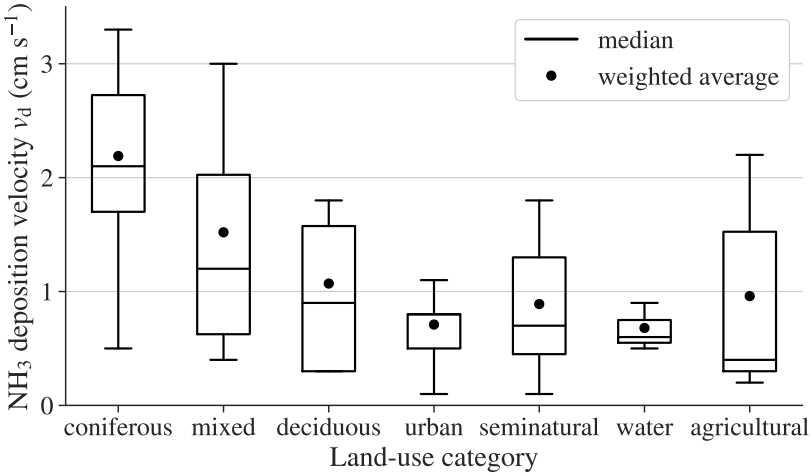

Figure 2.1: Distribution of ammonia deposition velocities grouped into different land-use categories. The boxes extend from the lower to upper 75 % quartiles of the data; the whiskers extend to the full range. The median and weighted average of each group is denoted by the horizontal bar and the dot, respectively. Note that the median and 75 % quartile of the urban sites are equal and thus not visually distinguishable in the figure.

Table 2.1: Medians, weighted averages and ranges of ammonia deposition velocities categorised by land-use. n is the number of individual data for each category.

		NH_3 DEPOSITION VELOCITY v_d ($cm\,s^{-1}$)			
LAND-USE	n (−)	MIN	MAX	MEDIAN	WEIGHTED AVG.
Coniferous forest	6	0.5	3.3	2.1	2.2
Mixed forest	4	0.4	3.0	1.2	1.5
Deciduous forest	4	0.3	1.8	0.9	1.1
Semi-natural	19	0.1	1.8	0.7	0.9
Urban	5	0.1	1.1	0.8	0.7
Water	3	0.5	0.9	0.6	0.7
Agricultural	18	0.2	7.1	0.4	1.0
Unspecified	2				

the same data set and two values could not unambiguously be attributed to a specific land-use class.

Staelens et al. (2012) compiled a literature review of deposition velocities for NH_3, NO_2 and SO_2 from the period 1972—2006. They report v_d of 1.14 cm s^{-1} (min. 0.65, max. 1.71, $n = 7$) for grassland and 1.56 cm s^{-1} (min. 0.80, max. 2.20, $n = 6$) for heathland, both thereby slightly higher but in the same range as our figure for semi-natural ecosystems of 0.9 cm s^{-1} (median 0.7; min 0.1, max. 1.8, $n = 19$). Their average numbers for deciduous forests, 1.54 cm s^{-1} (min. 0.81, max. 2.20, $n = 4$), and coniferous forests, 2.91 cm s^{-1} (min. 2.00, max. 3.80, $n = 12$), are likewise higher than ours of 1.1 cm s^{-1} (median 0.9, min. 0.3, max. 1.8, $n = 4$) and 2.2 cm s^{-1} (median 2.1, min. 0.5, max. 3.3, $n = 6$) for deciduous and coniferous forests, respectively. The Association of German Engineers (VDI, 2006) reports a deposition velocity of 1.5 cm s^{-1} for grass and 2.0 cm s^{-1} for forests, which is, again, slightly higher, but not inconsistent with our findings. Reasons for the mismatch might be the specific choices of categories for aggregation and the averaging procedure. In addition, one may want to calculate individual metrics for central tendency, e.g. a truncated mean, a weighted median, or include outlier corrections e.g. for the agricultural data set. Therefore, all data used in this study are made available as supplementary material, supported by a thoroughly commented IPython notebook that shows all analysis steps and may be modified by all users.

Further reasons for the significantly lower values found in more recent studies remain a matter of speculation. On the one hand, the choice of tower position, e.g., central vs. edge spot within a homogeneous fetch, might have had a considerable effect on NH_3 concentration measurements. Studies like Flechard et al. (2011) report data from sites where the positions of determination were almost exclusively located in central position in order to represent the chosen land-use as good as possible. In a number of former studies, however, research aims were more focused on local transport and dispersion away from point sources such as cattle urine patches, cattle sheds, and slurry tanks. Thus, higher values of NH_3 concentration formed the base for the derivation of deposition velocities. On the other hand, improvements in both measurement and modelling techniques could have also

led to a lowered deposition regime. Optical devices such as absorption spectrometers (von Bobrutzki et al., 2010) use short and heated inlet tubes, thereby avoiding more efficiently wall surface reactions and memory effects. Consequently, more accurate input data generates better parameterisations for canopy resistances in surface-atmosphere exchange schemes.

Due to missing information in many studies, it was not possible to derive a robust dependency of deposition velocity on reference height. It is well known that concentration profiles are usually not strictly linear and therefore a constant concentration gradient governing the deposition process is not always a valid assumption. However, a large number of authors did not report the respective reference height. If it was provided, in many cases no details e.g. on the consideration of zero plane displacement height were reported. The same holds true for reporting uncertainty estimates. Due to inconsistent use of terminology, omission of details on the uncertainty estimation techniques and on the nature of reported uncertainties (standard deviations, standard errors, confidence intervals, ranges), or simply no mention of uncertainty at all, it was not possible for us to do an error propagation and report more than ranges for the aggregated values of v_d.

Note that we did not distinguish agricultural sites by different management practices. Some authors, e.g. Cui et al. (2011), explicitly report v_d during different phases of management and include fertilisation periods in the annual average. In other cases, such as the data synthesis of Flechard et al. (2011), fertilisation periods were excluded from dry deposition velocity estimates. Furthermore, many authors did not report whether average v_d values were obtained from long-term average concentrations and fluxes, or as an average of multiple individual (e.g. daily or hourly) v_d estimates, which may lead to differences in the significance of singular events, like emission periods shortly after fertilisation, with regard to the average deposition velocity.

It is worth noting that more than half of the values for the ammonia deposition velocity are the results of inferential modelling or the use of chemical transport models and not of direct flux measurements, like those using aerodynamic gradient techniques, which may play a role regarding the fact that our v_d

values are lower than those of comparable studies. However, recent technical improvements, both in the area of modelling (Flechard et al., 2013) and in measurement (von Bobrutzki et al., 2010), especially in the field of optical techniques such as open path DOAS (e.g., Volten et al., 2012) or QCL spectroscopy (e.g. Ferrara et al., 2012, based on the concept of Nelson et al., 2004), may lead to an increase of, or at least to more reliable ammonia exchange studies in the near future.

ACKNOWLEDGEMENTS

Funding for this study was provided by the Federal Environmental Agency of Germany (Umweltbundesamt, UBA) under project number 29965 and by the Federal Ministry of Education and Research (BMBF) within the framework of the junior research group NITROSPHERE under support code FKZ 01LN1308A. We greatly acknowledge advice and valuable comments from Jakob Frommer and Markus Geupel.

3

NON-STOMATAL EXCHANGE

The great tragedy of science –
the slaying of a beautiful hypothesis by an ugly fact.

— Thomas Henry Huxley

This chapter is published as: *Schrader, F., et al. (2016). Non-stomatal exchange in ammonia dry deposition models: Comparison of two state-of-the-art approaches. Atmospheric Chemistry and Physics, 16(21), 13417–13430.*

ABSTRACT

The accurate representation of bidirectional ammonia (NH_3) biosphere-atmosphere exchange is an important part of modern air quality models. However, the cuticular (or external leaf surface) pathway, as well as other non-stomatal ecosystem surfaces, still pose a major challenge of translating our knowledge into models. Dynamic mechanistic models including complex leaf surface chemistry have been able to accurately reproduce measured bidirectional fluxes in the past, but their computational expense and challenging implementation into existing air quality models call for steady-state simplifications. We here qualitatively compare two semi-empirical state-of-the-art parameterisations of a unidirectional non-stomatal resistance (R_w) model after Massad et al. (2010a), and a quasi-bidirectional non-stomatal compensation point (χ_w) model after Wichink Kruit et al. (2010), with NH_3 flux measurements from five European sites. In addition, we tested the feasibility of using backward-looking moving averages of air NH_3 concentrations as a proxy for prior NH_3 uptake and driver of an alternative parameterisation of non-stomatal emission potentials (Γ_w) for bidirectional non-stomatal exchange models. Results indicate that the R_w-only model has a tendency to underestimate fluxes, while the χ_w model mainly overestimates fluxes, although systematic underestimations can occur under certain conditions, depending on temperature and ambient NH_3 concentrations at the site. The proposed Γ_w parameterisation revealed a clear functional relationship between backward-looking moving averages of air NH_3 concentrations and non-stomatal emission potentials, but further reduction of

uncertainty is needed for it to be useful across different sites. As an interim solution for improving flux predictions, we recommend to reduce the minimum allowed R_w and the temperature response parameter in the unidirectional model and to revisit the temperature dependent Γ_w parameterisation of the bidirectional model.

3.1 INTRODUCTION

Reactive nitrogen (N_r) deposition can contribute to a number of adverse environmental impacts, including ecosystem acidification, shifts in biodiversity, or climate change (Erisman et al., 2013). Breakthroughs in the measurement of biosphere-atmosphere exchange of ammonia (NH_3), the major constituent of N_r (Sutton et al., 2013), have been made in the recent past with the rising availability of high-frequency measurement devices that can be used within the eddy-covariance method (e.g. Famulari et al., 2004; Ferrara et al., 2012; Zöll et al., 2016), and a large body of flux measurements using other measurement techniques, e.g. the aerodynamic gradient method, has emerged from large-scale projects such as NitroEurope (Sutton et al., 2011). These measurements, however, are usually only representative for a specific location and difficult to interpolate in space. Surface-atmosphere exchange schemes that predict ammonia exchange fluxes from measured or modelled concentrations and micrometeorological conditions are used on both the local scale and within large-scale chemical transport models (CTMs). Following the discovery of the ammonia compensation point (Farquhar et al., 1980), these models are nowadays able to reproduce bidirectional exchange fluxes, i.e. both emission and deposition of ammonia, and typically feature at least a stomatal and a non-stomatal leaf surface pathway. The addition of a soil- or leaf litter pathway by Nemitz et al. (2001) has been recognised as an optimal compromise between model complexity and accuracy of the flux estimates (Flechard et al., 2013), although some uncertainties in the treatment of the ground layer still prevail.

While the representation of the stomatal pathway has received much attention in the literature due to its importance not only for ammonia, but also for a large number of other atmospheric

constituents, especially carbon dioxide (CO_2) and water vapour (H_2O) (e.g. Ball et al., 1987; Farquhar and Sharkey, 1982; Jarvis, 1976), modelling non-stomatal exchange is still subject to considerable uncertainty (Burkhardt et al., 2009). Ammonia is highly soluble in water and thus readily deposits to water layers on the leaf cuticle, and on any other environmental surface, following precipitation events, condensation of water vapour, or due to the presence of hygroscopic particles on the surface. This characteristic behavior is typically modelled with an exponential relative humidity response function as a proxy for canopy wetness, where a high relative humidity results in low non-stomatal resistances, and vice-versa (e.g. Erisman et al., 1994; Sutton and Fowler, 1993). A self-limiting effect of ambient ammonia concentrations on the deposition process, due to saturation effects and an increase in surface pH, has been observed in experiments (Cape et al., 2008; Jones et al., 2007a,b) and implemented in some non-stomatal exchange models (e.g. Wichink Kruit et al., 2010). Additionally, re-emission events during evaporation of leaf surface water layers have been measured in the field, which hints at the limits of these classical static and unidirectional approaches (Wyers and Erisman, 1998). Sutton et al. (1998) and Flechard et al. (1999) have successfully reproduced measurements of these events on the field scale by modelling the water films as charged capacitors for ammonia emissions; however, these models need complex dynamic leaf chemistry modules which drastically increase computational expense and necessary input variables and consequently limit their applicability in large scale simulations. Wichink Kruit et al. (2010) developed a static hybrid-model featuring a non-stomatal compensation point approach in order to simplify the model calculations and as an important step towards the use of a bidirectional non-stomatal exchange paradigm within large scale CTMs. In this paper, we compare the performance of two state-of-the-art parameterisations of non-stomatal exchange: The unidirectional approach of Massad et al. (2010a) and the quasi-bidirectional approach of Wichink Kruit et al. (2010).

The Massad et al. (2010a) parameterisation has received widespread acceptance in the community, with 53 citations according to the literature database *Thomson Reuters Web of Science* at the time of writing this article, and variants of it have been applied

in numerous studies, e.g. recently in Shen et al. (2016), Moring et al. (2016), Zöll et al. (2016), and others. Wichink Kruit et al. (2010) followed a unique approach by simplifying complex dynamic approaches towards an empirical steady-state formulation of a non-stomatal compensation point model, which is nowadays used within the DEPAC3.11 deposition module (van Zanten et al., 2010) and the chemistry transport model LOTOS-EUROS (Wichink Kruit et al., 2012), and it is structurally compatible with the Massad et al. (2010a) model. We highlight strengths and weaknesses of both approaches and apply them to five measurement sites in Germany, the UK, the Netherlands and Switzerland. Predicted (effective) non-stomatal resistances are compared to those inferred from nighttime flux measurements, when stomata are mostly closed and the contribution of the non-stomatal pathway to the total observed flux is dominant. In addition, we investigate the potential of parameterising a bidirectional non-stomatal exchange model by testing backwards-looking moving averages of air ammonia concentrations as a proxy for prior ammonia inputs into the ecosystem, eliminating the need for dynamic or iterative flux-based approaches with the use of a readily available, easy-to-calculate and easy-to-implement metric.

3.2 METHODS

3.2.1 *Bidirectional ammonia exchange models*

Ammonia dry deposition is typically modelled using an electrical analogy based on a network of serial and parallel resistances. The two-layer model structure introduced by Nemitz et al. (2001) has been recognised as a good compromise between model complexity, ease of use and accuracy of the resulting exchange fluxes (Flechard et al., 2013), and it is the foundation for the parameterisation of Massad et al. (2010a) that is used throughout this study. However, in the Massad et al. (2010a) formulation, the second (soil / leaf-litter) layer is essentially switched off for semi-natural ecosystems and managed ecosystems outside of management events, because soil emissions are expected to be negligible in these cases. We therefore focus on the one-layer big-leaf model (Figure 3.1) in this paper. For a list of variables

used throughout this article, the reader is referred to Table B.1 in the Supplement.

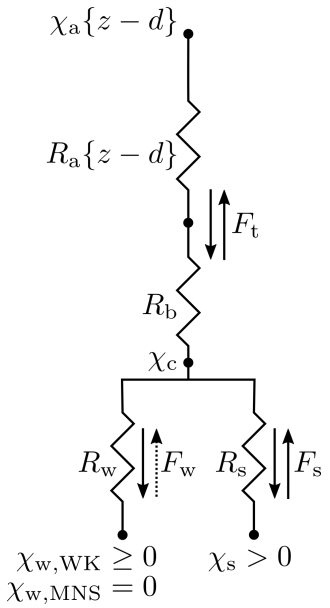

Figure 3.1: Structure of the single-layer model of NH_3 surface-atmosphere exchange used in this study. The non-stomatal pathway can be treated either uni- or bidirectionally, depending on the specific parameterisation. MNS = Massad et al. (2010a); WK = Wichink Kruit et al. (2010).

In the simplest form, the canopy resistance model (e.g. Erisman and Wyers, 1993; Wesely, 1989), surface-atmosphere-fluxes are limited by three resistances in series: The aerodynamic resistance $R_a\{z-d\}$ ($s\,m^{-1}$) at the reference height $z-d$ (m) (where z (m) is the measurement height above ground and d (m) is the zero-plane displacement height), the quasi-laminar boundary layer resistance R_b ($s\,m^{-1}$), and the canopy resistance R_c ($s\,m^{-1}$). While $R_a\{z-d\}$ and R_b are mainly dependent on micrometeorological conditions, surface roughness and chemical properties of the compound of interest, R_c is directly dependent on the characteristics of the vegetated surface. The inverse of the sum of these three resistances is called the deposition velocity, $v_d\{z-d\}$ ($m\,s^{-1}$).

R_c is further split into a stomatal pathway with the stomatal resistance R_s ($s\,m^{-1}$), and a non-stomatal (or cuticular) pathway

with the non-stomatal resistance R_w ($s\,m^{-1}$) (e.g. Erisman et al., 1994; Sutton et al., 1998). Stomatal exchange is usually modelled bidirectionally for ammonia in field scale studies and some CTMs, i.e. it is assumed that there is a non-zero gaseous ammonia concentration χ_s ($\mu g\,m^{-3}$) in equilibrium with dissolved ammonia in the apoplastic fluid. This concentration is often called the stomatal compensation point, although strictly speaking the compensation point is only met when χ_s is approximately equal to the air ammonia concentration at the reference height $\chi_a\{z-d\}$ ($\mu g\,m^{-3}$) and consequently the net flux F_t ($\mu g\,m^{-2}\,s^{-1}$) is zero (Farquhar et al., 1980). The non-stomatal pathway is modelled unidirectionally in many parameterisations, i.e. the gaseous ammonia concentration in equilibrium with the solution on the external leaf surfaces χ_w ($\mu g\,m^{-3}$) is assumed to be zero, although observational evidence indicates that this pathway is in fact bidirectional as well (e.g. Neirynck and Ceulemans, 2008). A canopy compensation point, χ_c ($\mu g\,m^{-3}$), that integrates these two pathways can be calculated as (e.g. Sutton et al., 1995; modified to include χ_w):

$$\chi_c = \frac{\chi_a\{z-d\}\cdot\left(R_a+R_b\right)^{-1}+\chi_s\cdot R_s^{-1}+\chi_w\cdot R_w^{-1}}{\left(R_a\{z-d\}+R_b\right)^{-1}+R_s^{-1}+R_w^{-1}}, \quad (3.1)$$

and the total net flux of ammonia to or from the ecosystem, F_t ($\mu g\,m^{-2}\,s^{-1}$) as

$$F_t = -\frac{\chi_a\{z-d\}-\chi_c}{R_a\{z-d\}+R_b}, \quad (3.2)$$

where by convention negative fluxes indicate deposition towards the surface and positive fluxes indicate emission. This is typically done on a half-hour basis for consistency with flux measurement practices. $R_a\{z-d\}$ and R_b are here modelled after Garland (1977) as:

$$R_a\{z-d\} = \frac{u\{z-d\}}{u_*^2} - \frac{\Psi_H\left\{\frac{z-d}{L}\right\}-\Psi_M\left\{\frac{z-d}{L}\right\}}{k\cdot u_*}, \quad (3.3)$$

and

$$R_b = u_*^{-1}\left[1.45\cdot\left(\frac{z_0\cdot u_*}{\nu_{air}}\right)^{0.24}\cdot\left(\frac{\nu_{air}}{D_{NH_3}}\right)^{0.8}\right], \quad (3.4)$$

where $u\{z-d\}$ ($\mathrm{m\,s^{-1}}$) is the wind speed at the reference height, u_* ($\mathrm{m\,s^{-1}}$) is the friction velocity, L (m) is the Obukhov length, k ($-$) is the von Kármán constant ($k = 0.41$), Ψ_H ($-$) and Ψ_M ($-$) are the integrated stability corrections for entrained scalars and momentum, respectively, after Webb (1970) and Paulson (1970), z_0 (m) is the roughness length, ν_air ($\mathrm{m^2\,s^{-1}}$) is the kinematic viscosity of air, and $D_{\mathrm{NH_3}}$ ($\mathrm{m^2\,s^{-1}}$) is the molecular diffusivity of ammonia in air. R_s can be modelled using at least a light and temperature response function (e.g. Wesely, 1989), often with additional reduction factors accounting for vapour pressure deficit, soil moisture and other environmental variables (e.g. Emberson et al., 2000). However, this study focuses on nighttime fluxes when non-stomatal fluxes are assumed to be dominant. If R_s is assumed to approach infinity at during nighttime, all terms involving R_s in Eq. (3.1) collapse to zero.

3.2.2 *Most recent non-stomatal resistance parameterisations*

3.2.2.1 *Massad et al. (2010a)*

Based on an extensive meta-analysis, Massad et al. (2010a) derived a parameterisation (henceforth referred to as *MNS*) for a unidirectional non-stomatal pathway model (i.e. $\chi_\mathrm{w} = 0$) that models the effect of the air pollution climate by incorporating a so-called acid ratio, AR ($-$), to scale the minimum allowed R_w. It is defined as the molar ratio of average total acid/$\mathrm{NH_3}$ concentrations, $AR = (2[\mathrm{SO_2}] + [\mathrm{HNO_3}] + [\mathrm{HCl}])/[\mathrm{NH_3}]$ and is an extension of the classical $[\mathrm{SO_2}]/[\mathrm{NH_3}]$ co-deposition proxy concept following the decline of $\mathrm{SO_2}$ emissions in Europe during the last few decades (e.g., Erisman et al., 2001). In addition, effects of leaf area index LAI ($\mathrm{m^2\,m^{-2}}$) and temperature T (°C) are modelled following Zhang et al. (2003) and Flechard et al. (2010), respectively. With all corrections R_w is given as:

$$R_{\mathrm{w,MNS}} = R_{\mathrm{w,min}} \cdot AR^{-1} \cdot e^{a\cdot(100-RH)} \cdot \frac{e^{\beta\cdot|T|}}{\sqrt{LAI}}, \tag{3.5}$$

where $R_{\mathrm{w,min}} = 31.5\ \mathrm{s\,m^{-1}}$ is the *baseline* minimum R_w, a ($-$) is an empirical ecosystem-specific parameter ranging from 0.0318 $\pm$ 0.0179 for forests to 0.176 $\pm$ 0.126 for grasslands, RH (%) is

relative humidity, LAI ($m^2\,m^{-2}$) is one-sided leaf area index, $\beta = 0.15\,°C^{-1}$ is a temperature response parameter, and T (°C) is the temperature. The exponential decay parameter a was calculated as an average of a values per land-use class reported in the literature (Massad et al., 2010a). Note that the temperature response was originally derived using temperatures scaled to the notional height of trace gas exchange $z_0{}'$ (m). Since sensible heat flux measurements, which are required for this extrapolation (e.g. Nemitz et al., 2009), were not available for all sites, we here used measured air temperatures instead. The influence of using T and RH at the reference height instead of $z_0{}'$ is discussed later in this paper. Contrary to the original formulation of Flechard et al. (2010), Massad et al. (2010a) do not use absolute values of $|T|$ (°C), but we chose to do so under the assumption that generally R_w increases in freezing conditions (e.g. Erisman and Wyers, 1993).

3.2.2.2 *Wichink Kruit et al. (2010)*

Following the bidirectional non-stomatal exchange paradigm introduced in the cuticular capacitance model of Sutton et al. (1998), Wichink Kruit et al. (2010) developed a simplified steady-state non-stomatal compensation point (χ_w) model (henceforth referred to as *WK*) using three years of flux measurements over an unfertilised grassland in the Netherlands. In this model, a simple exponential humidity response after Sutton and Fowler (1993) is used as an approximation for R_w under low ambient NH_3 concentrations, where saturation of the external leaf surfaces is unlikely (Milford et al., 2001a; Wichink Kruit et al., 2010):

$$R_{w,WK} = 2 \cdot e^{\frac{1}{12}\cdot(100-RH)}. \tag{3.6}$$

χ_w ($\mu g\,m^{-3}$) is calculated from the temperature response of the Henry equilibrium and the ammonium-ammonia dissociation equilibrium, similar to formulations used for the stomatal compensation point (e.g., Nemitz et al., 2000), as:

$$\chi_w = \frac{2.75 \cdot 10^{15}}{T + 273.15} \cdot e^{\left(-\frac{1.04\cdot 10^4}{T+273.15}\right)} \cdot \Gamma_w, \tag{3.7}$$

where Γ_w $(-)$ is the non-stomatal emission potential and corresponds to the molar ratio of $[NH_4^+]$ to $[H^+]$ in the leaf surface water layers. Wichink Kruit et al. (2010) derived a functional relationship for Γ_w from measurements of the ammonia air concentration at a reference height of 4 m:

$$\Gamma_w = 1.84 \cdot 10^3 \cdot \chi_a\{4\,\mathrm{m}\} \cdot e^{-0.11 \cdot T} - 850. \tag{3.8}$$

The WK model is only structurally bidirectional in that the effect of the air pollution climate is shifted from R_w to χ_w. In practice, as χ_w is parameterised as a fraction of χ_a, no emissions can occur (cf. van Zanten et al., 2010, Appendix F).

An effective non-stomatal resistance, $R_{w,\mathrm{eff.}}$ $(\mathrm{s\,m^{-1}})$, that produces identical results when used with a unidirectional non-stomatal resistance-only model, can be written as:

$$R_{w,\mathrm{eff.}} = \frac{\chi_c \cdot R_w}{\chi_c - \chi_w}, \tag{3.9}$$

or during nighttime conditions, when R_s is here assumed to approach infinity:

$$R_{w,\mathrm{eff.,nighttime}} = \frac{\chi_a\{z-d\} \cdot R_w + \chi_w \cdot (R_a\{z-d\} + R_b)}{\chi_a\{z-d\} - \chi_w}. \tag{3.10}$$

Note that Wichink Kruit et al. (2010) used surface temperatures estimated from outgoing longwave radiation and the Stefan-Boltzmann law, but in practice the model is routinely run with air temperatures within the DEPAC3.11 code (van Zanten et al., 2010). As with the MNS model, the difference between using air and surface temperatures when the latter was available was investigated in a small sensitivity study.

3.2.3 *Theoretical considerations and generation of hypotheses*

The MNS model uses a minimum non-stomatal resistance $R_{w,\mathrm{min}}$ of 31.5 $\mathrm{s\,m^{-1}}$, which is further significantly increased when $AR < 1$, $RH < 100\,\%$, $LAI < 1$ and $T \neq 0\,^\circ\mathrm{C}$ (Figure 3.2). For example, at $AR = 0.5$ and $T = 10\,^\circ\mathrm{C}$, the minimum allowed R_w at 100 % relative humidity lies between 163 and 282 $\mathrm{s\,m^{-1}}$ for an LAI

range of 1 to 3 $m^2\,m^{-2}$. It is evident from Table 1 of Massad et al. (2010a) that $AR < 1$ is no rare occurrence, but compared to minimum measured R_w (ibid.) predicted values appear to be rather high. It should also be noted that in the MNS model, the deposition velocity can never reach the maximum limit allowed by turbulence $v_{d,max}\{z-d\}$ ($m\,s^{-1}$):

$$v_{d,max}\{z-d\} = \left(R_a\{z-d\} + R_b\right)^{-1}. \tag{3.11}$$

The temperature dependent parameterisation of Γ_w in the WK model can lead to contrasting effects: When temperatures increase, the exponential decay function in Eq. (3.8) can completely counter the growth of Eq. (3.7). In other words, depending on NH_3 air concentration levels, after a certain cut-off temperature the non-stomatal compensation point χ_w decreases (Figure 3.2), although with a constant Γ_w, an equilibrium shift towards gaseous ammonia would be expected to lead to a further exponential increase of χ_w. Consequently, when T is high and χ_w approaches zero, χ_c is canceled out in Eq. (3.9) and $R_{w,eff.}$ becomes equal to the clean air $R_{w,WK}$ (Eq. (3.6)), which at 100 % relative humidity is as low as 2 $s\,m^{-1}$.

Based on these considerations, we hypothesise that:

1. The MNS model has a tendency to overestimate R_w and consequently to underestimate F_t, especially at sites with low acid ratios.

2. The WK model has a tendency to underestimate R_w and consequently to overestimate F_t, especially during high temperatures and low air ammonia concentrations.

3.2.4 *Derivation of nighttime non-stomatal resistances from flux measurements*

Non-stomatal resistance models are parameterised using flux measurements during reasonably turbulent, i.e. near neutral or only slightly stable, nighttime conditions. When stomatal closure is high and therefore $R_s \gg R_w$, we can assume that the canopy resistance R_c is approximately equal to R_w based on the

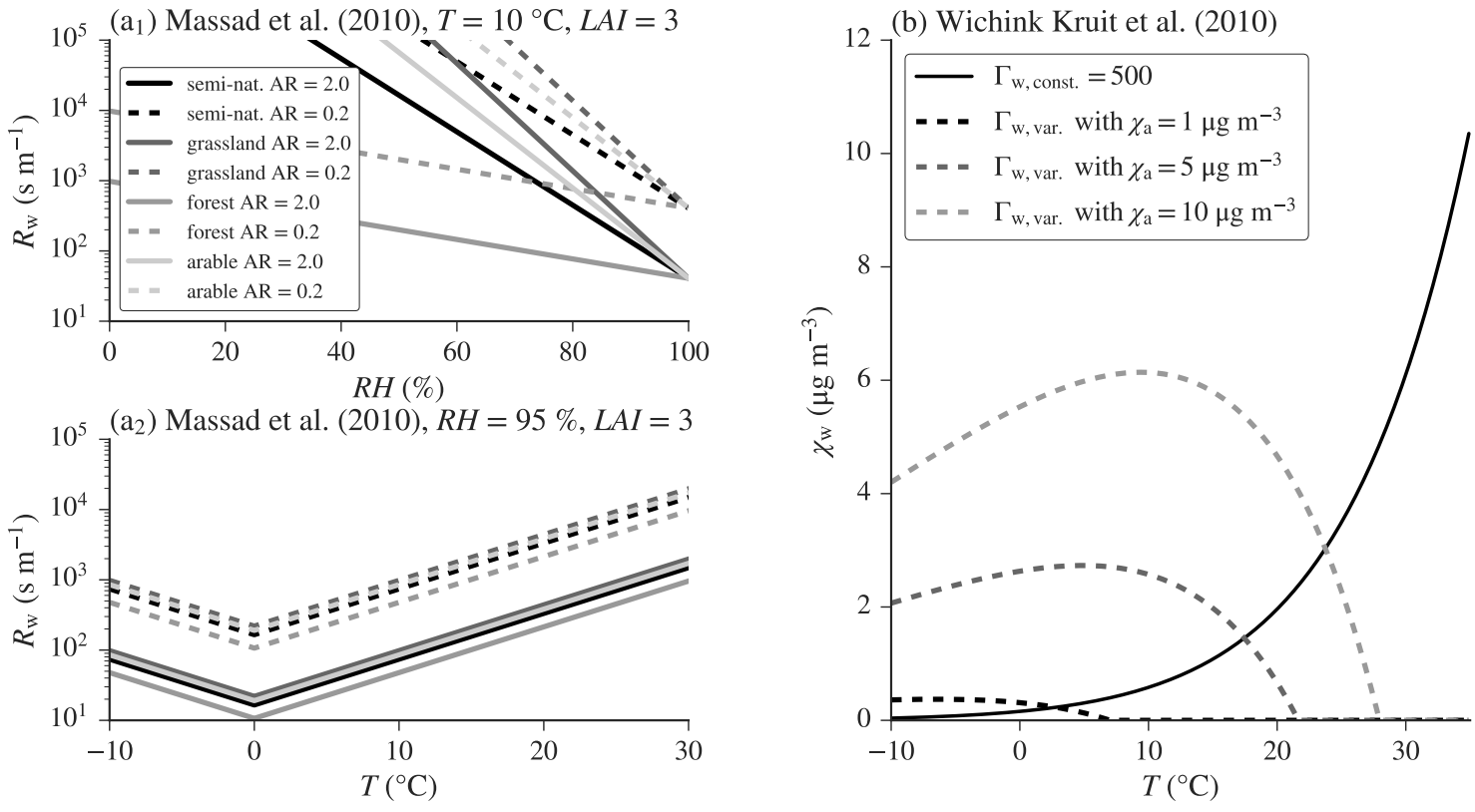

Figure 3.2: Theoretical considerations about the non-stomatal resistance parameterisations' response to changes in micrometeorological conditions. (a) Non-stomatal resistance (R_w) as a function of (a_1) relative humidity (RH) and (a_2) temperature (T) for different ecosystems and pollution climates according to the Massad et al. (2010a) parameterisation. (b) Non-stomatal compensation point (χ_w) as a function of air ammonia concentration (χ_a) and temperature (T) in the Wichink Kruit et al. (2010) parameterisation.

single-layer model when the non-stomatal pathway is treated unidirectional:

$$R_{\mathrm{w,obs.}} \approx -\frac{\chi_{\mathrm{a}}\{z-d\}}{F_{\mathrm{t}}} - \left(R_{\mathrm{a}}\{z-d\} + R_{\mathrm{b}}\right), \tag{3.12}$$

where $R_{\mathrm{w,obs.}}$ ($\mathrm{s\,m^{-1}}$) is the observed non-stomatal resistance, and F_{t} is in $\mu\mathrm{g\,m^{-2}\,s^{-1}}$. $R_{\mathrm{w,obs.}}$ values were selected from turbulent nighttime conditions (e.g. Wichink Kruit et al., 2010), when $R_{\mathrm{a}}\{z-d\} + R_{\mathrm{b}} < 200\,\mathrm{s\,m^{-1}}$, $u_* > 0.1\,\mathrm{m\,s^{-1}}$, and global radiation $< 10\,\mathrm{W\,m^{-2}}$.

Existing datasets of flux measurements were used for a comparison of measured and modelled R_{w}. These measurements were conducted at two peatland sites, Auchencorth Moss (AM) in the United Kingdom, and Bourtanger Moor (BM) in Germany, as well as three grassland sites, Oensingen (OE) in Switzerland, and Solleveld (SV) and Veenkampen (VK), both in the Netherlands. At AM, OE, SV and VK, the aerodynamic gradient and at BM the eddy-covariance method was used. For detailed site and measurement setup descriptions, the reader is referred to Flechard et al. (1999) for AM, Zöll et al. (2016) and Hurkuck et al. (2014) for BM, and Spirig et al. (2010) for OE. SV and VK datasets are unpublished as of now. SV is best characterised as a semi-natural grassland and is located in the dune area west of The Hague, NL. NH_3 concentration profiles were measured using a *Gradient Ammonia High Accuracy Monitor* (GRAHAM, Wichink Kruit et al., 2007) system with inlets at 0.8, 1.7 and 3.6 m above ground. VK is an experimental grassland site used by Wageningen UR for meteorological measurements, where NH_3 was sampled at 0.8 and 2.45 m above ground using *Differential Optical Absorption Spectroscopy* (DOAS, Volten et al., 2012). A brief overview of measurement conditions at the five sites is given in Table 3.1. *LAI* and canopy height h_{c} (m) measurements were available for AM and OE, and the default values proposed in Table 6 of Massad et al. (2010a) were used at the other sites. Emission events at OE not suitable for this study were filtered out by removing 9 days of measurements after a fertilisation event, based on the *e*-folding time of 2.88 days used for fertiliser emission potentials in Massad et al. (2010a), which translates into a 95 % *extinction time* of 8.63 days for the management influence. For VK, no management logs for the measurement site or the surrounding fields were

available and only two strong emission periods were removed manually after visual inspection of the dataset.

3.2.5 *Proposal for a semi-dynamic parameterisation of non-stomatal emission potentials*

The Wichink Kruit et al. (2010) parameterisation was developed for frameworks within which the use of dynamic cuticular capacitance models in conjunction with leaf surface chemistry modules may not be practical (e.g. to limit computation time of large scale CTMs). While it is capable of modelling saturation effects with an ambient ammonia concentration dependent non-stomatal compensation point, it only relies on χ_a at the current calculation step. A compromise between the truly dynamic models of Sutton et al. (1998) and Flechard et al. (1999) and the steady-state simplification of Wichink Kruit et al. (2010) would respect the site's history of reactive nitrogen inputs without falling back to a numerically dynamic model and, consequently, the same difficulties that limit the application of existing dynamic approaches in large-scale models, i.e. it would need to use a proxy for previous nitrogen deposition without relying on the model's flux predictions at an earlier calculation time. We here additionally investigate the feasibility of a Γ_w parameterisation based on backward-looking moving averages of air ammonia concentrations as a proxy for prior NH_3 inputs into the system which might saturate leaf water layers and enhance the compensation points. If such a relationship exists, it can provide an easy-to-use metric that can be calculated from readily available observations without the need for spinning up and iteratively solving a model for F_t estimates, while still allowing the use of a more mechanistic bidirectional approach to non-stomatal exchange. Γ_w values are derived as done by Wichink Kruit et al. (2010), i.e. R_w is parameterised for clean air according to Eq. (6), χ_w is calculated as

$$\chi_w = \chi_a\{z-d\} + F_t \cdot (R_a\{z-d\} + R_b + R_{w,WK}), \qquad (3.13)$$

and finally, Γ_w is calculated by rearranging Eq. (3.7) to:

$$\Gamma_w = \frac{T+273.15}{2.75\cdot 10^{15}} \cdot e^{\left(\frac{1.04\cdot 10^4}{T+273.15}\right)} \cdot \chi_w. \qquad (3.14)$$

Table 3.1: Summary of the five datasets. AGM = Aerodynamic gradient method; EC = Eddy-covariance, MNS = Massad et al. (2010a). Measurement period is the period during which flux measurement were available after final data filtering. T and χ_a ranges are minimum and maximum values during the measurement period and values in parentheses denote the 5 %, 50 %, and 95 % quantiles.

ID	SITE NAME	ECOSYSTEM TYPE IN MNS	MEASUREMENT PERIOD	MEASUREMENT TECHNIQUE	T (°C)	χ_a ($\mu g\,m^{-3}$)	AVG. AR (−)	REFERENCE
AM	Auchencorth Moss (UK)	semi-natural	02/1995–02/1996 05/1998–11/1998	AGM	−7.8–26.9 (0.0, 9.4, 17.3)	0.0–32.9 (0.1, 0.4, 2.9)	0.7	Flechard et al. (1999)
BM	Bourtanger Moor (DE)	semi-natural	02/2014–05/2014	EC	−4.4–22.3 (0.7, 7.3, 17.8)	1.6–62.0 (3.2, 9.0, 26.6)	0.1	Zöll et al. (2016)
OE	Oensingen (CH)	grassland	07/2006–10/2007	AGM	−3.0–33.1 (1.2, 12.3, 23.8)	0.0–24.7 (0.4, 2.2, 8.0)	0.4	Spirig et al. (2010)
SV	Solleveld (NL)	grassland	09/2014–08/2015	AGM	−1.5–31.7 (3.4, 11.6, 20.4)	0.1–15.6 (0.2, 1.2, 6.6)	0.5	unpublished
VK	Veenkampen (NL)	grassland	01/2012–10/2013	AGM	−5.4–31.6 (4.0, 15.2, 26.2)	0.3–116.9 (2.5, 8.8, 27.7)	0.3	unpublished

The relationship was investigated for moving-windows of different lengths (1 day, 3 days, 7 days, and 14 days) under exclusion of periods with substantial rainfall ($> 5\,\mathrm{mm\,d^{-1}}$).

3.3 RESULTS AND DISCUSSION

3.3.1 *Comparison of existing parameterisations with observations*

The MNS model tends to underestimate nighttime F_t at all five sites, whereas the WK model overestimates F_t for BM, OE and SV, underestimates it for VK, and only very slightly underestimates it for AM (Figure 3.3). Note that total cumulative F_t in Figure 3.3 is by no means representative for an estimate for total NH_3 input during these times, but based on non-gap filled nighttime fluxes only. Additionally, a mismatch between modelled and measured flux densities early in the time series propagates through the whole time series of cumulative fluxes. For example, at BM the MNS model performs very well after a mismatch during the first week, whereas the WK model fits the observations closely until mid-March 2014. Similarly, the strong measured deposition event early in the VK time series is not reproduced by either of the models. Comparing differences in modelled and measured nighttime R_w (Figure 3.4, upper row) supports these observations: While using the MNS model leads to an overestimation of the majority of observed R_w at all sites, as hypothesised, the picture is not as clear for WK. Here, the majority of modelled R_w values lies below the observations for BM, OE, SV and VK, however, for AM and VK both frequent over- and underestimations of R_w canceled each other out, thereby leading to fairly reasonable predicted net fluxes at these two sites. The inverse of these resistances, the non-stomatal conductance $G_w = R_w^{-1}$ may be a better predictor for the resulting fluxes, as very high resistances have a negligible effect on fluxes. Differences between modelled and measured G_w are shown in the lower row of Figure 3.4 and generally lead to similar conclusions (note that here underestimations of G_w directly lead to underestimations of F_t), but emphasise the relatively good predictive capabilities of MNS at BM and WK at VK during most times, which may not immediately be obvious from looking at cumulative fluxes (Figure 3.3).

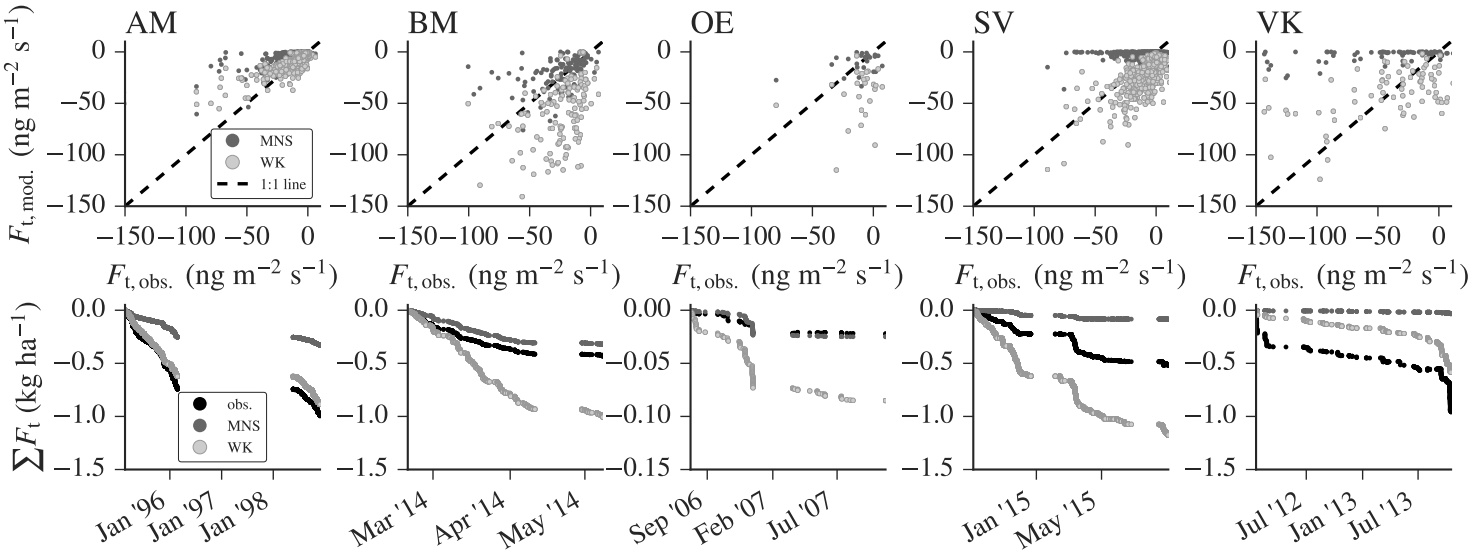

Figure 3.3: Measured and modelled ammonia dry deposition fluxes (F_t) during near-neutral or slightly stable nighttime conditions. Upper row: modelled vs. measured 6 h median flux densities. Lower row: Cumulative fluxes. obs. = observations; MNS = Massad et al. (2010a); WK = Wichink Kruit et al. (2010). Refer to the text for site descriptors. Note the different scaling of the axes.

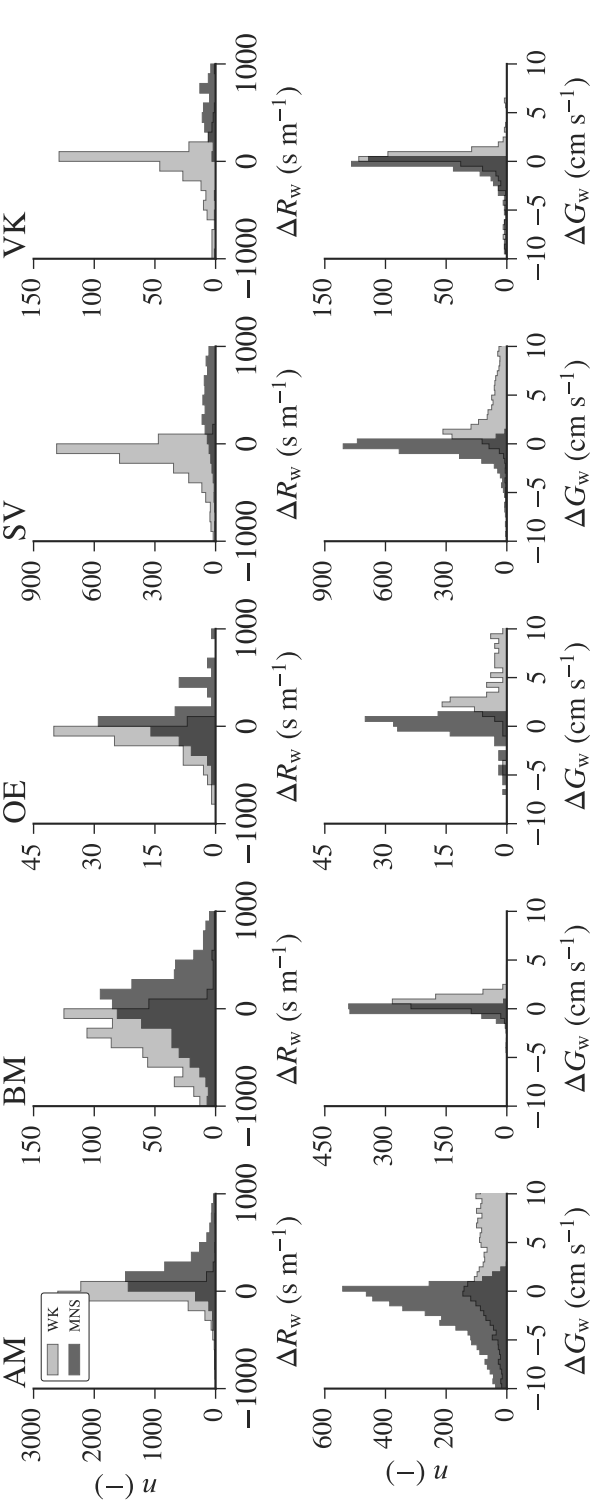

Figure 3.4: Differences in measured and modelled 30 min nighttime non-stomatal resistances (R_w, upper row, 100 s m^{-1} bins) and conductances (G_w, lower row, 0.5 cm s^{-1} bins). $\Delta R_w = R_{w,mod.} - R_{w,obs.}$ and $\Delta G_w = G_{w,mod.} - G_{w,obs.}$, i.e. positive values indicate an overestimation and negative values indicate an underestimation by the models. Note that an overestimation of R_w leads to an underestimation of fluxes F_t, whereas an overestimation of G_w leads to an overestimation of F_t.

We attribute the mismatch of the MNS model results and measurements to the relatively high baseline minimum allowed R_w and the strong response of the temperature correction function (Figure 3.5, left panel). Note that AR at all sites is lower than 1, ranging from 0.1 at BM to 0.7 at AM, which results in minimum R_w of 315 and 45 $s\,m^{-1}$ before LAI and T correction, respectively. For example, at OE with an AR of 0.4 and an average LAI of approximately 2 $m^2\,m^{-2}$, even under conditions highly favouring deposition towards the external leaf surface in the MNS model ($RH = 100\,\%$, $T = 0\,°C$), deposition velocity is restricted to an upper bound of 1.8 $cm\,s^{-1}$, although observations regularly exceeded this threshold. In their comprehensive literature review, Massad et al. (2010a) themselves report $R_{w,min}$ between 1 and 30 $s\,m^{-1}$ for grassland and between 0.5 and 24 $s\,m^{-1}$ for semi-natural ecosystems. In their parameterisation of R_w, on the other hand, the actual deposition velocity can never approach the theoretical limit allowed by turbulence (Eq. (3.11)), although this case was regularly observed in the field. This is of course true for all unidirectional R_w parameterisations of the commonly used $R_w = R_{w,min} \cdot e^{a\cdot(100-RH)}$ form, however, in the WK model a small minimum R_w of 2 $s\,m^{-1}$ allows $v_d\{z-d\}$ to approach $v_{d,max}\{z-d\}$ closely. Regarding the temperature correction, the parameter $\beta = 0.15\,°C^{-1}$ translates into an increase of R_w by a factor of 4.5 with a T increase of 10 K. Equation (3.7), however, only predicts an increase of the compensation point χ_w by a factor of approximately 2.8 to 4.1 for a T increase of 10 K, depending on the starting temperature, which translates into a significantly smaller factor for $R_{w,eff.}$ considering the influence of other variables in Eq. (3.9) and / or Eq. (3.10). Note, the relatively good agreement with measured fluxes at BM, despite the very low AR.

Reasons for strikingly diverse performance of the WK model are not straightforward, but may be explained based on the combined effect of T and χ_a on the Γ_w parameterisation, as depicted in Figure 3.2. For example, at BM the model performs relatively well until mid-March 2014 (Figure 3.3), when measured fluxes decrease, whereas modelled fluxes remain at a similar level and later even increase. This observation corresponds to an increase in both T and χ_a at the site cf. (cf. Zöll et al., 2016), leading to a

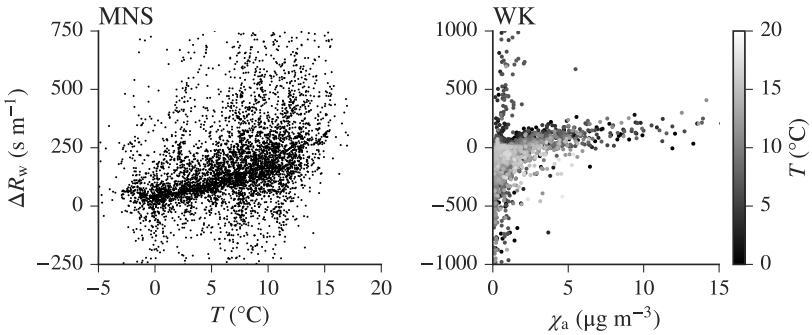

Figure 3.5: Differences between modelled and measured 30 min nighttime non-stomatal resistances (ΔR_w) as a function of T and / or χ_a. Left panel: Increasing mismatch of measured and modelled R_w in the MNS model due to a too strong T response. The line-shaped pattern emerges from times when observed R_w is zero and is equal in magnitude to the minimum allowed R_w in the parameterisation. Right panel: The WK model reveals a tendency for both stronger over- and underestimation of observed R_w with increasing χ_a, where overestimation occurs more frequently during colder and underestimation during warmer conditions.

decrease in effective R_w and therefore an increase in modelled F_t. In fact, with all sites pooled into one combined dataset, two interesting characteristics of the parameterisation emerge from a plot of differences in modelled and measured R_w against χ_a (Figure 3.5, right panel): (i) The underestimation of R_w does indeed increase with rising temperatures and χ_a, as hypothesised. (ii) There is an additional tendency to actually overestimate R_w when temperatures are relatively low, which strongly responds to increasing χ_a and may be an indication of a too high modelled Γ_w under these conditions. These two contrasting effects may explain the good agreement of net modelled and measured cumulative fluxes e.g. at AM, where concentrations were relatively low during most times and both low and high temperatures without extremes were measured.

3.3.2 *Semi-dynamic* Γ_w

Estimated non-stomatal emission potentials Γ_w appear to have a strong dependency on backward-looking moving averages of measured air ammonia concentrations $\chi_{a,MA}$ ($\mu g\,m^{-3}$) (Figure 3.6). While this may indicate some potential as an easy-to-use and readily available proxy for prior NH_3 inputs without the need for more complex and / or computationally intensive mechanistic models, estimated Γ_w values are extremely noisy and span multiple orders of magnitude in the $< 5\ \mu g\,m^{-3}$ range. An increase in the moving-window length from 1 day (Figure 3.6a) to 14 days (Figure 3.6d) does not lead to a substantial decrease in the magnitude of the noise. There is a very clear linear relationship when log-transforming both Γ_w and $\chi_{a,MA}$ ($R^2 = 0.62$ for the 1 day moving average case; not shown), however, the strong variability of the data, especially in the low-concentration region, leads to a best fit that predicts large Γ_w even at concentrations as low as 1 $\mu g\,m^{-3}$ ($\Gamma_w \approx 380$), which eventually ends in unreasonably high emission fluxes. Without further noise reduction, this approach appears unfeasible as an alternative to more sophisticated dynamic models (e.g. Flechard et al., 1999) or those featuring additional dependencies as the one of Wichink Kruit et al. (2010). Making the moving-window width dependent on time since the last substantial precipitation event might help reduce this noise and lead to a more realistic representation, but in turn complicates the implementation and increases the degrees of freedom in this approach, thereby reducing its advantage over mechanistically more accurate models.

3.3.3 *MNS with updated parameters*

Since we hypothesised the reasons for the mismatch between modelled R_w with the MNS model and measured $R_{w,obs.}$ to be based on two easily accessible parameters with relatively obvious effects on modelled resistances ($R_{w,min}$ and the temperature response parameter β in Eq. (3.5)), we additionally investigated the effects of adjusting them towards smaller values. Figure 3.7 shows the effects of simply halving both $R_{w,min}$ and β on predicted nighttime fluxes. Even though there still remains signi-

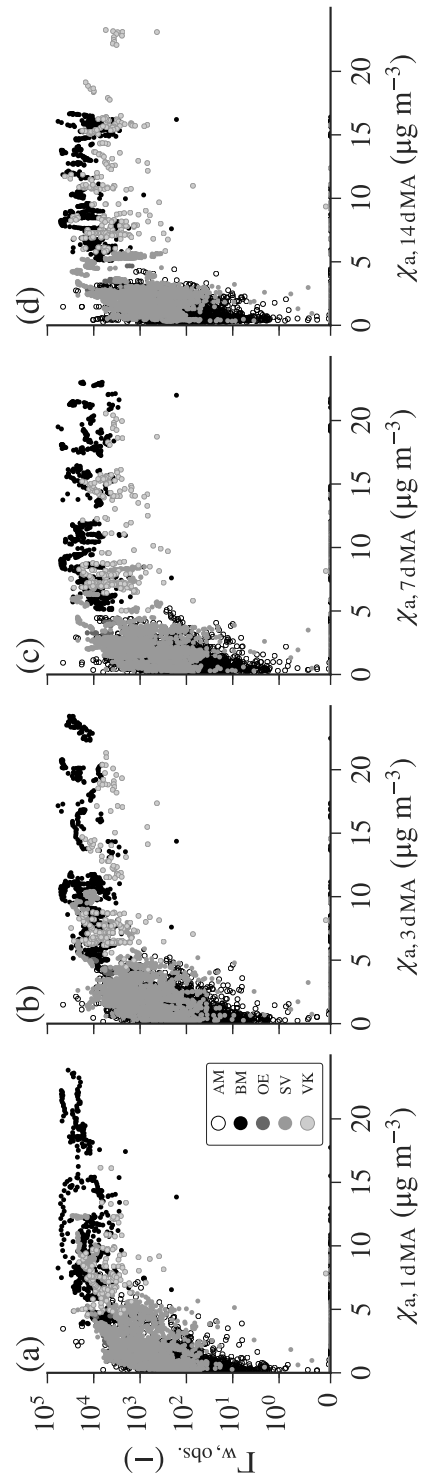

Figure 3.6: Non-stomatal emission potentials inferred from measurements (Γ_w) as a function of backward-looking moving averages of measured air ammonia concentrations (χ_a). (a) 1 day, (b) 3 day, (c) 7 day, (d) 14 day moving window. Periods with substantial precipitation were removed from the analysis.

ficant scatter, doing so decreases the mismatch between modelled and measured fluxes in most cases. However, in one case (BM) predicted fluxes actually turn out to fit the measurements worse than with the original parameters, and in another case (VK) this only leads to a marginal improvement. This exercise highlights the potential for a significant overall improvement in NH_3 flux predictions by optimising these two parameters based on independent data from all four ecosystem types (grassland, arable, forest and semi-natural ecosystems) used in the MNS parameterisation.

3.3.4 *Sensitivity of the main findings*

Parts of both models used in this study were developed using an estimate of surface temperatures, either by extrapolating T from the reference height $z - d$ to the notional height of trace gas exchange ${z_0}'$ using sensible heat flux H ($W\,m^{-2}$) measurements, or by estimating $T\{{z_0}'\}$ from outgoing long wave radiation measurements and the Stefan-Boltzmann law. Additionally, the temperature response function of Flechard et al. (2010), which is used within the MNS model, was fitted using surface level values of relative humidity, $RH\{{z_0}'\}$ which were derived using measured latent heat fluxes LE (cf. Nemitz et al., 2009). Since H and LE measurements were not available at all sites and introduce an additional source of uncertainty, especially during moderately stable nighttime conditions, and the WK model is routinely being used with air temperatures within the DEPAC3.11 code, we here used both T and RH at the reference height as input data. Figure 3.8 (upper row) illustrates the effects of using T and RH at different conceptual model heights for AM. While there are of course numerical differences, they do not lead to significant differences in the main findings of this study. Generally, the WK model appears to be less sensitive to these choices than the MNS model.

For both SV and VK, no measurements of $[HNO_3]$ and [HCl] were available. We estimated AR for the MNS model based on the observations of Fowler et al. (2009), that across NitroEurope sites, $[SO_2]$ makes up around 40 % of the sum $[SO_2] + [HNO_3] + [HCl]$ to be approximately 3.5 times the ratio of $[SO_2]/[NH_3]$. From

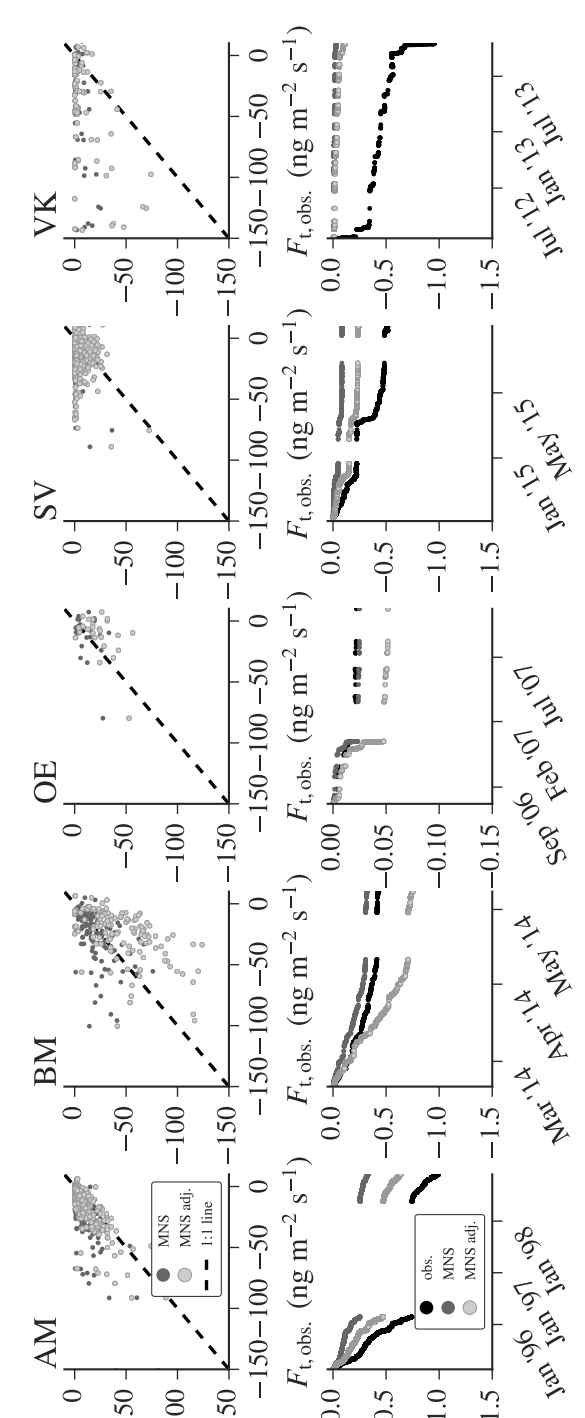

Figure 3.7: Measured and modelled ammonia dry deposition fluxes (F_t) during near-neutral or slightly stable nighttime conditions. Upper row: modelled vs. measured 6 h median flux densities. Lower row: Cumulative fluxes. MNS adj. = MNS with halved minimum R_w and temperature response parameter β.

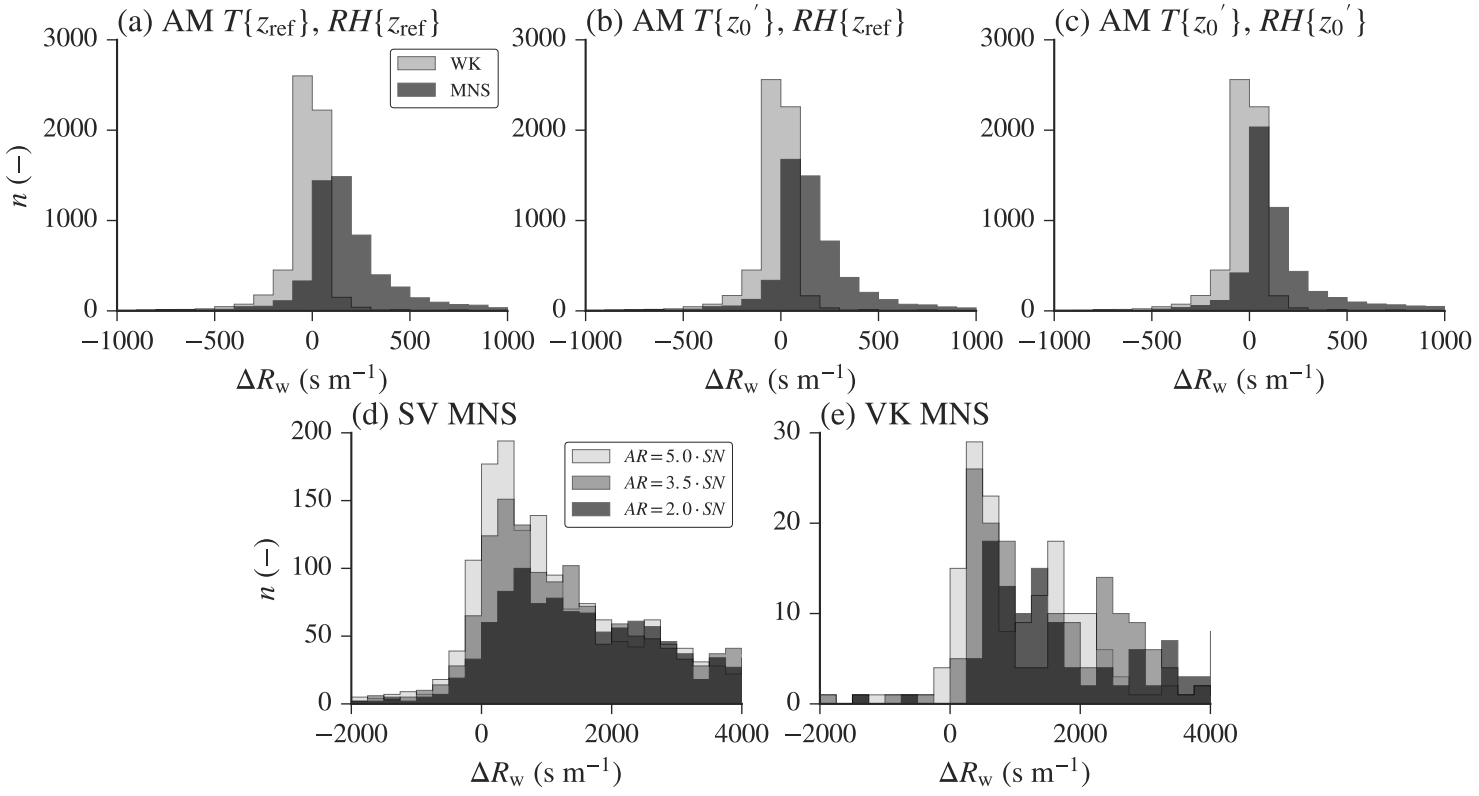

Figure 3.8: Sensitivity of differences in measured and modelled non-stomatal resistances to the use of measured air vs. surface temperature and relative humidity estimates. Upper row: Exemplary calculations for AM with (a) T and RH at the reference height, (b) T at the notional height of trace gas exchange (z_0'), and (c) T and RH at z_0'. Lower row: AR estimated as 2.0, 3.5 and 5.0 times the $[SO_2]/[NH_3]$ ratio SN for (d) Solleveld and (e) Veenkampen. Note the asymmetric horizontal axis in (d) and (e). Data are binned into 100 s m^{-1} bins for (a-c) and 250 s m^{-1} bins for (d-e) to ensure visual clarity.

the definitions $AR = (2[SO_2] + [HCl] + [HNO_3])/[NH_3]$ and $SN = [SO_2]/[NH_3]$, a lower bound of $AR \geq 2 \cdot SN$ is obvious. Using a symmetrical range around our initial estimate of $AR \approx 3.5 \cdot SN$, we set an additional upper bound of $AR \leq 5 \cdot SN$ and tested the effects of using these values on R_w differences for both affected sites (Figure 3.8, lower row). Again, there are apparent numerical differences, but they do not affect the main observations made here (i.e. they neither change the sign of the differences in modelled and measured R_w, nor do they change the general magnitude of the differences e.g. from a strong overestimation to an insignificant one).

3.3.5 *Sources of uncertainty*

Nighttime $R_{w,obs.}$ are affected by (i) the uncertainty in the flux measurements, which can be high due to insufficient turbulent mixing, and (ii) uncertainty in modelled $R_a\{z-d\}$ and R_b, which results from increasingly high stability corrections ($\Psi_M\left\{\frac{z-d}{L}\right\}$ and $\Psi_H\left\{\frac{z-d}{L}\right\}$) under increasing atmospheric stability, possible inaccuracy of estimated z_0 and d, and possible inadequacy of the R_b model for some surfaces. We therefore emphasise that the results of this study are to be interpreted qualitatively and can only reveal overall tendencies in the models' accuracy, not provide a precise quantification of the mismatch between models and measurements. Propagation of these uncertainties through the analysis resulted in some negative values of $R_{w,obs.}$. There are generally two possible reasons for negative canopy resistance values to occur: (i) emission (i.e. positive fluxes), or (ii) *overfast* deposition ($v_d\{z-d\} > v_{d,max}\{z-d\}$) that is not compatible with the resistance modelling framework used here. As a rule of thumb, we set an upper tolerance threshold for $v_d\{z-d\}$ of $1.5 \cdot v_{d,max}\{z-d\}$, considered to be within the limits of nighttime flux measurement uncertainty and representing perfect sink behavior, and consequently set $R_{w,obs.}$ to zero in these cases. Measurements where $v_d\{z-d\} > 1.5 \cdot v_{d,max}\{z-d\}$ were discarded and assumed to be either resulting from incompatibility with the atmospheric resistance ($R_a\{z-d\}$, R_b) model or from measurement error. During emission events, $R_{w,obs.}$ was set to

infinity. Ranges from 2 to 16 % invalid values, 63 to 93 % deposition and 4 to 29 % emission were observed across the five sites during near-neutral nighttime conditions. The latter especially highlights the importance of further research towards a truly bidirectional paradigm for non-stomatal exchange (i.e. cuticular desorption, ground-based emissions, or emission fluxes from other environmental surfaces).

An additional investigation of daytime non-stomatal exchange would be beneficial in terms of a significant reduction of uncertainty in the observations and in order to cover a much wider range of temperatures and humidity regimes. However, comparisons based on daytime flux estimates were not made in this study in order not to introduce an additional source of bias via the stomatal pathway. Both Massad et al. (2010a) and Wichink Kruit et al. (2010) also presented parameterisations for the stomatal emission potential, Γ_s $(-)$. However, for MNS information about annual total (dry and wet) N input into the system is necessary. While this issue can be overcome by iteratively solving a model with more reactive nitrogen species, so that N input is both a parameter, and a result of the simulation, we here used a model that only predicts NH_3 dry deposition, which we do not consider to be sufficient information to estimate total N input to our sites. At sites where total N input is known (e.g. BM, from Hurkuck et al. (2014), or from CTM results for other sites), the MNS and WK parameterisations both predict very different Γ_s estimates. The reasons for this mismatch have, to our knowledge, not been investigated to date. We therefore decided to not model the stomatal pathway explicitly and rely on nighttime fluxes only.

Explicitly modelling the stomatal pathway with physiologically accurate stomatal conductance models may have the additional benefit of being able to assess bias in the estimation of non-stomatal resistances introduced by nighttime stomatal opening, naturally resulting in a lower contribution of the non-stomatal pathway to the total observed flux. However, note that a distinction between physiological accuracy and the purpose which the derived resistances are used for has to be made. While nighttime stomatal opening is a well-known phenomenon (e.g. Caird et al., 2007), it is rarely respected in modelling studies (e.g. Fisher et al., 2007). A physiologically accurate R_w parameterisation used in

conjunction with a stomatal model that does not account for nighttime stomatal opening would result in biased fluxes. We here derived R_w under the assumption that stomata are closed at night to ensure comparability with R_w values predicted by the WK and MNS parameterisation, respectively, and compatibility with most operational biosphere-atmosphere exchange schemes, but we acknowledge that the physiological meaning may be confounded by stomatal flux contributions at night.

Another source of uncertainty lies in the fact that R_w models are often developed as *cuticular resistance* models with only leaf surface exchange in mind. However, in the one-layer resistance framework used here it is not possible to clearly differentiate between deposition towards or emission from wet leaf surfaces, leaf litter, the soil, stems and branches, and any other environmental surface. In fact, the MNS model was originally developed on the basis of the two-layer model of Nemitz et al. (2001), but outside of management events, the ground layer resistance was set to infinity in order to transform the model structure to that of a one-layer model (Massad et al., 2010a). While it is indeed conceptually unsatisfactory to ignore the source / sink strength of the ground-layer, an unambiguous identification of multiple non-stomatal pathways' flux contributions by simply inverting the model and inferring resistances from meteorological measurements is not possible, unless there is a signal that can confidently be attributed to originate from e.g. the ground layer (for instance after fertiliser application). Therefore, due to these methodological limitations, both the parameterisations and the measurements of R_w discussed in this paper may very well integrate exchange fluxes with not only wet leaves, but also e.g., the the soil, stems and branches, or other surfaces.

3.4 CONCLUSIONS

We presented a semi-quantitative assessment of the compared performances of two state-of-the-art non-stomatal resistance parameterisations for ammonia biosphere-atmosphere exchange models, supported by flux measurements from two semi-natural peatland and three grassland sites.

The unidirectional R_w-only approach of Massad et al. (2010a), which, in addition to the classical humidity response, reflects the effects of the air pollution climate, vegetation via the leaf area index, and an empirical temperature response, was found to overestimate R_w during nighttime at all five sites. Adjusting the temperature response and minimum R_w parameters in the MNS model towards smaller values resulted in a better match between modelled and measured NH_3 fluxes at most, but not all sites. We suggest to further investigate the potential of re-calibrating these parameters to flux data from all four ecosystem types represented in the MNS R_w parameterisation. Compared to measured values found in the literature (e.g. Massad et al., 2010a, Table 1), especially the minimum predicted R_w at sites with low atmospheric acid-to-ammonia ratios appear too high.

The quasi-bidirectional model of Wichink Kruit et al. (2010) shows a more complex response to varying air pollution climates and meteorological conditions, with both a tendency to underestimate R_w, as initially hypothesised, during warm conditions and moderately high ambient NH_3 concentrations, and a tendency to overestimate R_w during colder conditions, with an even stronger response to increasing χ_a. While there is likely no simple solution as may be the case for the MNS model, the WK parameterisation with its non-stomatal compensation point approach appears to be conceptually more compatible with field observations (e.g. morning peaks of NH_3 emission due to evaporation of leaf surface water). We suggest revisiting the Γ_w parameterisation with additional data from other ecosystems and investigating alternative approaches to model the effects of seasonality in Γ_w, e.g. by using a smoothed temperature response instead of an instantaneous one. An extension of the model with an SO_2 co-deposition response is currently being researched.

A simple alternative approach to dynamic models for the non-stomatal emission potential revealed a clear response of Γ_w to backward-looking moving averages of χ_a. These findings may turn out to be promising for CTMs, as they provide a first step towards a simplification of computationally intensive mechanistic model. However, further noise reduction, especially in the low concentration region, is needed for it to be useful for predicting NH_3 exchange fluxes.

CODE AND DATA AVAILABILITY

Python 2.7 code for the resistance model parameterised after Massad et al. (2010a) and Wichink Kruit et al. (2010), as well as the data analysis code, can be requested from the lead author via email (frederik.schrader@thuenen.de). Measurement data from AM, BM and OE are property of the respective authors (cf. Table 3.1); for the SV and VK datasets, please contact M. C. van Zanten (margreet.van.zanten@rivm.nl).

ACKNOWLEDEGEMENTS

We greatly acknowledge funding of this work by the German Federal Ministry of Education and Research (BMBF) within the junior research group NITROSPHERE under support code FKZ 01LN1308A. The authors are grateful to all scientific and technical staff involved in gathering the data used in this study. Many thanks to R.-S. Massad for her helpful comments and clarifications during the early stages of developing the program code used for the flux calculations. We are grateful to C. Ammann for his valuable comments on the manuscript and his contribution to the OE dataset. Finally, we would like to thank L. Zhang for handling the manuscript and two anonymous referees for their constructive reviews.

4

STOMATAL EXCHANGE

In science, one can learn the most by studying what seems the least.

— Marvin Minsky

This chapter is about to be submitted as: *Schrader, F., Erisman, J. W. & Brümmer, C. Towards a coupled paradigm of NH_3-CO_2 biosphere-atmosphere exchange modelling. Plant, Cell, & Environment.*

ABSTRACT

Stomatal conductance, one of the major plant physiological controls within ammonia (NH_3) biosphere-atmosphere exchange models, is nowadays commonly estimated from semi-empirical multiplicative schemes or simple light- and temperature-response functions. However, due to their inherent parameterisation on meteorological proxy variables, instead of a direct measure of stomatal opening, they are unfit for the use in climate change scenarios and of limited value for interpreting field-scale measurements. Alternatives based on water (H_2O) flux measurements suffer from uncertainties in the partitioning of evaporation and transpiration at humid sites, as well as a potential decoupling of transpiration from stomatal opening in the presence of hygroscopic particles on leaf surfaces. We argue that these problems may largely be avoided by directly deriving stomatal conductance from measured or modelled carbon dioxide (CO_2) fluxes instead. In a case study, we reanalyse a dataset of NH_3 flux measurements based on CO_2-derived stomatal conductances, successfully confirming the hypothesis that the increasing relevance of stomatal exchange with the onset of vegetation activity caused a rapid decrease of observed NH_3 deposition velocities. Finally, we argue that a focus on developing more mechanistic representations of NH_3 biosphere-atmosphere exchange can be of great benefit in many applications. These range from model-based flux partitioning approaches, over the implementation of deposition monitoring networks using low-cost samplers and inferential modelling, to a direct response of NH_3 exchange models to projected climate change impacts.

4.1 INTRODUCTION

Excessive dry deposition of reactive nitrogen has long been recognised as a major threat to both the environment and human health alike, as it can lead to shifts in biodiversity, especially in natural ecosystems, phytotoxic effects, elevated greenhouse-gas emissions, as well as respiratory and other health-related issues (Erisman et al., 2013). Ammonia (NH_3) is considered to be one of the most important constituents of total reactive nitrogen, with global emission estimates ranging from 46–85 $Tg\,N\,yr^{-1}$, likely more than half of which originate from agricultural production (Sutton et al., 2013). The accurate representation of NH_3 biosphere-atmosphere exchange within models is thus of great importance to build an adequate set of tools necessary to assess the whole lifecycle and impacts of reactive nitrogen compounds – from emission sources, over transport and chemical reactions in air, to their deposition. The difficulty with quantification of ammonia air-surface exchange is that because of the equilibrium with water NH_3 can easily be absorbed and desorbed if not fixed and therefore there is a high spatial and temporal variation in fluxes. There have been considerable efforts to improve the parameterisation of the bidirectional NH_3 exchange estimates in recent years (Massad et al., 2010a; Personne et al., 2009; Wichink Kruit et al., 2010; Zhang et al., 2010, and others); however, major uncertainties still prevail.

For instance, Schrader et al. (2016), among others, have recently highlighted uncertainties with the treatment of the non-stomatal pathway that can generally be attributed to (i) computational effort associated with a more realistic treatment of bidirectionality in the fluxes (e.g., Flechard et al., 1999; Sutton et al., 1998) and (ii) a lack of available measurement data across a wide range of ecosystems and pollution levels that are necessary for calibration and validation of new schemes (Flechard et al., 2013). Additionally, Flechard et al. (2013) note a lack of inter-species coupling in current models, not only in terms of often-neglected gas-particle interconversion within and above the canopy, or the still rather unrefined treatment of NH_3-SO_2-codeposition parameterisations based on relatively few observations (Nemitz et al., 2001; Wichink Kruit et al., 2017), but also within the repres-

entation of stomatal exchange. Most chemistry transport models (CTMs) nowadays employ multiplicative Jarvis (1976)-Type functions or other (semi-)empirical approaches for modelling stomatal conductance (e.g., Simpson et al., 2012; van Zanten et al., 2010), which is one of the most important plant physiological controls of NH_3 exchange. However, these models might be unfit for some tasks that require direct site-specific measurements of the stomatal conductance instead of parameterisations based on proxy variables. On the other hand, many measurement sites that are used for measuring and modelling NH_3 exchange are readily equipped with instrumentation that may be used to directly infer stomatal conductance from existing observations, thereby reducing the uncertainty associated with empirical approaches that were only built to be, on average, representative for a large number of potentially different sites within one land-use class.

One commonly used approach is to model the stomatal conductance based on measured fluxes of H_2O (e.g., Shuttleworth, 2012). However, these often suffer from an inherent uncertainty in the partitioning of transpiration and evaporation, especially at humid sites, where the latter is expected to be significant, since tower-based measurements of H_2O can generally only be representative for an ecosystem-integrated flux of evapotranspiration. Even if it can be partitioned successfully, recent research hints at a potential decoupling of transpiration fluxes and stomatal opening in the presence of hygroscopic particles on leaves (Grantz et al., 2018). Similar problems arise from directly inferring stomatal conductance of NH_3 from dry periods (e.g., Nemitz et al., 2004), assuming that deposition to non-stomatal surfaces is negligible below a certain relative humidity threshold. While this assumption may be valid to a certain degree given our current understanding of NH_3 exchange processes, measuring NH_3 exchange in itself is still highly uncertain and few studies span a long enough time to gather sufficient high-quality data during dry periods for a valid fit. Finally, purely empirical stomatal conductance parameterisations currently cannot account for stomatal responses to rising CO_2 concentrations (Ainsworth and Rogers, 2007), making them unfit for global change scenario modelling.

With this study, we aim to make a case for the use of a CO_2-exchange based treatment of the stomatal pathway within the

context of NH_3 dry deposition inferential modelling. Through the stomata CO_2 and NH_3 share a common major exchange pathway, and the underlying physiological mechanisms of CO_2 biosphere-atmosphere exchange are generally well understood. Since the emergence of continent-wide research infrastructures for monitoring CO_2 exchange, such as ICOS or NEON, and even global networks like FLUXNET, CO_2 exchange measurements have become widely available, with the eddy-covariance method as the de-facto standard measurement technique. The limited NH_3 exchange studies are often carried out at existing flux towers within one of those networks, and it is only natural to want to use as much additional available information as possible to improve our estimates of reactive nitrogen deposition. Further to pure modelling studies, information gained about stomatal behaviour may help interpret direct NH_3 flux measurements, as recently demonstrated by Hansen et al. (2017) and in the article at hand. But not only experimental studies at individual sites with standard half-hourly concentration measurements may benefit – it may also pave the road towards a valid low-cost model-based NH_3 deposition monitoring network, by equipping existing flux towers with inexpensive slow-response sensors, deriving site-specific parameterisations for the non-stomatal pathway as well as corrections for the lowered temporal resolution (Schrader et al., 2018), and using stomatal conductance estimates directly inferred from available CO_2 flux measurements. Finally, new knowledge gained from these applications can be useful to evaluate the potential benefits of coupling CO_2 and NH_3 exchange within large-scale CTMs.

In the following, we will briefly outline the fundamental assumptions and equations behind a modern bidirectional NH_3 exchange model, followed by a case-study on how we used CO_2-derived stomatal conductance for the interpretation of a decreasing NH_3 deposition velocity in spring observed in eddy-covariance measurements at a protected peatland site in Northwestern Germany, confirming a hypothesised ecosystem response that could not be explained with empirical models in an earlier analysis. In the end, we discuss options for how to incorporate existing information about CO_2 exchange in modelling and

data-analysis workflows, as well as future perspectives for the development of more mechanistic NH_3 exchange models.

4.2 MODELLING BIOSPHERE-ATMOSPHERE EXCHANGE OF AMMONIA

4.2.1 *Basic concepts*

Biosphere-atmosphere exchange of NH_3 is commonly modelled using an inferential resistance analogy, i.e. the total NH_3 flux density at a given time, F_t ($\mu g\,m^{-2}\,s^{-1}$) is estimated from a measured or modelled ambient concentration at a certain reference height, χ_a ($\mu g\,m^{-3}$), minus the canopy compensation point, χ_c ($\mu g\,m^{-3}$), divided by the sum of the aerodynamic and quasi-laminar boundary layer resistances, R_a ($s\,m^{-1}$) and R_b ($s\,m^{-1}$), respectively (Eq. (4.1)). By convention, a negative flux is directed to the surface and a positive flux is directed to the atmosphere.

$$F_t = -\frac{\chi_a - \chi_c}{R_a + R_b}. \tag{4.1}$$

χ_c can be interpreted as the equilibrium air NH_3 concentration at the mean notional height of trace-gas exchange and is calculated as:

$$\chi_c = \frac{\chi_s \cdot R_s^{-1} + \chi_a \cdot (R_a + R_b)^{-1}}{(R_a + R_b)^{-1} + R_s^{-1} + R_w^{-1}}. \tag{4.2}$$

for a simple single-layer model with parallel stomatal and non-stomatal pathways for surface exchange of NH_3 (Figure 4.1a; Nemitz et al. (2001)). R_s ($s\,m^{-1}$) and R_w ($s\,m^{-1}$) are the stomatal and non-stomatal resistance, respectively. The parameterisation of R_s is discussed in detail in the rest of this manuscript; R_w is most commonly modelled using humidity response functions (Sutton and Fowler, 1993), often with additional terms used to describe the effects of other atmospheric constituents on deposition (Massad et al., 2010a; Nemitz et al., 2001; Wichink Kruit et al., 2017). The stomatal pathway is nowadays usually modelled under consideration of a non-zero, near-surface air NH_3 concentration in equilibrium with NH_3 in the apoplastic fluid, called the stomatal compensation point, χ_s ($\mu g\,m^{-3}$), which allows for the

representation of bidirectional fluxes (i.e., both deposition and emission) within the model. It can be parameterised based on tabulated values for different ecosystems, direct or indirect estimates of deposition history to the site, or more mechanistic plant physiological approaches that directly relate the compensation point to the C- and N-metabolisms at the leaf-level (Massad et al., 2010a,b). Note that some researchers apply a similar concept to the non-stomatal pathway, with a non-stomatal compensation point, χ_w ($\mu g\,m^{-3}$), representing an air NH_3 concentration in equilibrium with NH_3 solved in water films or otherwise adsorbed to surfaces (Flechard et al., 2013; van Zanten et al., 2010; Wichink Kruit et al., 2010). Even so, to date, many chemistry transport models still employ a deposition-only paradigm for non-stomatal exchange, which is in contrast with observations of emission fluxes that are likely due to NH_3 release from non-stomatal surfaces (Wentworth et al., 2016), but much more straightforward to be parameterised from micrometeorological measurements. This can only be applied in background situations far away from NH_3 sources. In general, all models using the resistance analogy consider the surface component as a static parameter where the memory effects are not taken into account. The prior deposition of NH_3 and / or other components affect e.g. the acidity of water layers, the aerosol composition and the χ_w and χ_s concentrations.

For convenience, the model may be simplified to a strictly serial structure (Figure 4.1b) with a foliar resistance, R_f ($s\,m^{-1}$) and a foliar compensation point (sometimes called *total compensation point*), χ_f ($\mu g\,m^{-3}$), borrowing the notation of Wichink Kruit et al. (2010). An even further simplification to a quasi-unidirectional variant (Figure 4.1c) in which the effects of the compensation point are integrated in an effective foliar resistance, R_f^* ($s\,m^{-1}$) is possible and sometimes done to enforce compatibility with the concept of a deposition velocity. However, note that R_f^* can be negative in the case of emission fluxes, even though that is generally an ill-defined concept in a resistance modelling framework. R_f is equal to the sum of R_s and R_w; the derivation of expressions for χ_f and R_f^* is straightforward and documented e.g. in van Zanten et al. (2010). We here calculate χ_f as

$$\chi_f = \frac{R_f}{R_w} \cdot \chi_w + \frac{R_f}{R_s} \cdot \chi_s, \tag{4.3}$$

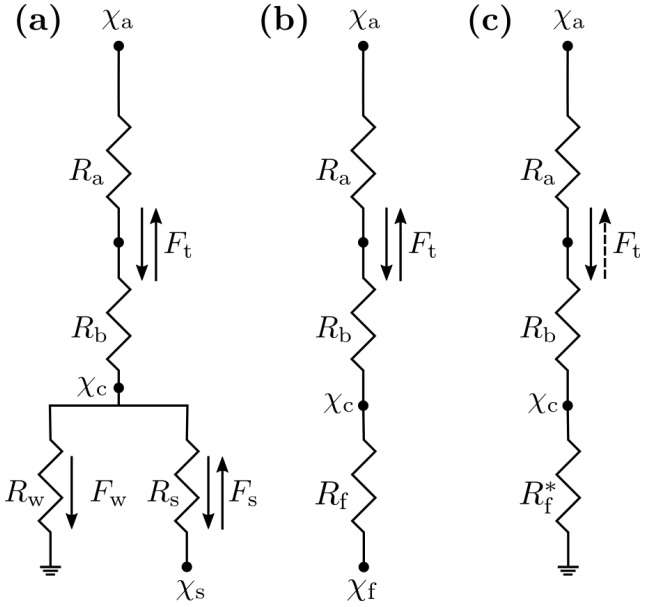

Figure 4.1: (a) Common structure of a canopy compensation point model with a unidirectional non-stomatal and a bidirectional stomatal NH_3 exchange pathway. (b) Serial bidirectional simplification with foliar resistance and foliar compensation point. (c) Serial unidirectional simplification with effective foliar resistance.

and R_f^* as

$$R_f^* = \frac{(R_a + R_b) \cdot \chi_f + R_f \chi_a}{\chi_a - \chi_f}. \tag{4.4}$$

The reciprocal of any resistance is called the corresponding conductance, i.e. $R_x^{-1} = G_x$. Both are used throughout this text, since conductances are the more commonly used quantity in some disciplines which we borrow concepts from. They also have the additional advantage of being directly (instead of inversely) proportional to the flux, as well as directly relatable to deposition velocities. Note that the units used in this context are sometimes inconsistent across communities: while micrometeorologists usually express conductances as length per time unit, plant physiologists tend to work with moles per area per second. We here follow the former convention unless specified otherwise.

4.2.2 *Stomatal controls and NH_3-CO_2 coupling*

The stomatal resistance to NH_3 exchange, or its inverse, the stomatal conductance G_s ($m\,s^{-1}$), can be modelled using a number of different approaches: Most commonly, chemistry transport models employ a multiplicative Jarvis (1976)-type scheme, such as the one of Emberson et al. (2000), which estimates the stomatal conductance as the product of a baseline resistance (or conductance) and a number of stress functions based on environmental factors (Flechard et al., 2013). Other authors use relatively simple light- and / or temperature response functions in the absence of more detailed measurements, such as the one of Wesely (1989). However, these models are usually not suitable to directly incorporate measurable effects of rising greenhouse gas concentrations and the physiological effects that are associated with them (Ainsworth and Rogers, 2007; Leakey et al., 2009). They also often rely on certain land-use specific effective parameters to be used over a wide array of ecosystems that can be aggregated into one class, but do not incorporate site-specific effects other than meteorological conditions. Finally, these models are usually used with ambient measurements of relative humidity, temperature, and other environmental factors as input data, even though the actual flux-controlling conditions near the surface may very well be significantly different. While this weakness is not inherently built into the models' structure and they can theoretically be used with surface values of the respective variables instead, this may lead to bias when they were originally parameterised on ambient measurements. However, whether or not modelling these processes with surface variables is possible and meaningful strongly depends on an individual models' configuration, spatial resolution and degree of simplification of related processes.

One approach to avoid these issues and to incorporate as much information about a specific ecosystem into their models as possible is to rely on using measured H_2O flux-based estimates of stomatal conductance (Shuttleworth, 2012). These, in turn, suffer from a number of uncertainties due to the non-trivial partitioning of measured evapotranspiration (ET) into evaporation (E) from wet surfaces and transpiration (T) through the stomata, which can be especially problematic at very humid sites where ground-

based fluxes and loss of water from leaf surfaces are a significant part of *ET*. Additional bias may be introduced from wick-effects due to hygroscopic particles lining the walls of the stomatal cavity, called *hydraulic activation of stomata* in the recent literature (Burkhardt, 2010; Burkhardt et al., 2012), which can lead to a decoupling of T and G_s (Grantz et al., 2018).

We argue that these issues may largely be avoided by basing site-specific estimates of G_s on measured or modelled CO_2 instead of H_2O fluxes. CO_2 fluxes are usually measured with the same instrumentation as H_2O (infrared gas analysers), are a routine measurement at many existing flux sites and tower networks (such as ICOS; Franz et al., 2018; or NEON; SanClements et al., 2014), and the underlying exchange processes are generally considered well understood. They are therefore suitable to directly base estimates of G_s to be used for modelling other compounds' exchange fluxes on measured data instead of uncertain empirical approaches. Additionally, CO_2 flux-based estimates of G_s may be used as an interpretation tool for measured fluxes of gaseous compounds that are exchanged via the stomata, such as NH_3 or NO_2.

We use the well-known Ball-Berry model (Ball et al., 1987) to derive G_s from measured or modelled fluxes of CO_2. It can be written as:

$$g_s = m \cdot \frac{A_n \cdot h_s}{C_s} + b, \tag{4.5}$$

where m $(-)$ is the slope and b $(\mathrm{mol\,m^{-2}\,s^{-1}})$ is the offset (minimum stomatal conductance) of the Ball-Berry function. For C_3 plants, m and b are commonly assumed to be around 9 and $0.01\,\mathrm{mol\,m^{-2}\,s^{-1}}$, respectively (Collatz et al., 1991; Sellers et al., 1996). Naturally these parameters are also subject to uncertainty, but we assume that the benefit of directly relating g_s to photosynthetic activity instead of similarly uncertain parameterisations based on proxy variables outweighs this fact. h_s is the leaf surface relative humidity (expressed as a fraction of 1) and C_s (ppm) is the leaf surface concentration of CO_2, which is obtained through simple resistance modelling-based extrapolation from measured or modelled concentrations and fluxes at the reference height to the notional height of trace gas exchange. A_n is net CO_2 uptake $(\mu\mathrm{mol\,m^{-2}\,s^{-1}})$. Lowercase g_s in Eq. (5) indicates that values

obtained through this method are representative for leaf-level fluxes; bulk canopy G_s can be obtained from an upscaling via measurements or modelled estimates of the leaf area index, as outlined e.g. by Sellers et al. (1992) and Anderson et al. (2000). To use it in an NH_3 inferential modelling context, the resulting bulk canopy G_s needs to be scaled by the ratio of NH_3 to H_2O molecular diffusivities.

4.3 CASE STUDY

4.3.1 *Site description and measurement setup*

Fast-response measurements of CO_2 and NH_3 were carried out at a temperate ombrotrophic bog in North-western Germany (*Bourtanger Moor*) from February to May 2014. Vegetation at the site is dominated by bog heather (*Erica tetralix*), purple moor-grass (*Molinia caerulea*), cotton grass (*Eriophorum vaginatum*, *E. angustifolium*), and few scattered birches (*Betula pubescens*) and Scots pines (*Pinus sylvestris*). CO_2 concentrations were measured with an open-path infrared gas analyser (IRGA; LI-7500, LI-COR Biosciences, Lincoln, USA), and NH_3 concentrations with a quantum cascade laser absorption spectrometer (Mini QC-TILDAS-76, Aerodyne Research, Inc., Billerica, MA, USA), both at a sampling frequency of 10 Hz. These high-frequency concentration measurements were used in conjunction with 10 Hz data from a 3D sonic anemometer (R3-50, Gill Instruments, Lymington, UK) to calculate half-hourly biosphere-atmosphere exchange fluxes of CO_2 and NH_3 using the eddy-covariance technique. For a detailed site-description and an in-depth discussion of data acquisition and post-processing steps, the reader is referred to Hurkuck et al. (2016) and Zöll et al. (2016).

4.3.2 *Reanalysis of observed NH_3 fluxes*

NH_3 fluxes at the Bourtanger Moor field site showed a sudden decrease in deposition around 15 March 2014, which in part coincided with a decrease in concentrations (Zöll et al., 2016). However, concentrations increased again later during the campaign whereas fluxes remained at a very low level (Figure 4.2a), and

the observed deposition velocities (i.e., essentially concentration-normalised flux rates) showed a similar pattern with a gradual decrease from up to 0.7 $cm\,s^{-1}$ down to daily averages of less than 0.2 $cm\,s^{-1}$ around mid- to end-March and staying on that level thereafter (Figure 4.2b). This coincided with a pressure drop, increasing precipitation and minimum air temperatures exceeding 5 °C for the first time at the site in 2014 (Zöll et al., 2016). Relative humidity was consistently very high (daily averages between 80 % and 100 %). The campaign-averaged NH_3 concentration was 11 $\mu g\,m^{-3}$ with management-related peaks in mid-March ($>$ 20 $\mu g\,m^{-3}$ daily average on 12 and 13 March) and early April ($>$ 20 $\mu g\,m^{-3}$ daily average from 1 to 4 April). Zöll et al. (2016) hypothesised that, among other reasons, this decline in deposition velocity may be attributed to the combined effects of an onset of vegetation activity and an increase in the stomatal compensation point due to rising temperatures. While an increasing compensation point is relatively straightforward to explain from theory, as it depends exponentially on temperature, accounting for the combined effect of gas solubility and dissociation of NH_3, observational evidence for an increasing stomatal contribution to the total flux is necessary. In this case-study, we examine how CO_2 flux-derived stomatal conductance can help us accept or reject the hypothesis of a stomatal effect on the lowered deposition velocity.

The traditional approach of separating measured fluxes into those measured during dry periods ($RH < 70\,\%$ or similar thresholds) and fitting a light-response function to the resulting observed foliar resistance (e.g., Nemitz et al., 2004) was not possible at this site due to the constantly humid conditions throughout the measurement campaign (cf. Zöll et al., 2016). Similarly, a permanently humid topsoil and even occasional ponding limited the applicability of latent heat flux measurements as a proxy for transpiration, thereby preventing their use in the derivation of a bulk stomatal conductance for H_2O.

Therefore, and as a test for its feasibility for the use in NH_3 modelling studies, CO_2 fluxes measured by Hurkuck et al. (2016) were used to derive bulk canopy stomatal conductance for NH_3 using the Ball-Berry model with canopy upscaling as described in Sellers et al. (1992). CO_2 net ecosystem exchange (NEE) was

partitioned into gross primary productivity (*GPP*) and ecosystem respiration (R_{eco}) following Reichstein et al. (2005), as described in Hurkuck et al. (2016), and the resulting *GPP* were used as bulk canopy A_n in the canopy-scale Ball-Berry model. G_s obtained via this procedure were used to model fluxes of NH_3 using the parameterisation of a two-layer canopy compensation point model after Massad et al. (2010a). Note that for semi-natural peatland sites like the Bourtanger Moor, the model is essentially reduced to a one-layer model by setting the ground-layer resistance to infinity, due to the difficult partitioning of ground-layer and other non-stomatal fluxes in unmanaged ecosystems. The minimum resistance and temperature response used in the non-stomatal resistance parameterisation were recently reported to be likely too high for some sites (Schrader et al., 2016). Thus, we derived site-specific values for these two parameters by assuming that foliar resistances derived from night-time flux measurements of NH_3 were representative for the non-stomatal resistance, R_w, i.e. assuming perfect stomatal closure at night. We then globally minimised the sum of squared residuals between measured and modelled non-stomatal conductance using a Python 3.7 implementation of the differential evolution method (*scipy.optimize.differential_evolution*; SciPy version 1.1.0; Jones et al., 2001–; Storn and Price, 1997) with bounds 0–1000 $s\,m^{-1}$ for minimum R_w and 0–1 $°C^{-1}$ for the temperature response parameter. Modelled results were used to interpret the observed flux patterns during the measurement campaign with focus on the validity of explaining the *tipping point* in mid-March with an onset of vegetation activity.

4.3.3 *Results and discussion*

Daily averages of stomatal conductance of NH_3 derived from CO_2 flux-measurements were relatively constant until the last week of March 2014, after which they exhibit a strong and seemingly linear increase up to more than twice their initial magnitude, whereas a selection of empirical models (Emberson et al., 2000; Wesely, 1989) show an initial increase at the beginning of the measurement campaign (mid-February) and remain on a relatively low level below 0.1 $cm\,s^{-1}$with an only slightly positive

trend (Figure 4.2c). At first glance, CO_2-derived stomatal conductance do not appear to be correlated with the strong decrease in observed deposition velocity (Figure 4.2c), while empirically modelled stomatal conductance seem to be anti-correlated to a certain degree. That said, it is unlikely that the decrease in deposition velocities can be attributed to the stomatal pathway in a mono-causal manner. In fact, this decrease is also observed in night-time data, where stomatal fluxes are assumed to play a negligible role, and both observed night-time foliar conductance (as a proxy for the non-stomatal conductance) and site-calibrated modelled non-stomatal conductance decrease at the same time. This is further reflected in an increasing contribution of CO_2-derived stomatal conductance to daytime foliar conductance from a minimum of around 20 % up to more than 80 %, which is apparently anti-correlated with observed deposition velocities (Figure 4.2d). Note that it follows from the governing equations of the resistance framework used in this study that this relation ($G_s\, G_f^{-1}$) is approximately equal to the ratio of stomatal to total exchange flux when the compensation point is considerably smaller than the ambient NH_3 concentration.

Indeed a regression of daytime observed deposition velocities against daytime CO_2-derived stomatal conductance contribution to the foliar conductance shows a significant anti-correlation ($r = -0.52$, intercept $= 0.46$, slope $= -0.53$, two-sided p-value (H_0: slope is zero) < 0.001; Figure 4.3), indicating that an increase in stomatal contribution to the flux leads to a decrease in the deposition velocity. While this may seem counter-intuitive at first, especially considering that the foliar conductance remains relatively constant from early March until the end of the campaign, this may be explained by a concurrent increase in temperatures and, consequently, the stomatal compensation point throughout the measurement period (Figure 4.2d). The Bourtanger Moor site has historically received annual N-deposition of up to five-fold above its critical load, with an estimated total (wet and dry) deposition in the order of $25\,\mathrm{kg\,N\,ha^{-1}\,yr^{-1}}$ (Hurkuck et al., 2014). Since the stomatal compensation point is expected to be dependent on historical N-inputs, it can reasonably be assumed to be significant at this site. To put it into context, the parameterisation of Massad et al. (2010a) predicts a stomatal emission potential of

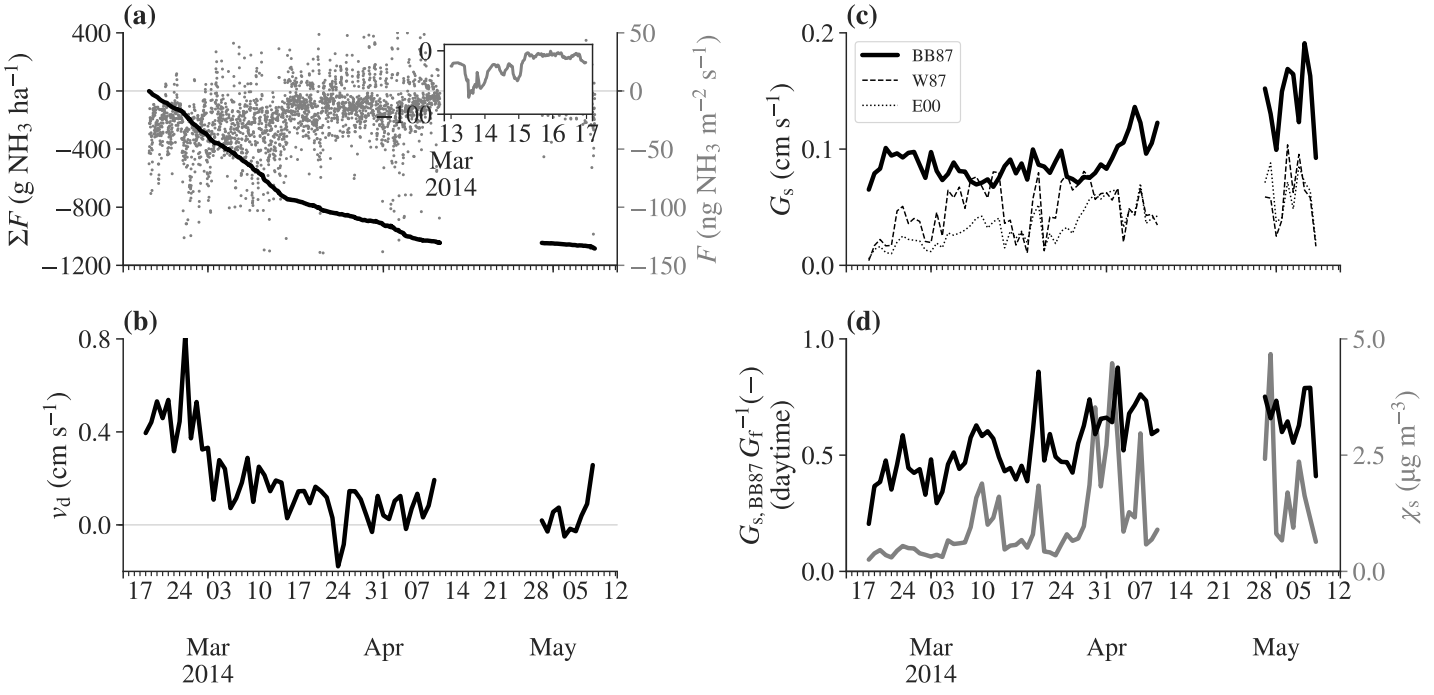

Figure 4.2: Results from the Bourtanger Moor case study. (a) Half-hourly NH_3 mass flux density (grey dots) and gap-filled cumulative NH_3 flux (black line) obtained with eddy-covariance measurements. Small inset shows sudden decline in 6 h moving average flux densities around 15 March. (b) Observed daily average NH_3 dry deposition velocity. (c) Modelled daily average stomatal conductance obtained from two empirical models (W89: Wesely (1989); E00: Emberson et al. (2000)) and from eddy-covariance fluxes of CO_2 using the Ball-Berry model (B87: Ball et al. (1987)) (d) Daily average daytime contribution of stomatal conductance to total foliar conductance (black line) and stomatal compensation point (grey line) using the Ball-Berry model.

635 for this site, which is well above the average (mean 502, median 190) for short semi-natural and forest ecosystems found in an extensive literature review by the same authors. An increase in the contribution of the stomatal conductance to the foliar conductance directly leads to an increase in the contribution of the stomatal compensation point to the foliar compensation point (Figure 4.4a). Assuming that the non-stomatal compensation point is zero, which is commonly done in modelling NH_3 exchange, this also directly leads to a reduced NH_3 concentration gradient and therefore a reduced deposition velocity. We thus conclude that the hypothesis of Zöll et al. (2016) regarding a reduction of the deposition velocity at least partially due to the onset of vegetation activity is justified and likely plays a significant role in the observed flux patterns, based on our reanalysis using CO_2-derived stomatal conductance.

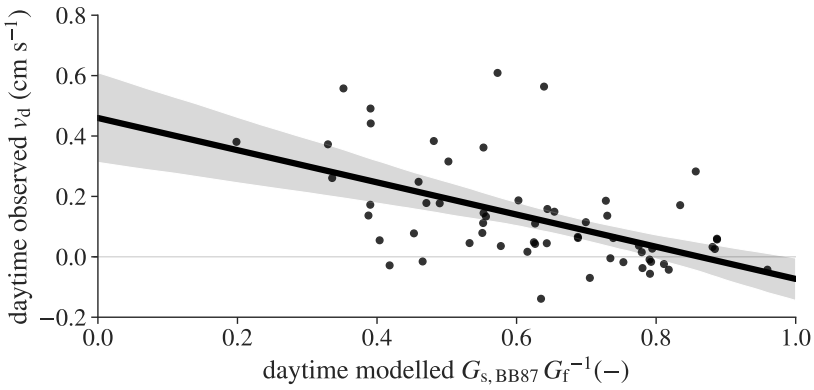

Figure 4.3: Linear regression of observed daily mean daytime NH_3 dry deposition velocities against daytime ratio of CO_2 flux-derived stomatal conductance to total modelled foliar conductance. One outlier ($v_d > 1.5\,\mathrm{cm\,s^{-1}}$ on 25 February 2014) was removed from the regression dataset. The shaded area envelopes a 95 % confidence interval of the regression based on 10 000 bootstrap samples.

Theoretically, the relationship explaining this phenomenon is linear when non-stomatal fluxes are modelled unidirectionally: If the stomatal compensation point is twice the air NH_3 concentration, a 50 % contribution of the stomatal conductance to the foliar conductance means zero gradient and therefore zero flux. This is

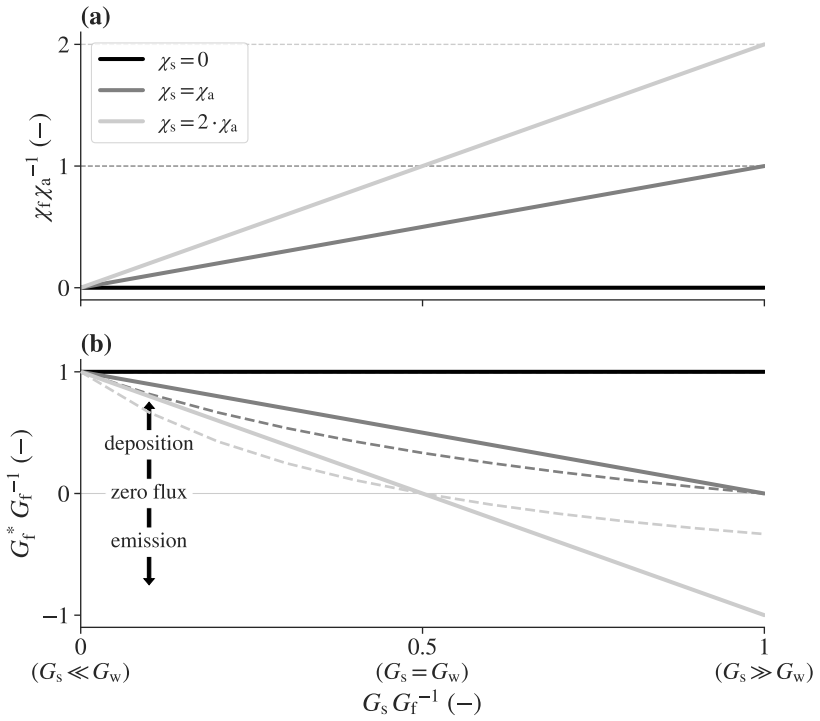

Figure 4.4: Theoretical explanation of the results from the Bourtanger Moor case study. (a) Evolution of the ratio of the foliar compensation point to ambient NH_3 concentration at the reference height and (b) the ratio of effective to actual foliar conductance with increasing stomatal contribution to the foliar conductance and varying stomatal compensation point levels. Black lines: no stomatal compensation point; dark grey lines: stomatal compensation point equal to ambient concentrations; light grey lines: stomatal compensation point twice as large as ambient concentrations. Dashed lines: Aerodynamic and quasi-laminar conductance equal in magnitude to foliar conductance; solid lines: aerodynamic and foliar conductance neglected. The non-stomatal pathway is assumed to be unidirectional (i.e., a hypothetical non-stomatal compensation point would be zero) in all cases.

irrespective of the magnitude of the aerodynamic and boundary layer conductance. However, note that taking these into account the relationship of an effective foliar resistance to the actual foliar resistance becomes non-linear between the extreme cases of zero compensation point or compensation point equal to the ambient concentration at the reference height (Figure 4.4b).

4.4 CONCLUSIONS AND FUTURE PERSPECTIVES

We successfully demonstrated that a model-driven approach for flux data analysis using CO_2 flux-derived stomatal conductance can help reveal otherwise hidden processes. Simple regression- and observation-based approaches only indirectly allowed the conclusions here drawn from a leaf-level analysis of drivers for the biosphere-atmosphere exchange of NH_3 at the Bourtanger Moor field site (Zöll et al., 2016). Yet, this case study is merely one example of how CO_2 flux data-based estimates of stomatal conductance can be used to improve our understanding of NH_3 biosphere-atmosphere exchange. There is great potential in improving the predictive power of inferential models, both on the field-scale, as well as in spatially explicit modelling studies, and global change projections, by linking NH_3 and CO_2 models at this shared pathway using well-known and easy-to-implement modelling tools. Potential applications include, but are certainly not limited to:

- Using CO_2-derived stomatal conductances in a model-driven flux data analysis workflow to interpret direct flux measurements of NH_3 (as demonstrated in the case study).
- Coupling an NH_3 inferential and a photosynthesis model and using measured CO_2 data to validate the latter. This has recently been demonstrated in an NH_3 flux-partitioning study with the SURFATM-NH_3 model (Personne et al., 2009) by Hansen et al. (2017).
- Improving the predictive capabilities for global change projections from large-scale CTMs by joining CO_2, NH_3, and potentially other compounds' exchange sub-modules, e.g. following the example of Anav et al. (2012) for O_3, as recognised by Flechard et al. (2013).

- Retrofitting existing flux tower networks such as ICOS with low-cost, low-labour NH_3 measurements (e.g. with passive samplers). Models for the non-stomatal pathway may be calibrated on short-term measurements of nighttime NH_3 fluxes acquired with a roving system, and using correction factors accounting for the lowered temporal resolution compared to fast-response analysers (Schrader et al., 2018). The stomatal pathway can be modelled by validating (or calibrating) a coupled photosynthesis-stomatal conductance model (e.g., Collatz et al., 1991) on the existing CO_2 measurements, giving a continuous dataset of stomatal conductance independent of data gaps in the CO_2 eddy-covariance setups.

To achieve optimal suitability for local air quality and global change studies alike, future research should strive towards a more mechanistic representation of all biosphere-atmosphere exchange pathways. Long-term simultaneous micrometeorological measurements of both greenhouse-gas and reactive nitrogen exchange across a wide range of ecosystems are desperately needed to further develop valid frameworks for modelling interrelations between them, and to accurately identify areas where action is necessary to mitigate negative effects of excess nitrogen deposition.

ACKNOWLEDGEMENTS

F.S. and C.B. greatly acknowledge financial support by the German Federal Ministry of Education and Research (BMBF) within the Junior Research Group NITROSPHERE under support code FKZ 01LN1308A and the German Environmental Protection Agency (UBA) under grant no. FKZ 3715512110. We highly appreciate technical assistance in the field by Jeremy Rüffer and Jean-Pierre Delorme from Thünen Institute. Finally, we would like to acknowledge Undine Zöll and Miriam Hurkuck, who conducted the measurements at the Bourtanger Moor site.

5

TEMPORAL RESOLUTION ISSUES

I have approximate answers, and possible beliefs, and different degrees of certainty about different things, but I'm not absolutely sure of anything.

— Richard P. Feynman

This chapter is published as: *Schrader, F., et al. (2018). The hidden cost of using low-resolution concentration data in the estimation of NH_3 dry deposition fluxes. Scientific Reports, 8(1), 969.*

ABSTRACT

Long-term monitoring stations for atmospheric pollutants are often equipped with low-resolution concentration samplers. In this study, we analyse the errors associated with using monthly average ammonia concentrations as input variables for bidirectional biosphere-atmosphere exchange models, which are commonly used to estimate dry deposition fluxes. Previous studies often failed to account for a potential correlation between ammonia exchange velocities and ambient concentrations. We formally derive the exact magnitude of these errors from statistical considerations and propose a correction scheme based on parallel measurements using high-frequency analysers. In case studies using both modelled and measured ammonia concentrations and micrometeorological drivers from sites with varying pollution levels, we were able to substantially reduce bias in the predicted ammonia fluxes. Neglecting to account for these errors can, in some cases, lead to significantly biased deposition estimates compared to using high-frequency instrumentation or corrected averaging strategies. Our study presents a first step towards a unified correction scheme for data from nation-wide air pollutant monitoring networks to be used in chemical transport and air quality models.

5.1 INTRODUCTION

Gaseous ammonia (NH_3) plays an important role in the atmosphere as part of the natural and anthropogenic N cycle and contributes to a number of adverse effects on the environment and public health (Erisman et al., 2013). Recent developments allow the direct quantification of NH_3 dry deposition and emission fluxes via the eddy-covariance method (Famulari et al., 2004; Ferrara et al., 2012; Zöll et al., 2016); however, the necessary instrumentation is costly, long-term continuous studies are yet to be published, and the method is not trivially applicable in every environment. Alternative methods, such as the aerodynamic gradient technique, are even more labour-intensive, usually require expensive wet-chemical analyses, and are prone to errors in non-ideal conditions (Sutton et al., 2007).

A cost- and labour-efficient alternative to flux measurements is the use of so-called dry deposition inferential models. If they are properly validated against flux measurements in different ecosystems, they can be applied for regional estimates of NH_3 dry deposition using only concentration measurements and a small number of (micro-)meteorological variables as input data (Flechard et al., 2013; Massad et al., 2010a; Wichink Kruit et al., 2010; Zhang et al., 2003, 2010). These models are usually ran on a 30 minute basis, in accordance with the typical temporal resolution of flux measurements, or on an hourly basis within some large-scale chemistry transport models (CTM), such as LOTOS-EUROS (Schaap et al., 2008; Wichink Kruit et al., 2012). However, in national monitoring networks, such as the Measuring Ammonia in Nature (MAN) network in the Netherlands (Lolkema et al., 2015), often passive samplers or denuders (e.g. DELTA; Sutton et al., 2001, or KAPS; Hurkuck et al., 2014; Peake and Legge, 1987) are used to measure ambient NH_3 concentrations, which typically only yield a temporal resolution of monthly averages. The impact of using such low-resolution concentration measurements as input data for bidirectional NH_3 dry deposition inferential models has, to our knowledge, not been thoroughly investigated in the published literature, although they have regularly been used from local studies (Shen et al., 2016; Walker et al., 2008) to integrated projects (Flechard et al., 2011). In order to systemat-

ically assess potential bias introduced by using low-resolution concentration data, we exemplarily analysed a 1 year gap-free record of ambient NH_3 concentrations predicted by the CTM LOTOS-EUROS in conjunction with ECMWF (European Centre for Medium-Range Weather Forecasts) meteorology as input data for an independent dry deposition inferential model by Massad et al. (2010a), as well as preliminary NH_3 concentration measurements using quantum cascade laser (QCL) spectroscopy at a remote site in Germany. We investigated the potential magnitude of errors introduced by using low-resolution concentration measurements and formally derived the fundamental equations necessary for the development of correction schemes. Our study lays the groundwork for the characterisation of errors and estimation of site-specific correction functions when using NH_3 dry deposition models with low-resolution input data.

5.2 METHODS

5.2.1 *Dry deposition inferential modelling*

Dry deposition of NH_3 is most commonly modelled using parameterisations of a big-leaf canopy compensation point model, or a two-layer variant thereof when exchange with the soil- or litter-layer is expected to be significant and can be parameterised within reasonable margins of uncertainty (Flechard et al., 2013; Massad et al., 2010a; Nemitz et al., 2001). We here use the parameterisation of Massad et al. (2010a) in a one-layer configuration to ensure independence from the dry deposition module (DEPAC within LOTOS-EUROS) involved in the generation of the synthetic data. In this model, the flux density of NH_3 is predicted from the difference of the measured air NH_3 concentration χ_a ($\mu g\,m^{-3}$) at the aerodynamic reference height $z - d$ (m) and the (modelled) canopy compensation point concentration, χ_c ($\mu g\,m^{-3}$) (Figure 5.1). The sign of this difference governs the direction of the flux ($\chi_a > \chi_c$ leads to a deposition flux, with a negative sign by convention, and $\chi_a < \chi_c$ leads to an emission flux). Furthermore, the magnitude of the predicted flux density is controlled by the magnitude (i) of $\chi_a - \chi_c$, and (ii) of a number of resistances towards deposition. Within this framework, the total net

biosphere-atmosphere exchange flux of NH_3, F ($\mu g\,m^{-2}\,s^{-1}$), is typically given as

$$F = -\frac{\chi_a - \chi_c}{R_a + R_b}, \tag{5.1}$$

where R_a ($s\,m^{-1}$) and R_b ($s\,m^{-1}$) are the aerodynamic and quasi-laminar boundary layer resistance, respectively, and are here modelled as described in detail by Massad et al. (2010a). Instead of calculating the canopy compensation point (which is a function of both stomatal and cuticular resistance and, if applicable, their respective compensation points, and the air NH_3 concentration), we can simplify the model scheme to strictly consist of serial resistances only (Figure 5.1b). The effective *foliar compensation point*, χ_f ($\mu g\,m^{-3}$), is then given as a weighted average of both leaf-layer pathways via

$$\chi_f = \frac{R_f}{R_w} \cdot \chi_w + \frac{R_f}{R_s} \cdot \chi_s, \tag{5.2}$$

where χ_w ($\mu g\,m^{-3}$) and χ_s ($\mu g\,m^{-3}$) are the cuticular and stomatal compensation point, respectively, R_w ($s\,m^{-1}$) is the cuticular resistance, parameterised after Massad et al. (2010a), and R_s ($s\,m^{-1}$) the stomatal resistance after Emberson et al. (2000). In the Massad et al. (2010a) parameterisation, χ_w is zero (i.e., only deposition to the cuticula is possible). R_f ($s\,m^{-1}$) is the *foliar resistance*, similar to the notation of Wichink Kruit et al. (2010), and is given as

$$R_f = \left(R_w^{-1} + R_s^{-1}\right)^{-1}. \tag{5.3}$$

To further simplify the calculations, we define an exchange velocity, v_{ex} ($m\,s^{-1}$), as the inverse of the total resistance to NH_3 exchange:

$$v_{ex} = \left(R_a + R_b + R_f\right)^{-1}. \tag{5.4}$$

Note that R_f is not necessarily equal to the so-called canopy resistance, which is usually only used in unidirectional (deposition-only) models (i.e., they are only equal when χ_f is zero). Similarly, v_{ex} is not equal to the common concept of a deposition velocity, in which R_f is replaced by the canopy resistance and which is not used in conjunction with a compensation point.

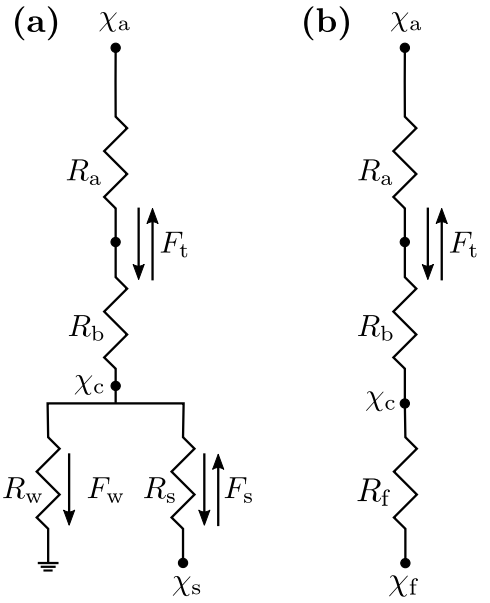

Figure 5.1: (a) Common structure of a bidirectional one-layer canopy compensation point model for biosphere-atmosphere exchange of NH_3. (b) Simplification of (a) to a serial resistance structure.

Given these definitions, the net NH_3 exchange flux can also be written as

$$\begin{aligned} F &= -v_{ex} \cdot (\chi_a - \chi_f) \\ &= \quad v_{ex} \cdot (\chi_f - \chi_a)\,, \end{aligned} \tag{5.5}$$

where a positive flux indicates emission and a negative flux indicates deposition.

5.2.2 *Flux prediction strategies for low-resolution input concentrations*

High-frequency concentration measurements are often cost- and labour-intensive, and usually not available within nationwide long-term monitoring networks. A number of different variants to predict long-term average or cumulative flux densities from low-frequency concentration measurements can be found in the literature (Andersen et al., 1999; Cape et al., 2004; Duyzer et al., 2001; Flechard et al., 2011; Poor et al., 2006; Rihm and Kurz, 2001;

Schmitt et al., 2005; Walker et al., 2008; Yang et al., 2010). We here discuss the case of monthly averages, which are a common outcome of passive sampler or denuder measurements, but the calculations remain the same for any other kind of averaging period. A sensitivity study for other averaging periods is given in the Supplementary Material.

Consider the case of (i) (micro-)meteorological input data available at a sampling frequency the model is usually run at, e.g. 1 hour in our sample datasets, and (ii) ambient NH_3 concentrations available at a lower sampling frequency, e.g. 1 month. We further assume that, from these data, reasonable flux predictions can only be made at the lowest available time scale, i.e. 1 month in this example. However, the model should still be run at a higher resolution in order to incorporate the effects of diurnal variations and day-to-day variability in meteorological conditions. There are generally two straightforward strategies to predict monthly averaged NH_3 fluxes under these conditions, the first being:

$$\bar{F} = \overline{v_{ex} \cdot (\chi_f - \overline{\chi_a})}. \tag{5.6}$$

Here, an overbar $\bar{x}$ denotes the arithmetic mean of some random variable x, and a prime x' denotes the instantaneous deviation from $\bar{x}$, i.e. $x = \bar{x} + x'$, similar to the notation commonly employed by the micrometeorological community. Consequently, equation (5.6) means that the model is run on an hourly basis with hourly meteorological input data, and the measured monthly average NH_3 concentration is used as a substitute for hourly concentration values. In other words, it is assumed that the monthly average NH_3 concentration is representative for hourly values and that internal mechanics of the model (such as the exponentially temperature dependent conversion of emission potentials to compensation points; Nemitz et al., 2001) effectively compensate the effect of the lowered input data resolution.

An alternative strategy would be to first calculate the exchange velocity and the compensation points at a high resolution (given that they are independent of χ_a), average them, and then calculate the monthly average flux from the monthly average of all other variables:

$$\bar{F} = \overline{v_{ex}} \cdot (\overline{\chi_f} - \overline{\chi_a}) \tag{5.7}$$

We will outline in the following section why both of these variants (equations (5.6) and (5.7)) will inevitably lead to biased results.

5.2.3 *Derivation of the error term*

A well-understood, but still often ignored fallacy is the assumption that the product of averages yields similar results to the average of products (Welsh et al., 1988). However, this is generally only the case when all variables involved are completely independent and uncorrelated. Even if not all of these variables are formally linked within the governing equations of a dry deposition model, they may be correlated through their inherent dependence on external environmental factors (e.g. temperature, radiation, or turbulence). Meyers and Yuen (1987) were among the first to observe the impacts of ignoring this fallacy with regards to (unidirectional) inferential modelling of SO_2 and O_3 fluxes. For a bidirectional NH_3 exchange scheme, the true mean flux over a certain period of time can be written as:

$$\begin{aligned} \bar{F} &= \overline{v_{\mathrm{ex}} \cdot (\chi_{\mathrm{f}} - \chi_{\mathrm{a}})} \\ &\neq \overline{v_{\mathrm{ex}}} \cdot (\overline{\chi_{\mathrm{f}}} - \overline{\chi_{\mathrm{a}}}) \,. \end{aligned} \tag{5.8}$$

Recall our definition of $\bar{x}$ and x', from which it follows that x'^2 is equal to the (non Bessel-corrected) variance of x, and $\overline{x' \cdot y'}$ to the covariance of two random variables x and y. With these additional definitions, we can calculate the true average flux from long-term average NH_3 concentrations using the linearity of expected values and the definition of the covariance, as follows:

$$\begin{aligned} \bar{F} &= \overline{v_{\mathrm{ex}} \cdot (\chi_{\mathrm{f}} - \chi_{\mathrm{a}})} \\ &= \overline{v_{\mathrm{ex}} \cdot \chi_{\mathrm{f}}} - \overline{v_{\mathrm{ex}} \cdot \chi_{\mathrm{a}}} \\ &= \overline{v_{\mathrm{ex}}} \cdot \overline{\chi_{\mathrm{f}}} + \overline{v_{\mathrm{ex}}' \cdot \chi_{\mathrm{f}}'} - \left(\overline{v_{\mathrm{ex}}} \cdot \overline{\chi_{\mathrm{a}}} + \overline{v_{\mathrm{ex}}' \cdot \chi_{\mathrm{a}}'}\right) \\ &= \overline{v_{\mathrm{ex}}} \cdot (\overline{\chi_{\mathrm{f}}} - \overline{\chi_{\mathrm{a}}}) + \overline{v_{\mathrm{ex}}' \cdot \chi_{\mathrm{f}}'} - \overline{v_{\mathrm{ex}}' \cdot \chi_{\mathrm{a}}'}. \end{aligned} \tag{5.9}$$

The difference between equation (5.7) and the last line of equation (5.9), i.e., the two covariance terms $\overline{v_{\mathrm{ex}}' \cdot \chi_{\mathrm{f}}'} - \overline{v_{\mathrm{ex}}' \cdot \chi_{\mathrm{a}}'}$ ($\mu g\, m^{-2}\, s^{-1}$), is equal to the exact error introduced when calculating average NH_3 fluxes from average exchange velocities and measured long-term average concentration measurements. When

directly calculating hourly fluxes with the long-term average NH_3 concentrations used as a substitute for hourly values and averaging afterwards (i.e., using equation (5.6)), the error is equal to $-\overline{v_{ex}{}' \cdot \chi_a{}'}$ ($\mu g\, m^{-2}\, s^{-1}$).

5.2.4 *A first step towards bias elimination*

If we run a dry deposition inferential model with only the ambient NH_3 concentration as a long-term average and all other driving variables measured at a higher temporal resolution, as is usually the case for monitoring stations, where the measurement of meteorological variables at a high temporal resolution is not very difficult, only the last term of equation (5.9), i.e. the covariance of v_{ex} and χ_a, is unknown. We can expand it to take the form

$$\overline{v_{ex}{}' \cdot \chi_a{}'} = \sqrt{\overline{v_{ex}{}'^2}} \cdot \sqrt{\overline{\chi_a{}'^2}} \cdot \frac{\overline{v_{ex}{}' \cdot \chi_a{}'}}{\sqrt{\overline{v_{ex}{}'^2}} \cdot \sqrt{\overline{\chi_a{}'^2}}}. \tag{5.10}$$

Note that here $\sqrt{\overline{v_{ex}{}'^2}} = \sigma_{v_{ex}}$ ($m\, s^{-1}$) and $\sqrt{\overline{\chi_a{}'^2}} = \sigma_{\chi_a}$ ($\mu g\, m^{-3}$) are identical to the empirical standard deviation of v_{ex} and χ_a, respectively, and $\overline{v_{ex}{}' \cdot \chi_a{}'} \cdot \left(\sqrt{\overline{v_{ex}{}'^2}} \cdot \sqrt{\overline{\chi_a{}'^2}} \right)^{-1} = r_{v_{ex},\chi_a}$ ($-$) is equal to the Pearson product-moment correlation of the two. Again, $\sigma_{v_{ex}}$ is known and can trivially be calculated from higher-resolution modelled estimates of v_{ex}. However, σ_{χ_a} and r_{v_{ex},χ_a} remain unknown at this point.

A simple approach to calculate less-biased fluxes from low-resolution concentration measurements could be based on accompanying high-resolution concentration measurements at the same site for a limited amount of time. E.g., one would use a single high-frequency (0.5 to 1 hour sampling rate) NH_3 monitor to take parallel measurements at a monitoring site for a few months to gather the necessary data to derive correction factors, and then move the instrument to the next site. We can assume an increase of the variation in air NH_3 concentrations with rising concentration levels, i.e. increasing σ_{χ_a}, with increasing mean $\overline{\chi_a}$, since (i) chemical measurement instruments often exhibit relative errors, and (ii) it is reasonable to suspect that, for instance,

emissions from nearby sources would not only lead to a steady increase of the mean NH_3 concentration, but also to a higher variability, depending on turbulent mixing, wind direction, and other factors. The most simple approach is to model this with a linear relationship:

$$\hat{\sigma}_{\chi_a}(\overline{\chi_a}) = m_0 \cdot \overline{\chi_a} + b_0, \tag{5.11}$$

where m_0 $(-)$ and b_0 $(\mu g\, m^{-3})$ are the slope and intercept of the resulting regression line, respectively.

Modelling the correlation between the exchange velocity and the air NH_3 concentration, r_{v_{ex},χ_a}, is substantially less straightforward. A o^{th}-order approach would consist of simply taking the mean correlation over the measurement period used for deriving correction functions. However, this would eliminate the possibility of registering potential seasonality in r_{v_{ex},χ_a}, and the next most simple alternative, a linear regression of r_{v_{ex},χ_a} against some environmental variable, would yield practically the same results if the slope of the regression is close to zero, leaving little reason not to favour at least a simple linear regression over the mean. Unfortunately, the choice of a suitable explanatory variable is far from trivial, as we essentially look for a correlation of a correlation, which is a somewhat ill-defined and difficult to understand concept. We will here exemplarily perform a linear regression against temperature, assuming that with rising temperature (as a measure for the energy content of the system), both volatilisation of NH_3 and buoyancy will increase and the correlation between the two might become stronger. However, this is merely an educated guess and not bound to be the most suitable model, nor is temperature guaranteed the most suitable regressor. In fact, we suspect that especially at remote sites with little to no diurnal variation in air NH_3 concentrations, but pronounced variation in v_{ex} (which is strongly linked to atmospheric turbulence), most variables with a strong diurnal cycle would work similarly well as a predictor for r_{v_{ex},χ_a}. The model is given as:

$$\hat{r}_{v_{ex},\chi_a}(\overline{T}) = m_1 \cdot \overline{T} + b_1, \tag{5.12}$$

with the slope m_1 $(-)$ and intercept b_1 $(-)$. Equation (5.9) then becomes:

$$\overline{F} = \overline{v_{ex}} \cdot (\overline{\chi_f} - \overline{\chi_a}) + \overline{v_{ex}' \cdot \chi_f'} - \sigma_{v_{ex}} \cdot \hat{\sigma}_{\chi_a}(\overline{\chi_a}) \cdot \hat{r}_{v_{ex},\chi_a}(\overline{T}). \tag{5.13}$$

5.2.5 *Comparison of flux prediction strategies*

A 12-month gap-free set of *synthetic* input data was generated by running the Eulerian grid model LOTOS-EUROS (Hendriks et al., 2016) in conjunction with ECMWF meteorology for the year 2016. Through a one-way nesting procedure a simulation over Germany was performed on a resolution of 0.125° longitude by 0.0625° latitude, approximately 7 by 7 km². The high resolution domain is nested in a European domain with a resolution of 0.5° longitude by 0.25° latitude, approximately 28 by 28 km². Emissions include the TNO MACC-III European emission inventory for the year 2014. For Germany, the national emission inventory of the German Environmental Protection Agency (UBA) was used to prescribe the gridded emissions. LOTOS-EUROS is one of the few CTMs that include SO_2-NH_3 co-deposition and bidirectional surface-atmosphere exchange of NH_3 (Wichink Kruit et al., 2017, 2012).

We here used data from one grid cell in the Allgäu region in southern Germany (47°41′34.80″ N, 10°2′6.00″ E) (Figure 5.2a). Average temperature during the year of 2016 was 8.1 °C, total precipitation 1690 mm, and the average NH_3 concentration was 5.6 µg m^{-3} (highest hourly means up to 60.6 µg m^{-3}) at an (aerodynamic) reference height of 2.5 m above zero-plane displacement. The annual course of the leaf area index was modelled as implemented in the DEPAC deposition module within LOTOS-EUROS (Emberson et al., 2000; Wichink Kruit et al., 2012). We here exemplarily used land-use parameters for grassy semi-natural vegetation; results for other land-use classes can be found in Figure C.1 of the Supplementary Material.

Additionally, we tested the correction scheme for measured data from a flux tower in the Bavarian Forest in Germany (Figure 5.2b) at 807 m a.s.l. (base of the tower), 48°56′50.27″ N, 13°25′12.22″ E (Beudert and Gietl, 2015). NH_3 concentrations were measured using a QCL absorption spectrometer from Aerodyne Research Inc., Billerica, MA, USA (cf. Zöll et al. (2016) for a detailed instrument description) at 31 m above ground level, and with an original sampling rate of 10 Hz averaged to 1 concentration value per hour. Turbulence measurements were taken with a sonic anemometer (model R3, Gill Instruments Ltd., Lyming-

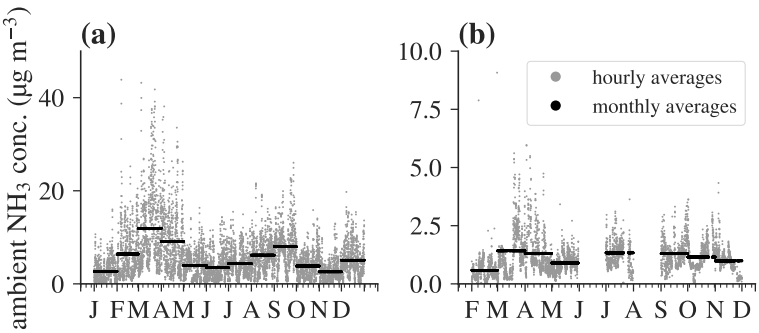

Figure 5.2: Hourly and monthly averaged air NH_3 concentrations for the year 2016 of (a) synthetic data predicted from LOTOS-EUROS for one grid cell in the Allgäu region in Germany and (b) measured data from a flux tower in the Bavarian Forest.

ton, UK) at the same height, as well as temperature and relative humidity using HC2S3 probes (Campbell Scientific, Inc., Logan, UT, USA). Leaf area index and canopy height were not measured at the site and parameterised as proposed in Massad et al. (2010a). Annual average temperature at the site was 7.4 °C, total precipitation was 1047 mm, and the average of NH_3 concentrations used in this study (approximately 56 % data coverage of the year) was 1.1 µg m^{-3} (maximum 14.5 µg m^{-3}). Measured ambient NH_3 concentrations at this site are preliminary, but have undergone common quality procedures, such as despiking, and system performance tests with regard to flow rate, temperature, and pressure stability. These data will be published in an ecological context in the near future. The purpose of using this dataset is solely meant for assessing the correction scheme, thus absolute numbers should not be cited for verifying ecosystem-specific thresholds. We also note that we here used the Massad et al. (2010a) parameterisation in its original form, despite the findings of Schrader et al. (2016) regarding a likely too large non-stomatal (cuticular) resistance in this parameterisation. While this leads to relatively low predicted fluxes, the derivation of the error term is unaffected. An additional case study for a moorland site in southern Scotland can be found in Figure C.2 in the Supplementary Material.

The dry deposition inferential model was run for four different scenarios for each site:

1. *control*: all variables at hourly resolution; flux calculation on hourly basis and subsequent averaging to monthly average fluxes (equation (5.8)).
2. *direct*: monthly average NH_3 concentrations and all other variables at hourly resolution; flux calculation on hourly basis with hourly NH_3 concentrations substituted by their monthly averages; subsequent averaging to monthly average fluxes (equation (5.6)).
3. *monthly*: monthly average NH_3 concentrations and all other variables at hourly resolution; calculation of exchange velocities and foliar compensation points on hourly basis; subsequent averaging to monthly average exchange velocities and foliar compensation points, and calculation of monthly fluxes via equation (5.7).
4. *corrected*: same as *monthly*, but with added correction terms from equations (5.11)–(5.13).

Note that *corrected* can also be written as equal to *direct* plus only the correction term for the covariance of v_{ex} and χ_a. Monthly deposition fluxes for months with gaps in the measured dataset were calculated by multiplying the arithmetic mean flux density of a given month with the number of data points at 100 % coverage (assuming no bias of the gaps towards a certain time of the day).

CODE AND DATA AVAILABILITY Synthetic data are available at reasonable request from M. Schaap. Measured data will be published separately after final analysis. A Python 2.7 implementation of the Massad et al. (2010a) parameterisation can be requested from the lead author. An open source version of LOTOS-EUROS is publicly available.

5.3 RESULTS AND DISCUSSION

Figure 5.3a–b exemplarily shows the results of the comparison between the different averaging strategies for the synthetic data-

set, using the parameterisation of the dry deposition model for semi-natural ecosystems. During some months, the relative error reaches over 100 % higher predicted deposition compared to *control* in a given month (e.g., January and April). The lowest error introduced by using uncorrected averaging strategies is in August (54 % for the *direct* variant, and 58 % for the *monthly* variant). Overall, the uncorrected variants overestimate total NH_3 dry deposition for the year 2016 roughly by a factor of two (Table 5.1). There is no clear dependency of the magnitude of the relative error on environmental drivers apparent from our observations; however, the magnitude of the error is naturally strongly linked to r_{v_{ex},χ_a}. Consequently, the performance of a correction scheme is directly proportional to the certainty with which the correlation of the exchange velocity and the air NH_3 concentration can be estimated. It also directly follows from a special case of equation (5.9), when χ_f is assumed to be zero, that the use of average deposition velocities instead of effective deposition velocities in a unidirectional framework is affected by the exact same type of error. In fact, due to the implicit integration of the compensation point in the deposition velocity, the error can be expected to be larger. Similar observations have been made by Matt and Meyers (1993) and Meyers and Yuen (1987) for SO_2 and O_3, in which they attempted to reduce the error by employing day- and night-sampling strategies. The proposed correction approach leads to a strong improvement during all months (Table 5.1, Figure 5.3a–b), especially considering its relative simplicity. These findings are also confirmed by running the model for different synthetic datasets with different land-use types (Table C.1 and Figure C.1 in the Supplementary Material).

For the measured data (Figure 5.3c–d), the picture is somewhat less clear, due to alternating over- and underestimations of averaged predicted deposition with respect to the control. While in some months, uncorrected *direct* or *monthly* flux prediction strategies give the best approximation to flux calculation using high-frequency data (e.g., May or October), the sum of all deviations from *control* is still lowest for the *corrected* variant (Table 5.1). However, the mean absolute deviation from *control* is lowest for the *direct* variant, albeit by a very small margin. Reasons for this less clear performance can be found in the very uncertain

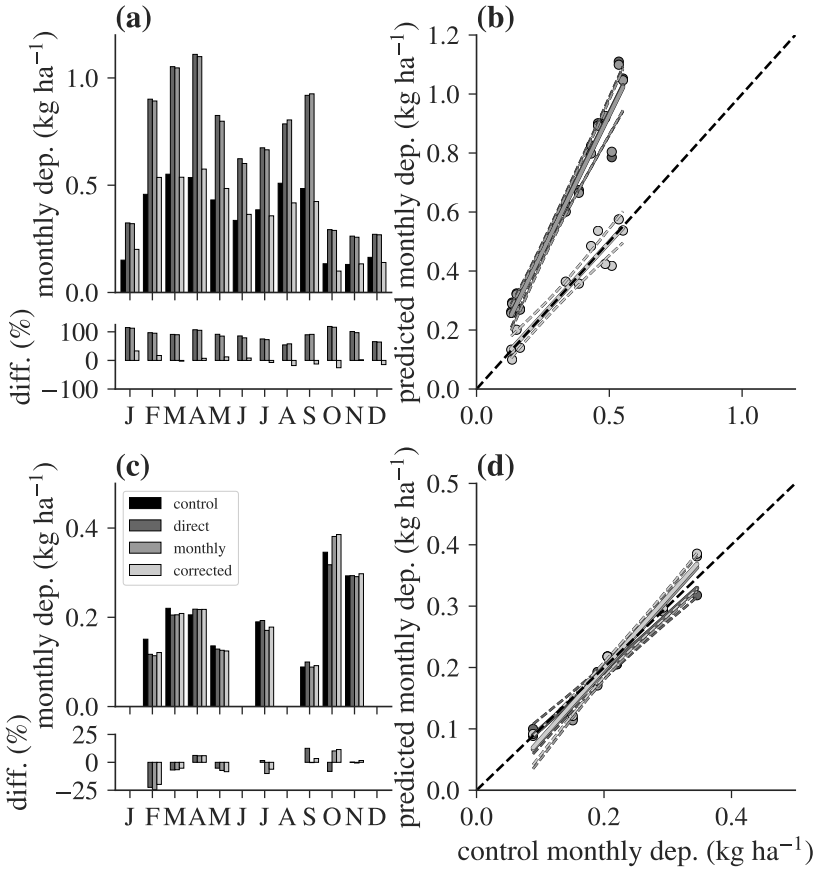

Figure 5.3: (a) Predicted cumulative monthly NH_3 deposition for the four scenarios *control*, *direct*, *monthly*, and *corrected* of the synthetic dataset (see text for description). Differences are given as percent deviation from *control*. (b) Predicted cumulative monthly NH_3 deposition of *direct*, *monthly*, and *corrected* variants against *control*. Dashed lines are 95 % bootstrapped confidence intervals of the regression lines. (c–d) Same as (a–b), but for the measured data. The legend in (c) is valid for all four panels.

Table 5.1: Performance of the different averaging strategies. Coverage: Raw data coverage of the year 2016; ΣF: Sum of all monthly fluxes (positive is deposition); Difference: difference from *control*; MAD: mean absolute monthly differences from *control*.

	SCENARIO	COVERAGE (%)	ΣF (g ha^{-1})	DIFFERENCE (g ha^{-1})	MAD (g ha^{-1})
synthetic	*control*	100	4347.0		
	direct		8126.5	3779.5	315.0
	monthly		8062.1	3715.0	309.6
	corrected		4329.0	−18.0	40.9
measured	*control*	56	1629.6		
	direct		1572.8	−56.8	13.9
	monthly		1594.5	−35.1	16.2
	corrected		1624.7	−4.9	15.5

regression of r_{v_{ex},χ_a} against ambient temperature (Figure 5.4d), leading to all estimates of r_{v_{ex},χ_a} close to its arithmetic mean, although it clearly changes throughout the measurement period. Furthermore, the error introduced by the different averaging strategies is already much lower ($< 25\,\%$) than for the synthetic dataset, which indicates a strong site-specificity of r_{v_{ex},χ_a}. This is supported by the observation that other measured datasets exhibit much larger errors (Figure C.2 in the Supplement).

The higher than observed anticorrelation between NH_3 concentrations and the exchange velocities may be due to the large difference in NH_3 levels between the synthetic and measured dataset (Figure 5.2). Firstly, in source areas primary emissions cause nighttime concentration maxima to occur, whereas exchange rates are highest during late morning hours when PBL growth has diluted the NH_3 concentrations. CTM modelled data from the grid-cell that includes the Bavarian Forest site (grey lines in Figure 5.4d) exhibit a weaker anticorrelation r_{v_{ex},χ_a} than the synthetic dataset from the Allgäu region. LOTOS-EUROS' resolution may explain why it is still somewhat more negative than observed: In each grid cell emissions of NH_3 take place, causing a slight nighttime maximum. In reality, the stagnant conditions do not allow these emissions to reach a hill site such

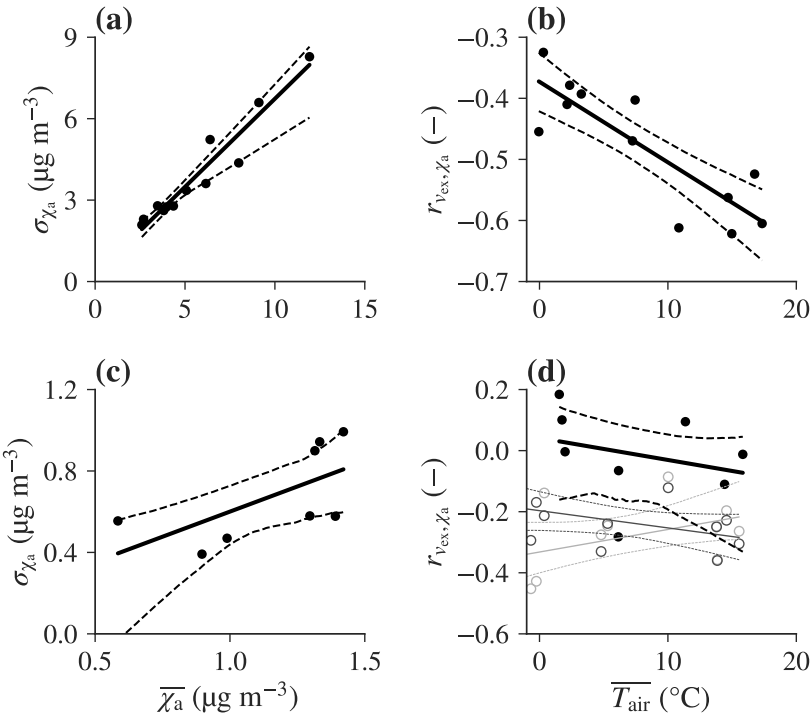

Figure 5.4: Linear regressions as an estimate for (a) the monthly standard deviation of air NH_3 concentrations and (b) the monthly Pearson correlation of exchange velocities and air NH_3 concentrations for the synthetic dataset. (c–d) Same as (a–b), but for the measured data. Grey lines in panel (d) are results for CTM data from the grid cell that includes the Bavarian Forest measurement tower. Light grey is modelled with land-use parameters for a coniferous, dark grey for a deciduous forest.

as the Bavarian Forest measurement tower. Hence, the implicit spatial mixing may explain the stronger anticorrelation found in the measurements.

It is evident from Figure 5.5, that, unfortunately for the purposes of correcting biased monthly flux estimates, the known part of the error term ($\overline{v_{ex}{}' \cdot \chi_f{}'}$) contributes much less to the total error than the unknown part ($-\overline{v_{ex}{}' \cdot \chi_a{}'}$). Consequently, the choice between *direct* and *monthly* flux calculation strategies does not substantially change the magnitude of the error. The assumption of a relative error in measured air NH_3 concentra-

tions appears to be justified from our observations with both modelled and measured concentrations (Fig 5.4a,c.). However, modelling the correlation of the exchange velocity and air NH_3 concentrations remains a challenge, as difficulties in the interpretation lead to difficulties in the conceptualisation of an adequate model for r_{v_{ex},χ_a} (Figure 5.4b,d). Also note that, for NH_3, both deposition, and emission can occur. We make no distinction between the two in our analysis, as all sites show net deposition on the monthly scale and no artificial management events were modelled. Contrary to deposition velocity models, information about the direction of the flux is removed from the exchange velocity by explicitly separating it from the compensation point in the derivations. Equation (5.12) appears to work acceptably well for modelling r_{v_{ex},χ_a} in the synthetic dataset, but not very well for the measured one. A better course of action than the one presented here might, for example, be based on a multivariate regression using more than one environmental driving factor. However, many potential candidate variables are highly correlated, and the number of parameters of such a multivariate model may quickly approach the number of data points, leading to an increased risk of overfitting and questionable predictive value. We have investigated the potential of fitting the correction factors on a smaller timescale than the averaging period, thereby increasing the number of data points for the regression, but this has been rather unsuccessful in terms of reducing uncertainty. With simple regression approaches, an adequate correction function will certainly be site-specific, and it will not be universally valid for different parameterisations of biosphere-atmosphere-exchange schemes. With the increasing availability of optical high-frequency NH_3 measurement instruments, fitting ecosystem-type and environmental condition specific multivariate correction functions, thereby potentially eliminating the need for site-specific parallel measurements, is a promising outlook, but we assume that the number of NH_3 concentration measurements currently available is simply too low for this task. However, truly site-independent correction functions that can be readily applied in existing modelling schemes may not even be possible to derive, as they likely depend on a multitude of factors which are not routinely measured. The relationship between v_{ex} and

χ_a may be vastly different depending on, for example, the N status of the ecosystem of interest, atmospheric composition, and even the measurement period. In agricultural ecosystems, for instance, there are times when the concentration is largely driven by emission fluxes from the surface, and times when the ambient concentration will drive the flux. The same can be the case for forests before and after leaf-fall (Hansen et al., 2017). Further research is necessary to develop an optimal strategy to handle these challenges.

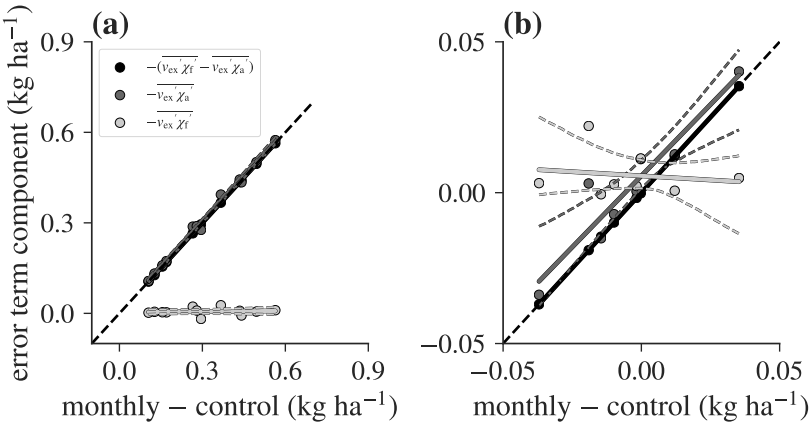

Figure 5.5: Variation of the individual error terms in equation (5.9) with the magnitude of the error for (a) synthetic and (b) measured data. Note that the signs are switched in this graph (deposition is positive) for consistency with Figure 5.3.

Readers should be aware that the observations and derivations made in this study are strictly only valid for a model parameterisation where both v_{ex} and χ_f are not directly dependent on high-frequency observations of the air NH_3 concentration, χ_a, such as the parameterisation of Massad et al. (2010a). For instance, Wichink Kruit et al. (2010) used an air NH_3 concentration dependent formulation for the cuticular compensation point to approximate saturation effects within leaf surface water layers. In this case, it would be advisable to use a corrected formulation based on the *direct* variant, so that one χ_a-dependent covariance in the correction term can be eliminated. Other than that, all derivations demonstrated here remain the same, should be ad-

aptable to other parameterisations and model structures in a straightforward manner, and they are valid for any arbitrary averaging period.

5.4 CONCLUSIONS

We have demonstrated and formally shown that commonly used averaging strategies for the prediction of long-term average fluxes from long-term average measurements of NH_3 concentrations (e.g., from denuder or passive sampler records) and high-frequency micrometeorology are biased. The magnitude and variation of this bias is dependent on the biosphere-atmosphere-exchange scheme used, and measurement site characteristics, such as surface, parameters, pollution level and the distance to NH_3 sources. The magnitude of errors in predicted fluxes introduced by using uncorrected averaging schemes is directly proportional to the (anti-)correlation of NH_3 exchange velocities and ambient concentrations, which is expected to be significant due to saturation effects on wet leaf surfaces (Cape et al., 2008; Jones et al., 2007a; Wentworth et al., 2016), deposition history-dependent compensation points (Massad et al., 2010a; Wichink Kruit et al., 2010), and their inherent dependence on the same environmental variables. Relative errors of up to 100 % deviation from *control* and higher were observed in the synthetic dataset, whereas measured data showed both over- and underestimations of less than 25 % that compensated each other over the course of the measurement period. The proposed correction scheme consists of

1. Measuring time-series of average NH_3 concentrations with low-frequency, low-cost monitoring equipment,

2. Measuring meteorological drivers at a high-frequency with standard instrumentation,

3. Taking parallel measurements with a high-frequency NH_3 monitor for a limited time to parameterise functions to estimate the standard deviation of NH_3 concentrations (equation (5.11)), and the correlation of air NH_3 concentrations with the exchange velocity (equation (5.12)),

4. Calculating corrected monthly average fluxes using equation (5.13).

The results of our first tests appear promising, but uncertainties in estimating aforementioned correlation have to be overcome in the future. In its current state, low-frequency concentration measurements need to be accompanied by high-frequency measurements for a certain (yet to be determined) amount of time to derive valid site-specific correction functions. In-depth model structure analyses and multi-site studies, especially at those with higher NH_3 concentrations and possibly emission fluxes, may give further valuable insight into the exact mechanics behind the dominant source of the error: the correlation of the NH_3 exchange velocities and air NH_3 concentrations.

ACKNOWLEDGEMENTS

F.S., M.S., U.Z., and C.B. greatly acknowledge financial support by the German Environmental Protection Agency (UBA) under grant no. FKZ 3715512110. F.S., U.Z., and C.B. are additionally funded by the German Federal Ministry of Education and Research (BMBF) within the Junior Research Group NITROSPHERE under support code FKZ 01LN1308A. We highly appreciate the contribution of additional data by C.R. Flechard. We would like to thank J. Rüffer, J.-P. Delorme, and M. Lewandowski from Thünen Institute for technical assistance in the field, and we highly acknowledge local support with the flux tower measurements by B. Beudert, W. Breit, and L. Höcker from the Nationalparkverwaltung Bayerischer Wald. Many thanks to J.W. Erisman for helpful comments on the manuscript.

AUTHOR CONTRIBUTIONS STATEMENT

F.S. and C.B. had the idea and designed the study. M.S. and R.K. contributed the synthetic data, U.Z. carried out the measurements. F.S. carried out all analyses and wrote the manuscript with equal contributions from all co-authors.

6

SUMMARY

Knowledge about the process being modelled starts fairly low,
then increases as understanding is obtained,
and tapers off to a high value at the end.

— Harold Chestnut

6.1 KEY FINDINGS

In this thesis, I have explored the state-of-the-art of NH_3 biosphere-atmosphere exchange modelling. I have tried to highlight the key issues that need to be addressed in future developments, and to give recommendations on how to deal with them in the context of plot- and regional-scale inference of NH_3 fluxes from measured or modelled concentrations. In doing so, I have always assumed the perspective of a *practical model developer*, i.e., I have made an effort to find solutions that are ready to be implemented both in an ecosystem-integrated setting, such as micrometeorological monitoring sites, and in large-scale CTMs. This often comes at the cost of sacrificing a fully mechanistic description of all processes; however, suitable, science-based, steady-state approximations to complex and dynamic NH_3 exchange processes are something we desparately need to address the challenges that we are facing. That is, to identify key areas that are in need of immediate action to preserve our few remaining natural ecosystems; to create nation-wide and even global budgets of N_r emission, transport, and deposition; to back up our predictions with observational evidence and work hand in hand with the people who run representative monitoring efforts; and to clearly communicate the shortcomings of our current tools and the need for further research.

6.1.1 *Deposition velocities*

In Chapter 2, I have compiled a database of recent measurements and modelled estimates of the NH_3 deposition velocity. While the general idea of using a single deposition velocity per land-use class and over large periods of time is an inherently unsatisfying concept for process modellers, I have come to learn and experience first-hand that it is indeed still being widely used nowadays. This is especially the case in regulatory processes, where consultants and government agents alike need easy-to-understand and easy-to-use tools that leave little to no room for interpretation in their application. Using approaches that represent the scientific state-of-the-art, no matter how simple from a researcher's point of view, may already be so complex that they would indubitably lead to legal battles about operator bias. To quote the great mathematician John von Neumann: *With four parameters I can fit an elephant, and with five I can make him wiggle his trunk.* From the experience I have gathered in the past five years, it seems to me that this is also more often than not the case for modelling biosphere-atmosphere exchange of N_r compounds, where there is a plethora of different tools for the same purpose, which not all necessarily arrive at similar answers.

That being said, it is our responsibility as researchers to provide policy with the necessary tools to do their jobs, while being as objective as possible at this task. In Schrader and Brümmer (2014) we have made an attempt at doing so, by weighting results from a literature research based on an assessment of their validity and reliability. All the necessary tools to modify this weighting scheme, be they due to a disagreement with our weighting choices, or for specific applications, have been made publicly available. Key results found in this study reflect the overall expectation regarding the order of magnitude of deposition velocities for certain ecosystems, as well as their variability. Ecosystems with large receptor areas, such as coniferous or mixed forests, were found to show the highest deposition velocities, and agricultural areas, while having the lowest median deposition velocity, likely due to N saturation and thus large emission potentials, are overall very variable. Weighted average and median deposition velocities were 2.2 and 2.1 $cm\,s^{-1}$ for coniferous forests, 1.5 and 1.2 $cm\,s^{-1}$

for mixed forests, 1.1 and 0.9 $cm\,s^{-1}$ for deciduous forests, 0.9 and 0.7 $cm\,s^{-1}$ for semi-natural sites, 0.7 and 0.8 $cm\,s^{-1}$ for urban sites, 0.7 and 0.6 $cm\,s^{-1}$ for water surfaces, and 1.0 and 0.4 $cm\,s^{-1}$ for agricultural sites, respectively.

Results of this study have since been used by numerous other researchers as a plausibility check for their experimental measurements and monitoring efforts (Adon et al., 2018; Häni et al., 2018; Hunova et al., 2016; Johnson et al., 2016; Thimonier et al., 2019; van der Graaf et al., 2018). Originally, this study emerged from the need for an update to the in Germany widely used tabulated deposition velocities by VDI (2006), and it was funded for that purpose (Schrader and Brümmer, 2013); however, it should be noted that at the time of writing this thesis, a task force responsible for updating the industry standard described in VDI (2006) is in the processes of exploring options for a simplified resistance model to be used in regulatory processes in the future instead.

6.1.2 *Non-stomatal exchange*

While Chapter 2 was the result of my first steps into the field of NH_3 research, Chapter 3 emerged from a deeper dive into the intricacies of modelling biosphere-atmosphere exchange of trace gases. Starting with the parameterisation of a two-layer canopy compensation point model (Nemitz et al., 2001) after Massad et al. (2010a), I noticed consistently low predicted non-stomatal deposition fluxes even at very humid measurement sites. A deeper investigation of the reasons for this revealed that this was very likely due to a too high minimum non-stomatal resistance prescribed in the parameterisation, especially at sites with large average acid-to-NH_3 ratios in the ambient air (Schrader et al., 2016). Observed average acid-to-NH_3 ratios ranged from 0.1 to 0.7 at the sites analysed in our study, leading to minimum non-stomatal resistance values at 100 % relative humidity between 45 to 315 $s\,m^{-1}$ before further corrections – considerably larger than values found in a meta-analysis by Massad et al. (2010a). This was further amplified by a too strong temperature response parameter in an empirical correction that essentially accounts for an increasing compensation point with rising temperatures, even

though this pathway is modelled unidirectionally in Massad et al. (2010a)

At the same time, I looked at alternatives for modelling exchange with non-stomatal surfaces, and I was intrigued by the ideas of Wichink Kruit et al. (2010). They have recognised the modeller's dilemma of having to find static approximations for processes that we know very well are dynamic in nature (Wentworth et al., 2016). While very sophisticated models exist that have been shown to successfully simulate phenomena such as early morning emission of NH_3 from leaf surfaces (Flechard et al., 1999; Sutton et al., 1998), they have not found widespread application in regional modelling due to limits in computational power for sub-grid processes and specific requirements about their input data. Wichink Kruit et al. (2010) attempted to solve these problems with the introduction and empirical parameterisation of a non-stomatal compensation point that does not require dynamically solving model equations at small time-steps. However, comparing this model to observational data I noticed a tendency to overestimate deposition under certain circumstances only. Their best parameterisation for the non-stomatal (and stomatal) emission potential included an instantaneous temperature response, accounting for seasonality in the emission potentials, which acts in the opposite direction of the temperature response that converts emission potentials into compensation point concentrations. This conversion is based on solubility and dissociation equilibria and can under some circumstances be considerably weaker than the seasonality function in the Wichink Kruit et al. (2010) model. In fact, as outlined in section 3.2.3, the equilibrium reaction temperature response may be completely countered by the seasonality response when temperatures increase. Consequently, under very warm conditions, when one would generally expect stronger volatilisation of NH_3 and thus a larger compensation point, it can actually fall to zero.

Comparing the two models against each other, as well as against micrometeorological measurement, led to an admittedly somewhat vague answer to the question which of the two parameterisations performs better in practice: *It depends.* The key lesson to learn from this observation is that there is, in fact, still a lot to do in terms of parameterising even these fairly simple

models, and that we should work towards a consensus on an appropriate framework to do so. The widely used unidirectional approach may work well in practice and be better validated on long-term budgets, but on finer temporal scales the approach of Wichink Kruit et al. (2010) allows for more realistic predicted fluxes and meaningful parameters, given that it will be updated with some modifications in the future, such as a delayed temperature response accounting for seasonality in the emission potential parameterisations.

6.1.3 *Stomatal exchange*

In Chapter 4 – part opinion piece, part case study – I describe first results on the way to a more mechanistic inter-compound coupling in biosphere-atmosphere exchange modelling. The desire to work towards such coupled models emerged from the goals of the junior research group I started my work in, called NITROSPHERE, in which we aimed to shine light on the interactions between N_r deposition and greenhouse gas exchange using both novel measurement techniques and biosphere-atmosphere exchange models. With regards to the modelling part, I found that there is relatively little overlap between those communities who model CO_2 exchange, and those who model NH_3 exchange. This came as a surprise, since they are fundamentally linked through a shared exchange pathway, as well as possible effects of acidity / alkalinity that are yet to be researched. Furthermore, many CTMs do model CO_2 exchange, albeit independent from other trace gases, and many, if not most sites at which NH_3 flux measurements are being made are already equipped with CO_2 flux measurement instrumentation.

In Schrader et al. (in preparation) we argue there are many potential benefits from modelling NH_3 and CO_2 exchange in a coupled manner, i.e., by linking them through the stomatal conductance via the well-known and well-understood model of Ball et al. (1987). This may be done in a number of different ways, e.g. either by directly inferring stomatal conductance from measured fluxes of CO_2, or by modelling photosynthesis and ecosystem respiration, validating them on measured CO_2 net ecosystem exchange, and deriving a gap- and noise-free dataset

of stomatal conductance from modelled photosynthesis. This is useful for both the modelling and measurement community: By deriving stomatal conductance directly from CO_2 fluxes, models gain the ability of directly reacting to rising atmospheric CO_2 concentrations and the assosciated effects on stomatal opening (Ainsworth and Rogers, 2007). The monitoring community can benefit from having valid, data-driven and site-specific estimates of the stomatal conductance instead of generalised *one-size-fits-all* empirical parameterisations for few ecosystem types, that in addition often require potentially unavailable ancillary data and / or complex sub-models that are prone to errors in their implementation. Finally, we demonstrated the advantages for the experimentalist through an increased confidence in the validity of NH_3 flux partitioning via resistance models on a case study using eddy-covariance measurements.

6.1.4 *Temporal resolution*

The question of *mean* versus *effective* deposition velocities, i.e., the difference between the mean of the flux divided by the concentration and the mean flux divided by the mean concentration, was the topic of conversations with many different colleagues throughout my academic journey. It was always clear, both numerically and logically, that they cannot be the same, but at the same time, it was almost never discussed in the literature. In fact, as the reader may have noticed, I was not fully aware myself of the full scope of this issue at the time of publishing Schrader and Brümmer (2013, 2014) / Chapter 2 in this thesis, although it should be noted that in the vast majority of studies that went into our results only one of the two was mentioned anyway. I therefore worked on trying to quantify, and later correct for it, not only with focus on deposition velocities, but especially on bidirectional models with low-resolution concentration measurements as input data – which would need an *effective* modelled exchange velocity, but have usually been applied with *mean* exchange velocities in the literature available at the time of writing.

Eventually, I found that the magnitude of the error can be quantified precisely: It directly depends on the correlation of ambient concentrations and the NH_3 exchange velocity, which, unfortu-

nately, is unknown when working with low-resolution concentration measurements. However, as demonstrated in Chapter 5 / Schrader et al. (2018), site-specific correction functions can be calibrated on temporary parallel measurements, and they allow for a remarkable reduction of bias in long-term NH_3 deposition budgets (e.g., from 86 % to less than 1 % in one example). Since it appears as though the correlation is not constant throughout the year, these parallel measurements need to be taken either over a longer period, or at least temporarily during the different seasons. As of writing this thesis, it is unknown how long exactly this period needs to be, and whether or not the correlation is significantly different if calculated over shorter time periods than the *target resolution*, i.e., the sampling resolution of the low-resolution concentration measurements. From a sensitivity study outlined in Appendix C.2 it seems that there is relatively little change in the magnitude of the error (and therefore the correlation) between one and four weeks, which indicates that probably more than one data point per month may be used for the calibration of correction functions for a monthly target resolution.

6.2 UNCERTAINTIES

Rigorous assessments of both model and measurement related uncertainties in the estimation of NH_3 dry deposition fluxes are extremely rare in the recent literature, likely due to considerable difficulties in estimating fundamental uncertainty ranges necessary for a reliable error propagation. Generally speaking, uncertainty results from a combination of random errors (*noise*) and systematic errors (*bias*), although in practice these two types often cannot be differentiated easily, and the same source of error may appear as either of them depending on the researcher's point of view and the scales of interest.

Random error in measurements mainly results from limited precision of the applied measurement techniques, but can be quantified to a certain degree from careful characterisation of individual instruments. However, it should be noted that laboratory characterisations in a controlled environment are not always necessarily representative of an instrument's behaviour in long-term field campaigns. Secondary sources of random uncertainty

are found in both temporal and spatial scales: Multiple point-measurements (e.g., with chambers) are likely to exhibit larger variation than those from field-integrated micrometeorological approaches (although each individual point-measurement may be regarded as systematically biased). Similarly, due to intra- and inter-annual variation in meteorological and chemical conditions, individual years may not be representative of a long-term deposition climatology, and week-long measurement campaigns may not be representative of a seasonal average, whereas an average over multiple such campaigns is likely to be.

Systematic measurement uncertainty, on the other hand, is related to accuracy instead of precision, and much more difficult to quantify. Sources include, but are not limited to, instrument bias (e.g. due to calibration errors, or actual quantities of interest below the limit of detection), bias in data-processing related parameters (e.g., stability correction functions), errors in measurement setups, neglection of advection errors, and vertical flux divergence due to chemical reactions between the reference height and the NH_3 sink level. Likewise, temporal and spatial issues can introduce systematic error as well: Sampling bias originating from generally higher data availability during daytime may subsequently lead to biased gap-filling results and ignorance of night-time production and consumption processes, as is known to be the case for CO_2 (Moncrieff et al., 1996). Spatially related sources of uncertainty in measurements are an individual measurement site's representativeness for the ecosystem of interest, and heterogeneity in the flux footprint.

Both random and systematic errors in the measurement directly translate into errors in modelled fluxes, since models are typically calibrated to fit our measurements, and, if applied outside of CTMs, driven with measured input variables. As a consequency, for example noisy concentration measurements will inevitably result in noisy modelled fluxes. Regarding fixed, land-use specific parameter values, it is debatable whether or not data availability for all ecosystem types of interest is enough to bridge the gap from systematic representativeness errors to random variation in parameterisations. For instance, the acid-to-NH_3 ratio in the non-stomatal resistance parameterisation of Massad et al. (2010a) is based on four to five individual data

points for three of the four land-use classes they consider, and the uncertainty range around the relative humidity response parameter they provide leads to coefficients of variation of up to 89 % for short semi-natural ecosystems. Given the exponential nature of the parameterisation, this leads to enormous (random and very likely systematic) uncertainties in non-stomatal fluxes. However, at the time of publication, it was virtually impossible to estimate the systematic proportion of it, since the extensive literature review behind the Massad et al. (2010a) parameterisation covered the majority of available literature on measured NH_3 fluxes at the time, leaving little room for independent validation. Note that this is not meant as criticism of their approach, but rather a demonstration of a dilemma that necessarily emerges from limited data availability.

In comparison to measurements, modelled fluxes likely suffer from even larger systematic uncertainties: In this thesis, I demonstrated physical implausibilities in state-of-the-art parameterisations of the non-stomatal exchange pathway (Chapter 3), as well as errors arising from temporal averaging (Chapter 5). Note that the latter can directly be translated into the same type of systematic error we found in Schrader et al. (2018) when averaging in space, although the extent of that is yet to be investigated. With regard to regional modelling, both random uncertainty and systematic uncertainty in the representativeness of grid-cell averages naturally arise from implicit mixing errors and systematic errors in land-use and parameter maps, model resolution issues in orographically variable regions, and low granularity of emission maps due to data protection regulations. That being said, perhaps the most significant sources of systematic uncertainty are unresolved physical and chemical processes, such as within-canopy gas-particle interconversion, or leaf-level chemical processes like cuticular desorption. These are often impossible to parameterise outside of specialised field trials, or limited in their application due to computational constraints (e.g., Flechard et al., 1999, 2013; Sutton et al., 1998). Last but not least, there may still be significant *unknown unknowns* left in our understanding of NH_3 exchange processes, which would naturally fall in the same category.

It is evident from this discussion how difficult it is to provide general estimates of uncertainty that are representative for the combined effects of all different types and sources, and that can be applied on different scales. All uncertainty estimates in this field need to be linked to a clearly defined reference frame in space, time, and application. Micrometeorological measurements at a given site can have low systematic uncertainty if the measurements are aimed at testing hypotheses about a specific site only, but very little certainty for general statements about an ecosystem type as a whole. To my knowledge, there has not been an attempt at quantifying uncertainties of state-of-the-art NH_3 biosphere-atmosphere exchange models at different scales in the recent literature. Erisman (1993), in one of the few simultaneous assessments of model- and measurement related uncertainties, estimated the total random uncertainy in the yearly average of modelled NH_3 dry deposition to be 130 % and the systematic uncertainty to be 58 % on a 5 by 5 km grid over the Netherlands. For the whole country, his random uncertainty estimates reduced to 17 % and systematic uncertainty to 45 %. Note that these numbers are based on the (likely not always valid) assumption of uncorrelated errors. In the *worst case*, perfectly correlated errors, systematic errors for total (wet and dry) reduced nitrogen deposition increase up to 89–98 %.

Strategies for a new comprehensive uncertainty analysis could be based on reanalysing instrument comparison field trials to obtain good estimates of measurement-related errors, following the example of Nemitz et al. (2009). Random uncertainty in models might be estimated by simultaneous parameter optimisation on existing flux datasets, potentially using Bayesian methods that yield credibility intervals and parameter distriubtions instead of single *best fit* values, or at best, approximate confidence intervals as obtained from traditional frequentist statistics. Forward error propagation from noisy input data and parameters whose distribution is known can nowadays easily be done with simple *brute force* Monte Carlo approaches for one-dimensional applications, thanks to abundant computing power. Systematic uncertainty should be analysed using model ensembles similar to the works of Flechard et al. (2011), but with higher temporal-resolution of the input data, and compared to direct flux measurements

obtained with micrometeorological methods. For sites where the necessary data are available, comparing mechanistically accurate models (or model-parts) (e.g., Flechard et al., 1999; Massad et al., 2010b) with the simpler compromises used in CTMs might be instructive with regard to their physical plasubility, and a first step towards developing approximate, easy-to-parameterise meta-models for missing processes.

In the work at hand I have not done any uncertainty calculations that are remotely as comprehensive as, e.g., shown in Erisman (1993) myself. However, the numbers Erisman (1993) arrives at are generally in agreement with my own expectations and experiences in field-scale application of NH_3 biosphere-atmosphere exchange models more than two decades later. Given that running existing state-of-the-art models in parallel with the same input data often yields a surprisingly large span of predicted fluxes, sometimes even in opposite directions for individual pathways, I generally assume that at the field scale, absolute total uncertainty in annual estimates of dry deposition is at the very least on the order of $1\,kg\,ha^{-1}\,yr^{-1}$, or in relative terms, usually a significant two-digit percentage. Note that it is generally accepted that micrometeorological measurements are usually only accurate to around 10–20 % anyway, due to natural variability in terrain, turbulence, and instrumentation (Moncrieff et al., 1996).

In a recent long-term measurement campaign at a remote site in the Bavarian Forest National Park, we compared eddy-covariance measurements of total N_r biosphere-atmosphere exchange (Brümmer et al., in press; Zöll et al., under review), the majority of which consisted of NH_3, with modelled estimates using different variants of the dry deposition module DEPAC (van Zanten et al., 2010), based on the parameterisation of a two-layer canopy compensation point model of Wichink Kruit et al. (2010). Depending on the specific scenario (inside the CTM LOTOS-EUROS and a measurement-driven 1D variant; with and without land-use corrected for site-specific conditions), modelled cumulative total N_r fluxes before gap-filling were within 20–70 % agreement with the measurements, although almost all variants showed a tendency to overestimate deposition (Brümmer et al., in press).

Despite not directly quantifying them, this thesis contributes to the overall reduction of uncertainty by isolating sources of systematic error in the non-stomatal pathway (Chapter 3), promoting the use of mechanistic, direct, and data-driven methods (Chapter 4), and providing a correction method for systematic errors arising from temporal averaging (Chapter 5).

6.3 IMPLICATIONS

In this thesis, I probably ask more new questions than I give answers to existing ones. Nevertheless, if we look at the overarching aim of developing practical tools for the assessment of N_r deposition, the better understanding of state-of-the-art model parameterisations and the errors that are associated with them can directly be put to good use. Most, if not all of the shortcomings that have been discussed may be revised with reasonable effort, possibly even without additional measurements, as further outlined in the final section of this summary. Others may directly be addressed on the local scale.

There is a clear need for large-scale N_r deposition monitoring, which, in many countries is not met. In Germany, apart from throughfall measurements in forests, only very few experimental measurement sites exist, much less any kind of nation-wide deposition monitoring efforts. However, the results presented in this thesis may be helpful to fill this gap. For instance, continent-wide research infrastructures like ICOS (Franz et al., 2018) in Europe or NEON (SanClements et al., 2014) in the US, which routinely measure turbulent fluxes of CO_2 using the eddy-covariance technique, may be used as a modular platform for low-cost NH_3 deposition monitoring. Their existing flux towers may be equipped with low-cost, low-effort concentration measurement devices like passive samplers, and complemented by individually calibrated biosphere-atmosphere exchange models. In such a monitoring network, the stomatal pathway would be parameterised through CO_2 flux-derived stomatal conductance, as well as estimates of the stomatal emission potential based on historical modelled or measured N inputs (Massad et al., 2010a), or directly on long-term average ambient NH_3 concentrations (Wichink Kruit et al., 2010). Site-specific parameterisations of the non-stomatal

resistance (in a unidirectional framework) or its emission potential (following the works of Wichink Kruit et al., 2010) may be based on a one-time calibration on nighttime flux measurements using a roving system. Finally, the same system would be used to calibrate correction functions for the lowered temporal resolution of passive samplers (which actually only needs concentration measurements instead of fluxes) and for site-specific model validation. The initial effort for setting up such a hybrid model-measurement-network would be largely outweighed by the benefits of an already existing infrastructure, finished site exploration, and low additional long-term cost of operation.

6.4 RECOMMENDATIONS

Finally, I would like to conclude this thesis with a few recommendations for future research, both related to NH_3 modelling in general, and to the specific questions that emerge from my research.

CONSENSUS ON AN OPTIMAL FRAMEWORK Finding the optimal balance between realism and applicability is probably the biggest challenge for modellers in every scientific discipline. As Flechard et al. (2013) noted, the level of complexity needs to be tailored to the specific application, but overall the two-layer canopy compensation point model after Nemitz et al. (2001) has been recognised as a good compromise between realism and accuracy on different scales. However, for site-level applications the unidirectional treatment of the non-stomatal pathway remains somewhat unsatisfying. Personally, I am convinced that a hybrid model, i.e. a steady-state approximation of cuticular desorption following the example of Wichink Kruit et al. (2010), should be the way to go in the future, as there is no clear justification for treating both stomatal and ground-layer fluxes bidirectionally, but fluxes from other non-stomatal surfaces (e.g., wet leaves and stems) not.

RECALIBRATION OF EXISTING MODELS As illustrated in Chapter 3, both the parameterisations of a two-layer model after Massad et al. (2010a) and Wichink Kruit et al. (2010) suffer from

some shortcomings in specific details of their implementation. I am convinced that feasible solutions to these can be found based on existing data and theoretical considerations. The temperature response parameter in Massad et al. (2010a) may be set with an effective one derived from equilibrium constants (cf. Section 3.3.1). The non-stomatal resistance can easily reach values of more than 1000 $s\,m^{-1}$ at relative humidities as high as 90 % at sites with low acid-to-NH_3 ratios, and it should be tested whether more suitable minimum values can be obtained through a recalibration on high-frequency flux measurements instead of campaign averages. Regarding the quasi-bidirectional approach of Wichink Kruit et al. (2010), an effort should be made to parameterise it on direct flux measurements from a larger variety of ecosystems. The issue of the seasonality countering thermodynamic equilibria needs to be addressed, as it affects not only the non-stomatal pathway discussed in Schrader et al. (2016), but also the stomatal pathway through a similar functional relationship. I propose researching options for smoother response functions in the seasonality parameterisation, e.g. by basing them on average instead of instantaneous measurements of the air temperature, or alternative variables with a distinct annual course with less intensive short-term fluctuations.

DISENTANGLING NON-STOMATAL EXCHANGE Presently, non-stomatal exchange pathways are often treated in an unsatisfying manner. For example, the parameterisation of Massad et al. (2010a) is run in a one-layer configuration for unmanaged ecosystems and managed ecosystems outside of management events, but in a two-layer configuration e.g. after fertilisation. While generally the motivation to do so is reasonable, as the ground-layer and other non-stomatal sources can only be separated in flux measurements when the majority of the signal can safely be attributed to one source, it leads to an awkward shift in the meaning of certain parameters. When there is no clear ground-layer signal, its resistance is set to infinity and exchange with it is lumped into the non-stomatal pathway, which is otherwise often interpreted as representing leaf-surfaces only. This may lead to misunderstandings and possibly bias in future parameterisations based on meta-analyses and should be addressed by carefully

unraveling the two pathways, e.g. through the help of chamber measurements.

MECHANISTIC TREATMENT OF CO-DEPOSITION Known parameterisations of co-deposition processes are mainly based on empirical relations (e.g., Massad et al., 2010a; Wichink Kruit et al., 2017). Future research should explore more mechanistic solutions, including their applicability to other trace gases than SO_2. Practical options worth exploring would be to derive effective co-deposition functions from acidity / alkalinity calculations, or attempting to build a steady-state meta-model based on the dynamic leaf-surface chemistry simulations of Flechard et al. (1999).

COMPARISON OF MEASUREMENT TECHNIQUES While the aerodynamic gradient technique has been the de-facto standard for NH_3 measurements in the past, the recent literature has seen an increased use of novel methods primarily using different optical spectroscopy systems (Ferrara et al., 2012; Hansen et al., 2015; Volten et al., 2012; von Bobrutzki et al., 2010; Whitehead et al., 2008; Zöll et al., 2016, and others). These should carefully be evaluated against each other and against gradient measurements in order to assess the uncertainties related with the techniques, and NH_3 flux measurements in general.

HARMONISED DATABASE OF FLUX MEASUREMENTS During my work on this thesis, I found that getting access to existing observational data is not a trivial task and can be extremely tedious when planning multi-site comparisons, and these data naturally come in an enormous variety of different formats and quality levels. There should be a global effort to build a harmonised database of not only NH_3, but all N_r exchange measurements, following the example of FLUXNET for eddy-covariance data. A better availability and accessibility of measured fluxes and other necessary variables would easily have one of the biggest impacts on boosting model development in the future.

MODEL VALIDATION A natural consequence of data scarcity is that models are often calibrated on virtually all available data,

which leaves litte to no room for independent model validation. Model developers should try to address this, e.g., by running cross-validation analyses and exploring other options to obtain validation data that were not used for the respective parameterisations.

As this list is by far not exhaustive, and only discusses the most pressing issues from the point of view of someone mainly working with very simple one- or two-layer models, it is evident that the field of NH_3 biosphere-atmosphere exchange modelling still has a lot of room to grow. We should embrace these challenges and do our best to work towards building good and practical models, as in light of data scarcity they are necessary tools to identify key areas at which we need to focus our environmental protection efforts.

I hope that my humble contribution to this exciting field of research can be of value for the scientific community.

REFERENCES

Adon, M., Galy-Lacaux, C., Serça, D., Guedant, P., Vongkhamsao, A., Rode, W., Meyerfeld, Y. & Guérin, F. (2018). First assessment of inorganic nitrogen deposition budget following the impoundment of a subtropical hydroelectric reservoir (Nam Theun 2, Lao PDR). *Journal of Geophysical Research: Atmospheres*, *123*(21), 12413–12428.

Ainsworth, E. A. & Rogers, A. (2007). The response of photosynthesis and stomatal conductance to rising [CO_2]: Mechanisms and environmental interactions. *Plant, Cell & Environment*, *30*(3), 258–270.

Anatolaki, C. & Tsitouridou, R. (2007). Atmospheric deposition of nitrogen, sulfur and chloride in Thessaloniki, Greece. *Atmospheric Research*, *85*(3-4), 413–428.

Anav, A., Menut, L., Khvorostyanov, D. & Viovy, N. (2012). A comparison of two canopy conductance parameterizations to quantify the interactions between surface ozone and vegetation over Europe. *Journal of Geophysical Research: Biogeosciences*, *117*(G03027).

Andersen, H. V., Hovmand, M. F., Hummelshoj, P. & Jensen, N. O. (1999). Measurements of ammonia concentrations, fluxes and dry deposition velocities to a spruce forest 1991-1995. *Atmospheric Environment*, *33*(9), 1367–1383.

Anderson, M. C., Norman, J. M., Meyers, T. P. & Diak, G. R. (2000). An analytical model for estimating canopy transpiration and carbon assimilation fluxes based on canopy light-use efficiency. *Agricultural and Forest Meteorology*, *101*(4), 265–289.

Baek, B. H., Todd, R., Cole, N. A. & Koziel, J. A. (2006). Ammonia and hydrogen sulphide flux and dry deposition velocity estimates using vertical gradient method at a commercial beef cattle feedlot. *International Journal of Global Environmental Issues*, *6*, 189–203.

Bajwa, K. S., Arya, S. P. & Aneja, V. P. (2008). Modeling studies of ammonia dispersion and dry deposition at some hog farms

in north carolina. *Journal of the Air & Waste Management Association*, *58*(9), 1198–1207.

Baldocchi, D. D. (2003). Assessing the eddy covariance technique for evaluating carbon dioxide exchange rates of ecosystems: Past, present and future. *Global Change Biology*, *9*(4), 479–492.

Ball, J. T., Woodrow, I. E. & Berry, J. A. (1987). A model predicting stomatal conductance and its contribution to the control of photosynthesis under different environmental conditions. In *Progress in photosynthesis research* (Chap. 48, pp. 221–224).

Behera, S. N., Sharma, M., Aneja, V. P. & Balasubramanian, R. (2013). Ammonia in the atmosphere: A review on emission sources, atmospheric chemistry and deposition on terrestrial bodies. *Environmental Science and Pollution Research*, *20*(11), 8092–8131.

Bell, M., Flechard, C., Fauvel, Y., Häni, C., Sintermann, J., Jocher, M., Menzi, H., Hensen, A. & Neftel, A. (2017). Ammonia emissions from a grazed field estimated by minidoas measurements and inverse dispersion modelling. *Atmospheric Measurement Techniques*, *10*(5), 1875–1892.

Benedict, K. B., Carrico, C. M., Kreidenweis, S. M., Schichtel, B., Malm, W. C. & Collett, J., J. L. (2013). A seasonal nitrogen deposition budget for rocky mountain national park. *Ecological Applications*, *23*(5), 1156–69.

Beudert, B. & Gietl, G. (2015). Long-term monitoring in the Große Ohe catchment, Bavarian Forest National Park. *Silva Gabreta*, *21*(1), 5–27.

Biswas, H., Chatterjee, A., Mukhopadhya, S. K., De, T. K., Sen, S. & Jana, T. K. (2005). Estimation of ammonia exchange at the land–ocean boundary condition of Sundarban mangrove, northeast coast of Bay of Bengal, India. *Atmospheric Environment*, *39*(25), 4489–4499.

Bouwman, A. F., Lee, D. S., Asman, W. A. H., Dentener, F. J., VanderHoek, K. W. & Olivier, J. G. J. (1997). A global high-resolution emission inventory for ammonia. *Global Biogeochemical Cycles*, *11*(4), 561–587.

Brümmer, C., Schrader, F., Wintjen, P., Zöll, U. & Schaap, M. (in press). *FORESTFLUX – Verbesserung der Beurteilungsinstrumente für Politikberatung und Vollzug durch standörtliche*

Validierung der Modellierung atmosphärischer Schadstoffeinträge. Umweltbundesamt. Dessau-Roßlau.

Builtjes, P., Hendriks, E., Koenen, M., Schaap, M., Banzhaf, S., Kerschbaumer, A., Gauger, T., Nagel, H. D., Scheuschner, T. & Schlutow, A. (2011). *Erfassung, Prognose und Bewertung von Stoffeinträgen und ihren Wirkungen in Deutschland– Zusammenfassender Abschlussbericht (UBA TEXTE 38/2011)*. Umweltbundesamt. Dessau-Roßlau.

Burkhardt, J. (2010). Hygroscopic particles on leaves: Nutrients or desiccants? *Ecological Monographs*, *80*(3), 369–399.

Burkhardt, J., Basi, S., Pariyar, S. & Hunsche, M. (2012). Stomatal penetration by aqueous solutions–an update involving leaf surface particles. *New Phytologist*, *196*(3), 774–87.

Burkhardt, J., Flechard, C. R., Gresens, F., Mattsson, M., Jongejan, P. A. C., Erisman, J. W., Weidinger, T., Meszaros, R., Nemitz, E. & Sutton, M. A. (2009). Modelling the dynamic chemical interactions of atmospheric ammonia with leaf surface wetness in a managed grassland canopy. *Biogeosciences*, *6*(1), 67–84.

Businger, J. A., Wyngaard, J. C., Izumi, Y. & Bradley, E. F. (1971). Flux-profile relationships in the atmospheric surface layer. *Journal of the Atmospheric Sciences*, *28*(2), 181–189.

Businger, J. A. & Oncley, S. P. (1990). Flux measurement with conditional sampling. *Journal of Atmospheric and Oceanic Technology*, *7*(2), 349–352.

Caird, M. A., Richards, J. H. & Donovan, L. A. (2007). Nighttime stomatal conductance and transpiration in C3 and C4 plants. *Plant Physiology*, *143*(1), 4–10.

Cape, J. N., Jones, M. R., Leith, I. D., Sheppard, L. J., van Dijk, N., Sutton, M. A. & Fowler, D. (2008). Estimate of annual NH_3 dry deposition to a fumigated ombrotrophic bog using concentration-dependent deposition velocities. *Atmospheric Environment*, *42*(27), 6637–6646.

Cape, J. N., Tang, Y. S., van Dijk, N., Love, L., Sutton, M. A. & Palmer, S. C. (2004). Concentrations of ammonia and nitrogen dioxide at roadside verges, and their contribution to nitrogen deposition. *Environmental Pollution*, *132*(3), 469–78.

Collatz, G. J., Ball, J. T., Grivet, C. & Berry, J. A. (1991). Physiological and environmental-regulation of stomatal conductance, photosynthesis and transpiration – a model that includes a laminar boundary-layer. *Agricultural and Forest Meteorology*, *54*(2-4), 107–136.

Cui, J., Zhou, J. & Yang, H. (2010). Atmospheric inorganic nitrogen in dry deposition to a typical red soil agro-ecosystem in southeastern China. *Journal of Environmental Monitoring*, *12*(6), 1287–94.

Cui, J., Zhou, J., Yang, H., Peng, Y., He, Y. & Chan, A. (2011). Atmospheric NO_2 and NH_3 deposition into a typical agro-ecosystem in Southeast China. *Journal of Environmental Monitoring*, *13*(11), 3216–21.

Dämmgen, U. (2007). Atmospheric nitrogen dynamics in Hesse, Germany: Creating the data base 2. atmospheric concentrations of ammonia, its reaction partners and products at Linden. *Landbauforschung Völkenrode*, *57*, 157–170.

Delon, C., Galy-Lacaux, C., Adon, M., Liousse, C., Serca, D., Diop, B. & Akpo, A. (2012). Nitrogen compounds emission and deposition in West African ecosystems: Comparison between wet and dry savanna. *Biogeosciences*, *9*(1), 385–402.

Duyzer, J., Nijenhuis, B. & Weststrate, H. (2001). Monitoring and modelling of ammonia concentrations and deposition in agricultural areas of The Netherlands. *Water, Air and Soil Pollution: Focus*, *1*(5/6), 131–144.

Dyer, A. J. & Hicks, B. B. (1970). Flux-gradient relationships in the constant flux layer. *Quarterly Journal of the Royal Meteorological Society*, *96*(410), 715–721.

Ellis, R. A., Murphy, J. G., Pattey, E., van Haarlem, R., O'Brien, J. M. & Herndon, S. C. (2010). Characterizing a Quantum Cascade Tunable Infrared Laser Differential Absorption Spectrometer (QC-TILDAS) for measurements of atmospheric ammonia. *Atmospheric Measurement Techniques*, *3*(2), 397–406.

Emberson, L. D., Ashmore, M. R., Cambridge, H. M., Simpson, D. & Tuovinen, J. P. (2000). Modelling stomatal ozone flux across Europe. *Environmental Pollution*, *109*(3), 403–13.

Endo, T., Yagoh, H., Sato, K., Matsuda, K., Hayashi, K., Noguchi, I. & Sawada, K. (2011). Regional characteristics of dry

deposition of sulfur and nitrogen compounds at EANET sites in Japan from 2003 to 2008. *Atmospheric Environment*, *45*(6), 1259–1267.

Erisman, J. W. (1993). Acid deposition to nature areas in the Netherlands: Part I. Methods and results. *Water, Air, and Soil Pollution*, *71*(1-2), 51–80.

Erisman, J. W., Galloway, J. N., Seitzinger, S., Bleeker, A., Dise, N. B., Petrescu, A. M., Leach, A. M. & de Vries, W. (2013). Consequences of human modification of the global nitrogen cycle. *Philosophical Transactions of the Royal Society London B: Biological Sciences*, *368*(1621), 20130116.

Erisman, J. W., van Pul, A. & Wyers, P. (1994). Parametrization of surface-resistance for the quantification of atmospheric deposition of acidifying pollutants and ozone. *Atmospheric Environment*, *28*(16), 2595–2607.

Erisman, J. W., Galloway, J., Seitzinger, S., Bleeker, A. & Butterbach-Bahl, K. (2011). Reactive nitrogen in the environment and its effect on climate change. *Current Opinion in Environmental Sustainability*, *3*(5), 281–290.

Erisman, J. W., Mosquera, J. & Hensen, A. (2001). Two options to explain the ammonia gap in The Netherlands. *Environmental Science & Policy*, *4*(2), 97–105.

Erisman, J. W., Sutton, M. A., Galloway, J., Klimont, Z. & Winiwarter, W. (2008). How a century of ammonia synthesis changed the world. *Nature Geoscience*, *1*, 636.

Erisman, J. W. & Wyers, G. P. (1993). Continuous measurements of surface exchange of SO_2 and NH_3; implications for their possible interaction in the deposition process. *Atmospheric Environment. Part A. General Topics*, *27*(13), 1937–1949.

Famulari, D., Fowler, D., Hargreaves, K., Milford, C., Nemitz, E., Sutton, M. A. & Weston, K. (2004). Measuring eddy covariance fluxes of ammonia using tunable diode laser absorption spectroscopy. *Water, Air, & Soil Pollution: Focus*, *4*(6), 151–158.

Fan, J. L., Hu, Z. Y., Wang, T. J., Zhou, J., Wu, C. Y. & Xia, X. (2009). Atmospheric inorganic nitrogen deposition to a typical red soil forestland in southeastern China. *Environmental Monitoring and Assessment*, *159*(1-4), 241–53.

Farquhar, G. D., Firth, P. M., Wetselaar, R. & Weir, B. (1980). On the gaseous exchange of ammonia between leaves and the environment - determination of the ammonia compensation point. *Plant Physiology*, *66*(4), 710–714.

Farquhar, G. D. & Sharkey, T. D. (1982). Stomatal conductance and photosynthesis. *Annual Review of Plant Physiology and Plant Molecular Biology*, *33*(1), 317–345.

Ferrara, R. M., Loubet, B., Di Tommasi, P., Bertolini, T., Magliulo, V., Cellier, P., Eugster, W. & Rana, G. (2012). Eddy covariance measurement of ammonia fluxes: Comparison of high frequency correction methodologies. *Agricultural and Forest Meteorology*, *158*, 30–42.

Fisher, J. B., Baldocchi, D. D., Misson, L., Dawson, T. E. & Goldstein, A. H. (2007). What the towers don't see at night: Nocturnal sap flow in trees and shrubs at two AmeriFlux sites in California. *Tree Physiology*, *27*(4), 597–610.

Flechard, C. R. & Fowler, D. (1998a). Atmospheric ammonia at a moorland site. I: The meteorological control of ambient ammonia concentrations and the influence of local sources. *Quarterly Journal of the Royal Meteorological Society*, *124*(547), 733–757.

Flechard, C. R. & Fowler, D. (1998b). Atmospheric ammonia at a moorland site. II: Long-term surface-atmosphere micrometeorological flux measurements. *Quarterly Journal of the Royal Meteorological Society*, *124*(547), 759–791.

Flechard, C. R., Fowler, D., Sutton, M. A. & Cape, J. N. (1999). A dynamic chemical model of bi-directional ammonia exchange between semi-natural vegetation and the atmosphere. *Quarterly Journal of the Royal Meteorological Society*, *125*(559), 2611–2641.

Flechard, C. R., Massad, R. S., Loubet, B., Personne, E., Simpson, D., Bash, J. O., Cooter, E. J., Nemitz, E. & Sutton, M. A. (2013). Advances in understanding, models and parameterizations of biosphere-atmosphere ammonia exchange. *Biogeosciences*, *10*(7), 5183–5225.

Flechard, C. R., Nemitz, E., Smith, R. I., Fowler, D., Vermeulen, A. T., Bleeker, A., Erisman, J. W., Simpson, D., Zhang, L., Tang, Y. S. & Sutton, M. A. (2011). Dry deposition of reactive nitrogen to European ecosystems: A comparison of infer-

ential models across the NitroEurope network. *Atmospheric Chemistry and Physics*, *11*(6), 2703–2728.

Flechard, C. R., Spirig, C., Neftel, A. & Ammann, C. (2010). The annual ammonia budget of fertilised cut grassland – Part 2: Seasonal variations and compensation point modeling. *Biogeosciences*, *7*(2), 537–556.

Fowler, D., Pilegaard, K., Sutton, M. A., Ambus, P., Raivonen, M., Duyzer, J., Simpson, D., Fagerli, H., Fuzzi, S., Schjoerring, J. K., Granier, C., Neftel, A., Isaksen, I. S. A., Laj, P., Maione, M., Monks, P. S., Burkhardt, J., Daemmgen, U., Neirynck, J., Personne, E., Wichink-Kruit, R., Butterbach-Bahl, K., Flechard, C., Tuovinen, J. P., Coyle, M., Gerosa, G., Loubet, B., Altimir, N., Gruenhage, L., Ammann, C., Cieslik, S., Paoletti, E., Mikkelsen, T. N., Ro-Poulsen, H., Cellier, P., Cape, J. N., Horváth, L., Loreto, F., Niinemets, Ü., Palmer, P. I., Rinne, J., Misztal, P., Nemitz, E., Nilsson, D., Pryor, S., Gallagher, M. W., Vesala, T., Skiba, U., Brüggemann, N., Zechmeister-Boltenstern, S., Williams, J., O'Dowd, C., Facchini, M. C., de Leeuw, G., Flossman, A., Chaumerliac, N. & Erisman, J. W. (2009). Atmospheric composition change: Ecosystems–atmosphere interactions. *Atmospheric Environment*, *43*(33), 5193–5267.

Franz, D., Acosta, M., Altimir, N., Arriga, N., Arrouays, D., Aubinet, M., Aurela, M., Ayres, E., López-Ballesteros, A., Barbaste, M., Berveiller, D., Biraud, S., Boukir, H., Brown, T., Brümmer, C., Buchmann, N., Burba, G., Carrara, A., Cescatti, A., Ceschia, E., Clement, R., Cremonese, E., Crill, P., Darenova, E., Dengel, S., D'Odorico, P., Filippa, G., Fleck, S., Fratini, G., Fuß, R., Gielen, B., Gogo, S., Grace, J., Graf, A., Grelle, A., Gross, P., Grünwald, T., Haapanala, S., Hehn, M., Heinesch, B., Heiskanen, J., Herbst, M., Herschlein, C., Hörtnagl, L., Hufkens, K., Ibrom, A., Jolivet, C., Joly, L., Jones, M., Kiese, R., Klemedtsson, L., Kljun, N., Klumpp, K., Kolari, P., Kolle, O., Kowalski, A., Kutsch, W., Laurila, T., de Ligne, A., Linder, S., Lindroth, A., Lohila, A., Longdoz, B., Mammarella, I., Manise, T., Jiménez, S. M., Matteucci, G., Mauder, M., Meier, P., Merbold, L., Mereu, S., Metzger, S., Migliavacca, M., Mölder, M., Montagnani, L., Moureaux, C., Nelson, D., Nemitz, E., Nicolini, G., Nils-

son, M. B., de Beeck, M. O., Osborne, B., Löfvenius, M. O., Pavelka, M., Peichl, M., Peltola, O., Pihlatie, M., Pitacco, A., Pokorný, R., Pumpanen, J., Ratié, C., Rebmann, C., Roland, M., Sabbatini, S., Saby, N. P. A., Saunders, M., Schmid, H. P., Schrumpf, M., Sedlák, P., Ortiz, P. S. et al. (2018). Towards long-term standardised carbon and greenhouse gas observations for monitoring Europe's terrestrial ecosystems: A review. *International Agrophysics*, *32*(4), 439–455.

Galloway, J. N., Leach, A. M., Bleeker, A. & Erisman, J. W. (2013). A chronology of human understanding of the nitrogen cycle. *Philosophical Transactions of the Royal Society B: Biological Sciences*, *368*(1621), 20130120.

Galloway, J. N., Aber, J. D., Erisman, J. W., Seitzinger, S. P., Howarth, R. W., Cowling, E. B. & Cosby, B. J. (2003). The Nitrogen cascade. *BioScience*, *53*(4), 341–356.

Garland, J. A. (1977). The dry deposition of sulphur dioxide to land and water surfaces. *Proceedings of the Royal Society A: Mathematical, Physical and Engineering Sciences*, *354*(1678), 245–268.

Grantz, D. A., Zinsmeister, D. & Burkhardt, J. (2018). Ambient aerosol increases minimum leaf conductance and alters the aperture-flux relationship as stomata respond to vapor pressure deficit (VPD). *New Phytologist*, *219*(1), 275–286.

Haber, F. (1908). *Verfahren zur synthetischen darstellung von Ammoniak aus den Elementen*. DE235421. Badische Anilin- & Soda-Fabrik in Ludwigshafen.

Häni, C., Flechard, C., Neftel, A., Sintermann, J. & Kupper, T. (2018). Accounting for field-scale dry deposition in backward Lagrangian stochastic dispersion modelling of NH_3 emissions. *Atmosphere*, *9*(4).

Hansen, K., Personne, E., Skjoth, C. A., Loubet, B., Ibrom, A., Jensen, R., Sorensen, L. L. & Boegh, E. (2017). Investigating sources of measured forest-atmosphere ammonia fluxes using two-layer bi-directional modelling. *Agricultural and Forest Meteorology*, *237*, 80–94.

Hansen, K., Pryor, S. C., Boegh, E., Hornsby, K. E., Jensen, B. & Sorensen, L. L. (2015). Background concentrations and fluxes of atmospheric ammonia over a deciduous forest. *Agricultural and Forest Meteorology*, *214*, 380–392.

Hansen, K., Sorensen, L. L., Hertel, O., Geels, C., Skjoth, C. A., Jensen, B. & Boegh, E. (2013). Ammonia emissions from deciduous forest after leaf fall. *Biogeosciences*, *10*(7), 4577–4589.

Hayashi, K. & Yan, X. Y. (2010). Airborne nitrogen load in Japanese and Chinese agroecosystems. *Soil Science and Plant Nutrition*, *56*(1), 2–18.

Hayashi, K., Ono, K., Tokida, T., Takimoto, T., Mano, M., Miyata, A. & Matsuda, K. (2012). Atmosphere-rice paddy exchanges of inorganic particles and relevant gases during a week in winter and a week in summer. *Journal of Agricultural Meteorology*, *68*, 55–68.

Heil, G. W. & Diemont, W. H. (1983). Raised nutrient levels change heathland into grassland. *Vegetatio*, *53*(2), 113–120.

Hendriks, C., Kranenburg, R., Kuenen, J. J. P., Van den Bril, B., Verguts, V. & Schaap, M. (2016). Ammonia emission time profiles based on manure transport data improve ammonia modelling across north western Europe. *Atmospheric Environment*, *131*, 83–96.

Hensen, A., Nemitz, E., Flynn, M. J., Blatter, A., Jones, S. K., Sorensen, L. L., Hensen, B., Pryor, S. C., Jensen, B., Otjes, R. P., Cobussen, J., Loubet, B., Erisman, J. W., Gallagher, M. W., Neftel, A. & Sutton, M. A. (2009). Inter-comparison of ammonia fluxes obtained using the relaxed eddy accumulation technique. *Biogeosciences*, *6*(11), 2575–2588.

Hertel, O., Skjoth, C. A., Reis, S., Bleeker, A., Harrison, R. M., Cape, J. N., Fowler, D., Skiba, U., Simpson, D., Jickells, T., Kulmala, M., Gyldenkaerne, S., Sorensen, L. L., Erisman, J. W. & Sutton, M. A. (2012). Governing processes for reactive nitrogen compounds in the european atmosphere. *Biogeosciences*, *9*(12), 4921–4954.

Hertel, O., Reis, S., Skjoth, C. A., Bleeker, A., Harrison, R., Cape, J. N., Fowler, D., Skiba, U., Simpson, D., Jickells, T., Baker, A., Kulmala, M., Glydenkarne, S., Sorensen, L. L. & Erisman, J. W. (2011). Nitrogen processes in the atmosphere. In M. A. Sutton, C. M. Howard, J. W. Erisman, G. Billen, A. Bleeker, P. Grennfelt, H. van Grinsven & B. Grizzetti (Eds.), *The European Nitrogen Assessment: Sources, Effects and Policy Perspectives* (pp. 177–208). Cambridge University Press.

Hicks, B. B., Baldocchi, D. D., Meyers, T. P., Hosker, R. P. & Matt, D. R. (1987). A preliminary multiple resistance routine for deriving dry deposition velocities from measured quantities. *Water, Air, and Soil Pollution*, *36*(3-4), 311–330.

Hole, L. R., Brunner, S. H., Hanssen, J. E. & Zhang, L. (2008). Low cost measurements of nitrogen and sulphur dry deposition velocities at a semi-alpine site: Gradient measurements and a comparison with deposition model estimates. *Environmental Pollution*, *154*(3), 473–81.

Horvath, L., Asztalos, M., Führer, E., Meszaros, R. & Weidinger, T. (2005). Measurement of ammonia exchange over grassland in the Hungarian Great Plain. *Agricultural and Forest Meteorology*, *130*(3-4), 282–298.

Hunova, I., Kurfürst, P., Vlcek, O., Straník, V., Stoklasova, P., Schovankova, J. & Srbova, D. (2016). Towards a better spatial quantification of nitrogen deposition: A case study for Czech forests. *Environmental Pollution*, *213*, 1028–1041.

Hurkuck, M., Brümmer, C. & Kutsch, W. L. (2016). Near-neutral carbon dioxide balance at a seminatural, temperate bog ecosystem. *Journal of Geophysical Research-Biogeosciences*, *121*(2), 370–384.

Hurkuck, M., Brümmer, C., Mohr, K., Grünhage, L., Flessa, H. & Kutsch, W. L. (2014). Determination of atmospheric nitrogen deposition to a semi-natural peat bog site in an intensively managed agricultural landscape. *Atmospheric Environment*, *97*, 296–309.

Janicke, L. (2002). Lagrangian dispersion modelling. *Landbauforschung Völkenrode*, *235*, 37–41.

Jarvis, P. G. (1976). The interpretation of the variations in leaf water potential and stomatal conductance found in canopies in the field. *Philosophical Transactions of the Royal Society B: Biological Sciences*, *273*(927), 593–610.

Johnson, J., Cummins, T. & Aherne, J. (2016). Critical loads and nitrogen availability under deposition and harvest scenarios for conifer forests in Ireland. *Science of the Total Environment*, *541*, 319–328.

Jones, E., Oliphant, T., Peterson, P. et al. (2001–). SciPy: Open source scientific tools for Python. [Online; accessed 12.1.2019].

Jones, M. R., Leith, I. D., Fowler, D., Raven, J. A., Sutton, M. A., Nemitz, E., Cape, J. N., Sheppard, L. J., Smith, R. I. & Theobald, M. R. (2007a). Concentration-dependent NH_3 deposition processes for mixed moorland semi-natural vegetation. *Atmospheric Environment*, *41*(10), 2049–2060.

Jones, M. R., Leith, I. D., Raven, J. A., Fowler, D., Sutton, M. A., Nemitz, E., Cape, J. N., Sheppard, L. J. & Smith, R. I. (2007b). Concentration-dependent NH_3 deposition processes for moorland plant species with and without stomata. *Atmospheric Environment*, *41*(39), 8980–8994.

Katata, G., Hayashi, K., Ono, K., Nagai, H., Miyata, A. & Mano, M. (2013). Coupling atmospheric ammonia exchange process over a rice paddy field with a multi-layer atmosphere-soil-vegetation model. *Agricultural and Forest Meteorology*, *180*, 1–21.

Kirchner, M., Jakobi, G., Felcht, E., Bernhardt, M. & Fischer, A. (2005). Elevated NH_3 and NO_2 air concentrations and nitrogen deposition rates in the vicinity of a highway in Southern Bavaria. *Atmospheric Environment*, *39*(25), 4531–4542.

Kramm, G. & Dlugi, R. (1994). Modelling of the vertical fluxes of nitric acid, ammonia, and ammonium nitrate. *Journal of Atmospheric Chemistry*, *18*(4), 319–357.

Leakey, A. D., Ainsworth, E. A., Bernacchi, C. J., Rogers, A., Long, S. P. & Ort, D. R. (2009). Elevated CO_2 effects on plant carbon, nitrogen, and water relations: Six important lessons from FACE. *Journal of Experimental Botany*, *60*(10), 2859–76.

Lolkema, D. E., Noordijk, H., Stolk, A. P., Hoogerbrugge, R., van Zanten, M. C. & van Pul, W. A. J. (2015). The Measuring Ammonia in Nature (MAN) network in the Netherlands. *Biogeosciences*, *12*(16), 5133–5142.

Loubet, B., Laville, P., Lehuger, S., Larmanou, E., Flechard, C., Mascher, N., Genermont, S., Roche, R., Ferrara, R. M., Stella, P., Personne, E., Durand, B., Decuq, C., Flura, D., Masson, S., Fanucci, O., Rampon, J. N., Siemens, J., Kindler, R., Gabrielle, B., Schrumpf, M. & Cellier, P. (2011). Carbon, nitrogen and greenhouse gases budgets over a four years crop rotation in northern France. *Plant and Soil*, *343*(1-2), 109–137.

Lovett, G. M., Reiners, W. A. & Olson, R. K. (1982). Cloud droplet deposition in subalpine balsam fir forests: Hydrological and chemical inputs. *Science*, *218*(4579), 1303–1304.

Lucas-Moffat, A. M., Schrader, F. & Brümmer, C. (in preparation). Evaluating statistical properties and gap filling strategies for any kind of eddy covariance flux dataset.

Massad, R. S., Nemitz, E. & Sutton, M. A. (2010a). Review and parameterisation of bi-directional ammonia exchange between vegetation and the atmosphere. *Atmospheric Chemistry and Physics*, *10*(21), 10359–10386.

Massad, R. S., Tuzet, A., Loubet, B., Perrier, A. & Cellier, P. (2010b). Model of stomatal ammonia compensation point (STAMP) in relation to the plant nitrogen and carbon metabolisms and environmental conditions. *Ecological Modelling*, *221*(3), 479–494.

Matt, D. R. & Meyers, T. P. (1993). On the use of the inferential technique to estimate dry deposition of SO_2. *Atmospheric Environment Part A: General Topics*, *27*(4), 493–501.

Meyers, T. P., Luke, W. T. & Meisinger, J. J. (2006). Fluxes of ammonia and sulfate over maize using relaxed eddy accumulation. *Agricultural and Forest Meteorology*, *136*(3-4), 203–213.

Meyers, T. P. & Yuen, T. S. (1987). An assessment of averaging strategies associated with day/night sampling of dry-deposition fluxes of SO_2 and O_3. *Journal of Geophysical Research*, *92*(D6), 6705–6712.

Milford, C., Hargreaves, K. J., Sutton, M. A., Loubet, B. & Cellier, P. (2001a). Fluxes of nh3 and co2 over upland moorland in the vicinity of agricultural land. *Journal of Geophysical Research-Atmospheres*, *106*(D20), 24169–24181.

Milford, C., Theobald, M. R., Nemitz, E., Hargreaves, K. J., Horvath, L., Raso, J., Dämmgen, U., Neftel, A., Jones, S. K., Hensen, A., Loubet, B., Cellier, P. & Sutton, M. A. (2009). Ammonia fluxes in relation to cutting and fertilization of an intensively managed grassland derived from an intercomparison of gradient measurements. *Biogeosciences*, *6*(5), 819–834.

Milford, C., Theobald, M. R., Nemitz, E. & Sutton, M. a. (2001b). Dynamics of ammonia exchange in response to cutting and

fertilising in an intensively-managed grassland. *Water, Air and Soil Pollution*, *1*, 167–176.

Mohr, K., Meesenburg, H., Horvath, B., Meiwes, K. J., Schaaf, S. & Dämmgen, U. (2005). *Bestimmung von Ammoniak-Einträgen aus der Luft und deren Wirkungen auf Waldökosystem (ANSWER-Projekt)*. Umweltbundesamt. Dessau-Roßlau.

Moncrieff, J., Malhi, Y. & Leuning, R. (1996). The propagation of errors in long-term measurements of land-atmosphere fluxes of carbon and water. *Global Change Biology*, *2*(3), 231–240.

Moring, A., Vieno, M., Doherty, R. M., Laubach, J., Taghizadeh-Toosi, A. & Sutton, M. A. (2016). A process-based model for ammonia emission from urine patches, GAG (Generation of Ammonia from Grazing): Description and sensitivity analysis. *Biogeosciences*, *13*(6), 1837–1861.

Myles, L., Kochendorfer, J., Heuer, M. W. & Meyers, T. P. (2011). Measurement of trace gas fluxes over an unfertilized agricultural field using the flux-gradient technique. *Journal of Environmental Quality*, *40*(5), 1359–1365.

Myles, L., Meyers, T. P. & Robinson, L. (2007). Relaxed eddy accumulation measurements of ammonia, nitric acid, sulfur dioxide and particulate sulfate dry deposition near Tampa, FL, USA. *Environmental Research Letters*, *2*(3), 34004–34004.

Neirynck, J. & Ceulemans, R. (2008). Bidirectional ammonia exchange above a mixed coniferous forest. *Environmental Pollution*, *154*(3), 424–38.

Neirynck, J., Kowalski, A. S., Carrara, A. & Ceulemans, R. (2005). Driving forces for ammonia fluxes over mixed forest subjected to high deposition loads. *Atmospheric Environment*, *39*(28), 5013–5024.

Neirynck, J., Kowalski, A. S., Carrara, A., Genouw, G., Berghmans, P. & Ceulemans, R. (2007). Fluxes of oxidised and reduced nitrogen above a mixed coniferous forest exposed to various nitrogen emission sources. *Environmental Pollution*, *149*(1), 31–43.

Nelson, D. D., McManus, B., Urbanski, S., Herndon, S. & Zahniser, M. S. (2004). High precision measurements of atmospheric nitrous oxide and methane using thermoelectrically cooled mid-infrared quantum cascade lasers and detectors. *Spec-*

trochimica Acta Part A: Molecular and Biomolecular Spectroscopy, *60*(14), 3325–35.

Nemitz, E., Hargreaves, K. J., Neftel, A., Loubet, B., Cellier, P., Dorsey, J. R., Flynn, M., Hensen, A., Weidinger, T., Meszaros, R., Horvath, L., Dämmgen, U., Fruhauf, C., Lopmeier, F. J., Gallagher, M. W. & Sutton, M. A. (2009). Intercomparison and assessment of turbulent and physiological exchange parameters of grassland. *Biogeosciences*, *6*(8), 1445–1466.

Nemitz, E., Milford, C. & Sutton, M. A. (2001). A two-layer canopy compensation point model for describing bi-directional biosphere-atmosphere exchange of ammonia. *Quarterly Journal of the Royal Meteorological Society*, *127*(573), 815–833.

Nemitz, E., Sutton, M. A., Schjoerring, J. K., Husted, S. & Wyers, G. P. (2000). Resistance modelling of ammonia exchange over oilseed rape. *Agricultural and Forest Meteorology*, *105*(4), 405–425.

Nemitz, E., Sutton, M. A., Wyers, G. P. & Jongejan, P. A. C. (2004). Gas-particle interactions above a Dutch heathland: I. Surface exchange fluxes of NH_3, SO_2, HNO_3 and HCl. *Atmospheric Chemistry and Physics*, *4*, 989–1005.

Pan, Y. P., Wang, Y. S., Tang, G. Q. & Wu, D. (2012). Wet and dry deposition of atmospheric nitrogen at ten sites in Northern China. *Atmospheric Chemistry and Physics*, *12*(14), 6515–6535.

Paulson, C. A. (1970). The mathematical representation of wind speed and temperature profiles in the unstable atmospheric surface layer. *Journal of Applied Meteorology*, *9*(6), 857–861.

Peake, E. & Legge, A. H. (1987). Evaluation of methods used to collect air quality data at remote and rural sites in Alberta, Canada. In *Proc. 1987 EPA/APCA Symposium on Measurements of Toxic and Related Air Pollutants*. APCA.

Personne, E., Loubet, B., Herrmann, B., Mattsson, M., Schjoerring, J. K., Nemitz, E., Sutton, M. A. & Cellier, P. (2009). SURFATM-NH3: A model combining the surface energy balance and bi-directional exchanges of ammonia applied at the field scale. *Biogeosciences*, *6*(8), 1371–1388.

Phillips, S. B., Arya, S. P. & Aneja, V. P. (2004). Ammonia flux and dry deposition velocity from near-surface concentration gradient measurements over a grass surface in North Carolina. *Atmospheric Environment*, *38*(21), 3469–3480.

Poor, N., Pollman, C., Tate, P., Begum, M., Evans, M. & Campbell, S. (2006). Nature and magnitude of atmospheric fluxes of total inorganic nitrogen and other inorganic species to the Tampa Bay watershed, FL, USA. *Water, Air, and Soil Pollution*, *170*(1-4), 267–283.

Reichstein, M., Falge, E., Baldocchi, D., Papale, D., Aubinet, M., Berbigier, P., Bernhofer, C., Buchmann, N., Gilmanov, T., Granier, A., Grünwald, T., Havránková, K., Ilvesniemi, H., Janous, D., Knohl, A., Laurila, T., Lohila, A., Loustau, D., Matteucci, G., Meyers, T., Miglietta, F., Ourcival, J.-M., Pumpanen, J., Rambal, S., Rotenberg, E., Sanz, M., Tenhunen, J., Seufert, G., Vaccari, F., Vesala, T., Yakir, D. & Valentini, R. (2005). On the separation of net ecosystem exchange into assimilation and ecosystem respiration: Review and improved algorithm. *Global Change Biology*, *11*(9), 1424–1439.

Rihm, B. & Kurz, D. (2001). Deposition and critical loads of nitrogen in Switzerland. *Water, Air, and Soil Pollution*, *130*(1-4), 1223–1228.

Russow, R. & Böhme, F. (2005). Determination of the total nitrogen deposition by the N-15 isotope dilution method and problems in extrapolating results to field scale. *Geoderma*, *127*(1-2), 62–70.

Russow, R. & Weigel, A. (2000). Atmogener N-Eintrag in Boden und Pflanze am Standort Bad Lauchstädt: Ergebnisse aus 15N-Gestützten direktmessungen (ITNI-System) im Vergleich zur indirekten Quantifizierung aus N-Bilanzen des Statischen Dauerdüngungsversuches. *Archives of Agronomy and Soil Science*, *45*, 399–416.

SanClements, M., Luo, H., Pingintha-Durden, N., Metzger, S., Zulueta, R. & Loescher, H. W. (2014). The National Ecological Observatory's Terrestrial Infrastructure: A standardized framework for decadal ecosystem observations at the continental scale. *iLEAPs Newsletter*, *14*, 23–26.

Schaap, M., Timmermans, R. M. A., Roemer, M., Boersen, G. A. C., Builtjes, P. J. H., Sauter, F. J., Velders, G. J. M. & Beck, J. P. (2008). The LOTOS-EUROS model: Description, validation and latest developments. *International Journal of Environment and Pollution*, *32*(2), 270–290.

Schmitt, M., Thöni, L., Waldner, P. & Thimonier, A. (2005). Total deposition of nitrogen on Swiss long-term forest ecosystem research (LWF) plots: Comparison of the throughfall and the inferential method. *Atmospheric Environment*, *39*(6), 1079–1091.

Schrader, F. & Brümmer, C. (2013). *Genfer Luftreinhaltekonvention der UNECE: Literaturstudie zu Messungen der Ammoniak-Depositionsgeschwindigkeit (UBA TEXTE 67/2014)*. Umweltbundesamt. Dessau-Roßlau.

Schrader, F. & Brümmer, C. (2014). Land use specific ammonia deposition velocities: A review of recent studies (2004–2013). *Water, Air, and Soil Pollution*, *225*(10), 2114.

Schrader, F., Brümmer, C., Flechard, C. R., Wichink Kruit, R. J., van Zanten, M. C., Zöll, U., Hensen, A. & Erisman, J. W. (2016). Non-stomatal exchange in ammonia dry deposition models: Comparison of two state-of-the-art approaches. *Atmospheric Chemistry and Physics*, *16*(21), 13417–13430.

Schrader, F., Erisman, J. W. & Brümmer, C. (in preparation). Towards a coupled paradigm of NH_3-CO_2 biosphere-atmosphere exchange modelling.

Schrader, F., Schaap, M., Zöll, U., Kranenburg, R. & Brümmer, C. (2018). The hidden cost of using low-resolution concentration data in the estimation of NH_3 dry deposition fluxes. *Scientific Reports*, *8*(1), 969.

Sellers, P. J., Berry, J. A., Collatz, G. J., Field, C. B. & Hall, F. G. (1992). Canopy reflectance, photosynthesis and transpiration, III. a reanalysis using enzyme kinetics-electron transport models of leaf physiology. *Remote Sensing of Environment*, *42*, 187–216.

Sellers, P. J., Randall, D. A., Collatz, G. J., Berry, J. A., Field, C. B., Dazlich, D. A., Zhang, C., Collelo, G. D. & Bounoua, L. (1996). A revised land surface parameterization (SiB2) for atmospheric GCMS. Part I: Model formulation. *Journal of Climate*, *9*(4), 676–705.

Shen, J., Chen, D., Bai, M., Sun, J., Coates, T., Lam, S. K. & Li, Y. (2016). Ammonia deposition in the neighbourhood of an intensive cattle feedlot in Victoria, Australia. *Scientific Reports*, *6*, 32793.

Shuttleworth, W. J. (2012). *Terrestrial Hydrometeorology*. Chichester, UK: John Wiley & Sons, Ltd.

Simpson, D., Benedictow, A., Berge, H., Bergstrom, R., Emberson, L. D., Fagerli, H., Flechard, C. R., Hayman, G. D., Gauss, M., Jonson, J. E., Jenkin, M. E., Nyiri, A., Richter, C., Semeena, V. S., Tsyro, S., Tuovinen, J. P., Valdebenito, A. & Wind, P. (2012). The EMEP MSC-W chemical transport model – technical description. *Atmospheric Chemistry and Physics*, *12*(16), 7825–7865.

Sintermann, J., Dietrich, K., Häni, C., Bell, M., Jocher, M. & Neftel, A. (2016). A miniDOAS instrument optimised for ammonia field measurements. *Atmospheric Measurement Techniques*, *9*(6), 2721–2734.

Sintermann, J., Spirig, C., Jordan, A., Kuhn, U., Ammann, C. & Neftel, A. (2011). Eddy covariance flux measurements of ammonia by high temperature chemical ionisation mass spectrometry. *Atmospheric Measurement Techniques*, *4*(3), 599–616.

Smith, A. M., Keene, W. C., Maben, J. R., Pszenny, A. A. P., Fischer, E. & Stohl, A. (2007). Ammonia sources, transport, transformation, and deposition in coastal new england during summer. *Journal of Geophysical Research-Atmospheres*, *112*(D10).

Sommer, S. G., Ostergard, H. S., Lofstrom, P., Andersen, H. V. & Jensen, L. S. (2009). Validation of model calculation of ammonia deposition in the neighbourhood of a poultry farm using measured NH_3 concentrations and N deposition. *Atmospheric Environment*, *43*(4), 915–920.

Spirig, C., Flechard, C. R., Ammann, C. & Neftel, A. (2010). The annual ammonia budget of fertilised cut grassland – part 1: Micrometeorological flux measurements and emissions after slurry application. *Biogeosciences*, *7*(2), 521–536.

Staelens, J., Wuyts, K., Adriaenssens, S., Van Avermaet, P., Buysse, H., Van den Bril, B., Roekens, E., Ottoy, J. P., Verheyen, K., Thas, O. & Deschepper, E. (2012). Trends in atmospheric nitrogen and sulphur deposition in northern Belgium. *Atmospheric Environment*, *49*, 186–196.

Staelens, J., De Schrijver, A., Van Avermaet, P., Genouw, G. & Verhoest, N. (2005). A comparison of bulk and wet-only

deposition at two adjacent sites in Melle (Belgium). *Atmospheric Environment*, *39*(1), 7–15.

Storn, R. & Price, K. (1997). Differential evolution - a simple and efficient heuristic for global optimization over continuous spaces. *Journal of Global Optimization*, *11*(4), 341–359.

Sutton, M. A., Burkhardt, J. K., Guerin, D., Nemitz, E. & Fowler, D. (1998). Development of resistance models to describe measurements of bi-directional ammonia surface–atmosphere exchange. *Atmospheric Environment*, *32*(3), 473–480.

Sutton, M. A. & Fowler, D. (1993). A model for inferring bi-directional fluxes of ammonia over plant canopies. In *Proceedings of the WMO conference on the measurement and modelling of atmospheric composition changes including pollutant transport*. WMO/GAW-91.

Sutton, M. A., Howard, C. M., Erisman, J. W., Billen, G., Bleeker, A., Grennfelt, P., van Grinsven, H. & Grizzetti, B. (Eds.). (2011). *The European Nitrogen Assessment: Sources, effects and policy perspectives*. Cambridge, UK: Cambridge University Press.

Sutton, M. A., Nemitz, E., Erisman, J. W., Beier, C., Bahl, K. B., Cellier, P., de Vries, W., Cotrufo, F., Skiba, U., Di Marco, C., Jones, S., Laville, P., Soussana, J. F., Loubet, B., Twigg, M., Famulari, D., Whitehead, J., Gallagher, M. W., Neftel, A., Flechard, C. R., Herrmann, B., Calanca, P. L., Schjoerring, J. K., Daemmgen, U., Horvath, L., Tang, Y. S., Emmett, B. A., Tietema, A., Penuelas, J., Kesik, M., Brueggemann, N., Pilegaard, K., Vesala, T., Campbell, C. L., Olesen, J. E., Dragosits, U., Theobald, M. R., Levy, P., Mobbs, D. C., Milne, R., Viovy, N., Vuichard, N., Smith, J. U., Smith, P., Bergamaschi, P., Fowler, D. & Reis, S. (2007). Challenges in quantifying biosphere-atmosphere exchange of nitrogen species. *Environmental Pollution*, *150*(1), 125–39.

Sutton, M. A., Nemitz, E., Theobald, M. R., Milford, C., Dorsey, J. R., Gallagher, M. W., Hensen, A., Jongejan, P. A. C., Erisman, J. W., Mattsson, M., Schjoerring, J. K., Cellier, P., Loubet, B., Roche, R., Neftel, A., Hermann, B., Jones, S. K., Lehman, B. E., Horvath, L., Weidinger, T., Rajkai, K., Burkhardt, J., Lopmeier, F. J. & Daemmgen, U. (2009). Dynamics of ammonia exchange with cut grassland: Strategy

and implementation of the graminae integrated experiment. *Biogeosciences*, *6*(3), 309–331.

Sutton, M. A., Reis, S., Riddick, S. N., Dragosits, U., Nemitz, E., Theobald, M. R., Tang, Y. S., Braban, C. F., Vieno, M., Dore, A. J., Mitchell, R. F., Wanless, S., Daunt, F., Fowler, D., Blackall, T. D., Milford, C., Flechard, C. R., Loubet, B., Massad, R., Cellier, P., Personne, E., Coheur, P. F., Clarisse, L., Van Damme, M., Ngadi, Y., Clerbaux, C., Skjoth, C. A., Geels, C., Hertel, O., Wichink Kruit, R. J., Pinder, R. W., Bash, J. O., Walker, J. T., Simpson, D., Horvath, L., Misselbrook, T. H., Bleeker, A., Dentener, F. & de Vries, W. (2013). Towards a climate-dependent paradigm of ammonia emission and deposition. *Philosophical Transactions of the Royal Society of London. Series B.: Biological Sciences*, *368*(1621), 20130166.

Sutton, M. A., Tang, Y. S., Miners, B. & Fowler, D. (2001). A new diffusion denuder system for long-term, regional monitoring of atmospheric ammonia and ammonium. *Water, Air and Soil Pollution: Focus*, *1*(5/6), 145–156.

Sutton, M. A., Schjorring, J. K., Wyers, G. P., Duyzer, J. H., Ineson, P. & Powlson, D. S. (1995). Plant—atmosphere exchange of ammonia. *Philosophical Transactions of the Royal Society of London. Series A: Physical and Engineering Sciences*, *351*(1696), 261–278.

Sutton, M. A., Erisman, J. W., Dentener, F. & Möller, D. (2008). Ammonia in the environment: From ancient times to the present. *Environmental Pollution*, *156*(3), 583–604.

Tauchnitz, N., Meissner, R., Bernsdorf, S. & Wegener, U. (2010). Nitrogen fluxes of a slope mire in the German Harz mountains. *Water, Air, and Soil Pollution*, *205*(1-4), 107–112.

Thimonier, A., Kosonen, Z., Braun, S., Rihm, B., Schleppi, P., Schmitt, M., Seitler, E., Waldner, P. & Thöni, L. (2019). Total deposition of nitrogen in swiss forests: Comparison of assessment methods and evaluation of changes over two decades. *Atmospheric Environment*, *198*, 335–350.

Trebs, I., Lara, L. L., Zeri, L. M. M., Gatti, L. V., Artaxo, P., Dlugi, R., Slanina, J., Andreae, M. O. & Meixner, F. X. (2006). Dry and wet deposition of inorganic nitrogen compounds to a tropical pasture site (Rondonia, Brazil). *Atmospheric Chemistry and Physics*, *6*, 447–469.

van der Graaf, S. C., Dammers, E., Schaap, M. & Erisman, J. W. (2018). Technical note: How are NH_3 dry deposition estimates affected by combining the LOTOS-EUROS model with IASI-NH_3 satellite observations? *Atmospheric Chemistry and Physics*, *18*(17), 13173–13196.

van Breemen, N., Burrough, P. A., Velthorst, E. J., van Dobben, H. F., de Wit, T., Ridder, T. B. & Reijnders, H. F. R. (1982). Soil acidification from atmospheric ammonium sulphate in forest canopy throughfall. *Nature*, *299*, 548.

van Zanten, M. C., Sauter, F. J., Wichink Kruit, R. J., van Jaarsveld, J. A. & van Pul, W. A. J. (2010). *Description of the DEPAC module; Dry deposition modeling with DEPAC_GCN2010*. RIVM. Bilthoven, NL.

VDI. (2006). *VDI-Guideline 3782 Part 5: Environmental meteorology – Atmospheric dispersion models – Deposition parameters*. Verein Deutscher Ingenieure. Düsseldorf, DE.

Voglmeier, K., Jocher, M., Häni, C. & Ammann, C. (2018). Ammonia emission measurements of an intensively grazed pasture. *Biogeosciences*, *15*(14), 4593–4608.

Volten, H., Bergwerff, J. B., Haaima, M., Lolkema, D. E., Berkhout, A. J. C., van der Hoff, G. R., Potma, C. J. M., Kruit, R. J. W., van Pul, W. A. J. & Swart, D. P. J. (2012). Two instruments based on differential optical absorption spectroscopy (DOAS) to measure accurate ammonia concentrations in the atmosphere. *Atmospheric Measurement Techniques*, *5*(2), 413–427.

von Bobrutzki, K., Braban, C. F., Famulari, D., Jones, S. K., Blackall, T., Smith, T. E. L., Blom, M., Coe, H., Gallagher, M., Ghalaieny, M., McGillen, M. R., Percival, C. J., Whitehead, J. D., Ellis, R., Murphy, J., Mohacsi, A., Pogany, A., Junninen, H., Rantanen, S., Sutton, M. A. & Nemitz, E. (2010). Field inter-comparison of eleven atmospheric ammonia measurement techniques. *Atmospheric Measurement Techniques*, *3*(1), 91–112.

von Liebig, J. (1840). *Die organische Chemie in ihrer Anwendung auf Agricultur und Physiologie*. Braunschweig: Vieweg.

Walker, J., Spence, P., Kimbrough, S. & Robarge, W. (2008). Inferential model estimates of ammonia dry deposition in the

vicinity of a swine production facility. *Atmospheric Environment*, *42*(14), 3407–3418.

Webb, E. K. (1970). Profile relationships: The log-linear range, and extension to strong stability. *Quarterly Journal of the Royal Meteorological Society*, *96*(407), 67–90.

Weigel, A., Russow, R. & Korschens, M. (2000). Quantification of airborne N-input in long-term field experiments and its validation through measurements using N-15 isotope dilution. *Journal of Plant Nutrition and Soil Science*, *163*(3), 261–265.

Welsh, A. H., Peterson, A. T. & Altmann, S. A. (1988). The fallacy of averages. *American Naturalist*, *132*(2), 277–288.

Wentworth, G. R., Murphy, J. G., Benedict, K. B., Bangs, E. J. & Collett Jr, J. L. (2016). The role of dew as a nighttime reservoir and morning source for atmospheric ammonia. *Atmospheric Chemistry and Physics Discussions*, *16*, 1–36.

Wesely, M. L. (1989). Parameterization of surface resistances to gaseous dry deposition in regional-scale numerical-models. *Atmospheric Environment*, *23*(6), 1293–1304.

Wesely, M. L. & Hicks, B. B. (2000). A review of the current status of knowledge on dry deposition. *Atmospheric Environment*, *34*(12-14), 2261–2282.

Whitehead, J. D., Twigg, M., Famulari, D., Nemitz, E., Sutton, M. A., Gallagher, M. W. & Fowler, D. (2008). Evaluation of laser absorption spectroscopic techniques for eddy covariance flux measurements of ammonia. *Environ Sci Technol*, *42*(6), 2041–6.

Wichink Kruit, R. J., Aben, J., de Vries, W., Sauter, F., van der Swaluw, E., van Zanten, M. C. & van Pul, W. A. J. (2017). Modelling trends in ammonia in the Netherlands over the period 1990–2014. *Atmospheric Environment*, *154*, 20–30.

Wichink Kruit, R. J., Schaap, M., Sauter, F. J., van Zanten, M. C. & van Pul, W. A. J. (2012). Modeling the distribution of ammonia across europe including bi-directional surface–atmosphere exchange. *Biogeosciences*, *9*(12), 5261–5277.

Wichink Kruit, R. J., van Pul, W. A. J., Otjes, R. P., Hofschreuder, P., Jacobs, A. F. G. & Holtslag, A. A. M. (2007). Ammonia fluxes and derived canopy compensation points over non-fertilized agricultural grassland in the netherlands using the

new gradient ammonia—high accuracy—monitor (graham). *Atmospheric Environment*, *41*(6), 1275–1287.

Wichink Kruit, R. J., van Pul, W. A. J., Sauter, F. J., van den Broek, M., Nemitz, E., Sutton, M. A., Krol, M. & Holtslag, A. A. M. (2010). Modeling the surface–atmosphere exchange of ammonia. *Atmospheric Environment*, *44*(7), 945–957.

Wolff, V., Trebs, I., Ammann, C. & Meixner, F. X. (2010). Aerodynamic gradient measurements of the nh3-hno3-nh4no3 triad using a wet chemical instrument: An analysis of precision requirements and flux errors. *Atmospheric Measurement Techniques*, *3*(1), 187–208.

Wyers, G. P. & Erisman, J. W. (1998). Ammonia exchange over coniferous forest. *Atmospheric Environment*, *32*(3), 441–451.

Wyers, G. P., Vermeulen, A. T. & Slanina, J. (1992). Measurement of dry deposition of ammonia on a forest. *Environ Pollut*, *75*(1), 25–8.

Yang, R., Hayashi, K., Zhu, B., Li, F. & Yan, X. (2010). Atmospheric NH_3 and NO_2 concentration and nitrogen deposition in an agricultural catchment of Eastern China. *Science of the Total Environment*, *408*(20), 4624–32.

Zhang, L., Brook, J. R. & Vet, R. (2003). A revised parameterization for gaseous dry deposition in air-quality models. *Atmospheric Chemistry and Physics*, *3*(6), 2067–2082.

Zhang, L., Vet, R., O'Brien, J. M., Mihele, C., Liang, Z. & Wiebe, A. (2009). Dry deposition of individual nitrogen species at eight Canadian rural sites. *Journal of Geophysical Research-Atmospheres*, *114*(D02301).

Zhang, L., Wright, L. P. & Asman, W. A. H. (2010). Bi-directional air-surface exchange of atmospheric ammonia: A review of measurements and a development of a big-leaf model for applications in regional-scale air-quality models. *Journal of Geophysical Research-Atmospheres*, *115*(D20310).

Zhou, J., Cui, J., Fan, J. L., Liang, J. N. & Wang, T. J. (2010). Dry deposition velocity of atmospheric nitrogen in a typical red soil agro-ecosystem in Southeastern China. *Environmental Monitoring and Assessment*, *167*(1-4), 105–13.

Zimmermann, F., Plessow, K., Queck, R., Bernhofer, C. & Matschullat, J. (2006). Atmospheric N- and S-fluxes to a spruce forest – comparison of inferential modelling and

the throughfall method. *Atmospheric Environment*, *40*(25), 4782–4796.

Zöll, U., Lucas-Moffat, A. M., Wintjen, P., Schrader, F., Beudert & B., C., Brümmer. (under review). Is the biosphere-atmosphere exchange of total reactive nitrogen above forest driven by the same factors as carbon dioxide? an analysis using artificial neural networks. *Atmospheric Environment*.

Zöll, U., Brümmer, C., Schrader, F., Ammann, C., Ibrom, A., Flechard, C. R., Nelson, D. D., Zahniser, M. & Kutsch, W. L. (2016). Surface–atmosphere exchange of ammonia over peatland using QCL-based eddy-covariance measurements and inferential modeling. *Atmospheric Chemistry and Physics*, *16*(17), 11283–11299.

A

SUPPLEMENT TO CHAPTER 2

A.1 LITERATURE REVIEW

Table A.1: List of ammonia deposition velocities sorted by land-use category. Values listed under the column *Mean* were used in calculating weighted averages and medians, with the exception of duplicate values in Neirynck et al. (2007) and Neirynck and Ceulemans (2008). *CTM:* chemical transport model, *LIT:* literature study, *AGM*: aerodynamic gradient method, *BIO*: biomonitoring; *SUS*: surrogate surfaces; *CHA*: chamber measurements.

REFERENCE	METHOD	v_d ($cm\,s^{-1}$) SPECIFIC	v_d ($cm\,s^{-1}$) MEAN	COMMENT	WEIGHTS (−) w_s	WEIGHTS (−) w_c
Coniferous forests						
Builtjes et al. (2011)	CTM	1.6		Annual mean at z_R = 25 m	4	4
		2.1		Annual mean at z_R = 2.5 m		
		2.3		Annual mean at z_R = 1.0 m		
			2.0	Mean over all z_R		
Kirchner et al. (2005)	LIT	0.8–4.5		Literature research ($n = 1$)	4	4
			2.2	Center of range		
Mohr et al. (2005)	INF		1.6	Annual mean	4	4
Staelens et al. (2012)	LIT		2.9	Literature research ($n = 12$)	4	4
Zhang et al. (2009)	INF		0.5	Mean of two sites	3	2
Zimmermann et al. (2006)	INF		3.3	Annual mean	4	4
Deciduous forests						

(Continued on next page)

REFERENCE	METHOD	v_d ($cm\,s^{-1}$) SPECIFIC	v_d ($cm\,s^{-1}$) MEAN	COMMENT	WEIGHTS (−) w_s	WEIGHTS (−) w_c
Builtjes et al. (2011)	CTM	1.4		Annual mean at z_R = 25 m	4	4
		1.9		Annual mean at z_R = 2.5 m		
		2.1		Annual mean at z_R = 1.0 m		
			1.8	Mean over all z_R		
Fan et al. (2009)	INF		0.3	Annual mean	4	4
Staelens et al. (2012)	LIT		1.5	Literature research ($n = 4$)	4	4
Zhang et al. (2009)	INF		0.3	Mean of two sites	2	2
Mixed forests						
Endo et al. (2011)	INF	0.5–0.9		Range of ten sites	4	4
			0.7	Center of range		
Flechard et al. (2011)	INF		1.7	Mean of 29 sites	4	4
Neirynck et al. (2005)	AGM	3.5		Daytime	4	4
		2.4		Nighttime		
		2.9		High NH_3 daytime		
		1.5		High NH_3 nighttime		
		3.7		Low NH_3 daytime		
		2.6		Low NH_3 nighttime		
			3.0	Annual mean		
Neirynck and Ceulemans (2008)	AGM		3.0	Annual mean	4	4
Neirynck et al. (2007)	AGM	3.2		Winter	4	4
		2.8		Summer		
		3.4		Summer daytime		

(Continued on next page)

REFERENCE	METHOD	v_d (cm s^{-1}) SPECIFIC	v_d (cm s^{-1}) MEAN	COMMENT	WEIGHTS (−) w_s	WEIGHTS (−) w_c
		1.7		Summer nighttime		
		3.6		Winter daytime		
		3.0		Winter nighttime		
			3.0	Annual mean		
Zhang et al. (2009)	INF		0.4	Mean of three sites	4	2
Semi-natural sites						
Bajwa et al. (2008)	CTM	1.0		Summer, daytime	4	1
		0.1		Summer, nighttime		
		1.7		Spring, daytime		
		0.1		Spring, nighttime		
		0.8		Fall, daytime		
		0.1		Fall, nighttime		
		0.5		Winter, daytime		
		0.1		Winter nighttime		
			0.6	Annual mean		
Benedict et al. (2013)	INF	0.1–2.3		Annual range	4	4
			1.2	Center of range		
Cape et al. (2008)	CHA + INF		1.6	Annual mean	4	4
			0.3	Annual mean, fumigated		
Endo et al. (2011)	INF	0.2–0.6		Range of ten sites	4	4
			0.4	Center of range		
Flechard et al. (2011)	INF		0.6	Annual mean of 17 sites	4	4

(Continued on next page)

REFERENCE	METHOD	v_d ($cm\,s^{-1}$) SPECIFIC	v_d ($cm\,s^{-1}$) MEAN	COMMENT	WEIGHTS (−) w_s	WEIGHTS (−) w_c
Hole et al. (2008)	AGM		0.1	Annual mean from measurements	4	4
	INF		0.3	Model result for scenario *Grass*		
			0.6	Model result for scenario *Tundra*		
Horvath et al. (2005)	AGM	1.1		Vegetation period, daytime	4	4
		1.0		Vegetation period, nighttime		
		1.1		Vegetation period, whole day		
		1.1		Dormant season, daytime		
		0.7		Dormant season, nighttime		
		0.9		Dormant season, whole day		
			1.0	Annual mean		
Hurkuck et al. (2014)	AGM		0.7	Annual mean	4	4
Jones et al. (2007a)	CHA	0.4–0.6		Range during spring	1	1
			0.5	Center of range		
Kirchner et al. (2005)	LIT	0.5–2.2		Literature research ($n = 3$)	4	4
			1.4	Center of range		
Milford et al. (2009)	AGM		0.2	Summer	1	1
Myles et al. (2011)	LIT		1.8	Literature research ($n = 4$)	4	4

(Continued on next page)

REFERENCE	METHOD	v_d (cm s^{-1}) SPECIFIC	v_d (cm s^{-1}) MEAN	COMMENT	WEIGHTS (−) w_s	WEIGHTS (−) w_c
Nemitz et al. (2004)	AGM	0.6		Daytime, dry	1	2
		0.7		Nighttime, dry		
		1.8		Daytime, wet		
		1.6		Nighttime, wet		
			1.2	Spring mean		
Phillips et al. (2004)	AGM	3.9		Summer, daytime	4	1
		0.8		Summer, nighttime		
		2.9		Spring, daytime		
		0.6		Spring, nighttime		
		2.8		Fall, daytime		
		0.1		Fall, nighttime		
		2.4		Winter, daytime		
		0.2		Winter, nighttime		
			1.7	Annual mean		
Staelens et al. (2012)	LIT		1.4	Literature research (n = 13)	4	4
Trebs et al. (2006)	INF		1.0	Fall	1	2
Water						
Biswas et al. (2005)	AGM	0.4		Monsoon	4	4
		0.6		Pre-monsoon		
		0.5		Post-monsoon		
			0.5	Mean		
Builtjes et al. (2011)	CTM	0.7		Annual mean at z_R = 25 m	4	4
		1.0		Annual mean at z_R = 2.5 m		

(Continued on next page)

REFERENCE	METHOD	v_d ($cm\,s^{-1}$) SPECIFIC	v_d ($cm\,s^{-1}$) MEAN	COMMENT	WEIGHTS (−) w_s	WEIGHTS (−) w_c
		1.1		Annual mean at z_R = 1.0 m		
			0.9	Mean over all z_R		
Smith et al. (2007)	INF		0.6	Summer	1	2
Urban sites						
Anatolaki and Tsitouridou (2007)	SUS		0.8	Annual mean	4	4
Builtjes et al. (2011)	CTM	0.7		Annual mean at z_R = 25 m	4	4
		0.8		Annual mean at z_R = 2.5 m		
		0.9		Annual mean at z_R = 1.0 m		
			0.8	Mean over all z_R		
Hayashi and Yan (2010)	LIT		0.5	Annual mean from data synthesis	4	4
Poor et al. (2006)	CTM		1.1	Annual mean	4	4
Yang et al. (2010)	INF		0.1	Annual mean	4	1
Agricultural sites						
Baek et al. (2006)	AGM		6.3	Summer	1	1
Builtjes et al. (2011)	CTM	1.2		Annual mean at z_R = 25 m	4	4
		1.7		Annual mean at z_R = 2.5 m		
		1.9		Annual mean at z_R = 1.0 m		
			1.6	Mean over all z_R		
Cui et al. (2010)	INF	0.3		Spring	4	4
		0.2		Summer		
		0.2		Fall		
		0.3		Winter		
			0.3	Annual mean		
Cui et al. (2011)	INF		0.3	Annual mean	4	4
	LIT		0.4	Literature research ($n = 3$)		

(Continued on next page)

REFERENCE	METHOD	v_d ($cm\,s^{-1}$) SPECIFIC	v_d ($cm\,s^{-1}$) MEAN	COMMENT	WEIGHTS (−) w_s	WEIGHTS (−) w_c
Delon et al. (2012)	INF		0.3	Annual mean of five sites	4	4
Flechard et al. (2011)	INF		0.2	Annual mean of eight sites	4	4
Hayashi et al. (2012)	AGM	0.6		Winter, fallow, daytime	2	1
		0.2		Winter, fallow, nighttime		
		0.2		Summer, crop period, daytime		
		0.2		Summer, crop period, nighttime		
			0.3	Mean		
Katata et al. (2013)	INF	0.4–0.8		Fallow	2	1
		0.2–1.0		Crop period		
			0.6	Center of range		
Loubet et al. (2011)	INF	0.1–0.6		Annual mean	4	4
			0.4	Center of range		
Meyers et al. (2006)	REA		4.7	Summer	1	1
Myles et al. (2007)	REA		1.3	Daytime mean	1	1
Myles et al. (2011)	AGM		7.1	Fall	1	1
	LIT		2.2	Literature research ($n = 4$)	4	4
Sommer et al. (2009)	CTM + BIO		0.5	Fall	1	2
Yang et al. (2010)	INF		0.2	Annual mean	4	1
Zhang et al. (2009)	INF		0.3	Spring	1	1
Zhou et al. (2010)	INF	0.3		Spring	4	4
		0.2		Summer		
		0.2		Fall		
		0.3		Winter		

(Continued on next page)

REFERENCE	METHOD	v_d ($cm\,s^{-1}$) SPECIFIC	v_d ($cm\,s^{-1}$) MEAN	COMMENT	WEIGHTS (−) w_s	WEIGHTS (−) w_c
			0.3	Mean		
Unspecified						
Hayashi and Yan (2010)	LIT		0.4	Annual mean of twelve sites	4	4
Pan et al. (2012)	INF	0.4–2.0		Annual mean of ten sites	4	4
			1.2	Center of range		

A.2 RAW DATA FOR REANALYSIS

Listing A.1: Raw .csv data used for the calculation of statistics.

```
reference,use_for_averaging,land_use,vd,vd_sig,vd_min,vd
    _max,period,method,c,c_sig,c_min,c_max,w_seasons,w_
    coverage
Phillips et al. (2004),0,seminatural,3.9,2.8,,,"Summer,
    daytime",AGM,4.8,,,,,
Phillips et al. (2004),0,seminatural,0.8,1.7,,,"Summer,
    nighttime",AGM,3,,,,,
Phillips et al. (2004),0,seminatural,2.9,2,,,"Spring,
    daytime",AGM,5.6,,,,,
Phillips et al. (2004),0,seminatural,0.6,1,,,"Spring,
    nighttime",AGM,3.6,,,,,
Phillips et al. (2004),0,seminatural,2.8,2,,,"Fall,
    daytime",AGM,8,,,,,
Phillips et al. (2004),0,seminatural,0.1,0.2,,,"Fall,
    nighttime",AGM,7.5,,,,,
Phillips et al. (2004),0,seminatural,2.4,1.9,,,"Winter,
    daytime",AGM,1.7,,,,,
Phillips et al. (2004),0,seminatural,0.2,0.3,,,"Winter,
    nighttime",AGM,1.4,,,,,
Phillips et al. (2004),1,seminatural,1.7,,,,Annual mean,
    AGM,,,,,4,1
Zhou et al. (2010),0,agricultural,0.3,,,,Spring,INF
    ,,,,,,
Zhou et al. (2010),0,agricultural,0.2,,,,Summer,INF
    ,,,,,,
Zhou et al. (2010),0,agricultural,0.2,,,,Fall,INF,,,,,
```

```
Zhou et al. (2010),0,agricultural,0.3,,,,Winter,INF
    ,,,,,,
Zhou et al. (2010),1,agricultural,0.3,,0.1,0.4,Annual
    mean,INF,,,,,4,4
Hurkuck et al. (submitted),1,seminatural,0.7,,0.2,1.9,
    Annual mean,AGM,,,2.5,15.4,4,4
Anatolaki & Tsitouridou (2007),1,urban,0.8,,,,Annual
    mean,SUS,2.3,1.5,0,5.8,4,4
Biswas et al. (2005),0,water,0.4,0.2,,,during monsoon,
    AGM,2.7,1.3,,,,
Biswas et al. (2005),0,water,0.6,0.3,,,pre-monsoon,AGM
    ,8.7,4.1,,,,
Biswas et al. (2005),0,water,0.5,0.2,,,post-monsoon,AGM
    ,8.2,3,,,,
Biswas et al. (2005),1,water,0.5,,,,average,AGM
    ,6.5,,,,4,4
Cape et al. (2008),1,seminatural,1.6,0.5,,,Annual mean,
    CHA + INF,0.7,,,,4,4
Cape et al. (2008),1,seminatural,0.3,,,,Annual mean,CHA
    + INF,100,,,,4,4
Hole et al. (2008),1,seminatural,0.1,,,,Annual mean from
     measurements,AGM,,,0.1,1,4,4
Hole et al. (2008),1,seminatural,0.3,,,,Annual mean for
    scenario "Grass",INF,,,,,4,4
Hole et al. (2008),1,seminatural,0.6,,,,Annual mean for
    scenario "Tundra",INF,,,,,4,4
Delon et al. (2012),1,agricultural,0.3,0.1,0.1,0.5,
    Annual mean of five sites,INF,1.4,8.3,,,4,4
Hayashi & Yan (2010),1,unspecified,0.4,,,,Annual mean of
     twelve sites,LIT,7.8,,,,4,4
Hayashi & Yan (2010),1,urban,0.5,,,,Annual mean from
    data synthesis,LIT,0.7,,,,4,4
Cui et al. (2010),0,agricultural,0.3,,,,spring,INF,,,,,,
Cui et al. (2010),0,agricultural,0.2,,,,summer,INF,,,,,,
Cui et al. (2010),0,agricultural,0.2,,,,fall,INF,,,,,,
Cui et al. (2010),0,agricultural,0.3,,,,winter,INF,,,,,,
Cui et al. (2010),1,agricultural,0.3,,0.1,0.4,Annual
    mean,INF,201.5,,77,317.1,4,4
Flechard et al. (2011),1,mixed,1.7,1.2,,,Mean of 29
    sites,INF,1,0.3,2.8,,4,4
Flechard et al. (2011),1,seminatural,0.6,0.2,,,Annual
    mean of 17 sites,INF,1.6,0.3,4.3,,4,4
Flechard et al. (2011),1,agricultural,0.2,0.1,,,Annual
    mean of eight sites,INF,3.7,0.9,11.3,,4,4
```

```
Katata et al. (2013),0,agricultural,,,0.4,0.8,Fallow,INF
    ,,,,,,
Katata et al. (2013),0,agricultural,,,0.2,1,Crop period,
    INF,,,,,,
Katata et al. (2013),1,agricultural,0.6,,,,Center of
    ranges,INF,,,,,2,1
Horvath et al. (2005),0,seminatural,1.1,1,0,80.9,"
    Veteation period, daytime",AGM,3.8,,,,,
Horvath et al. (2005),0,seminatural,1,1,0,75.4,"
    Vegetation period, nighttime",AGM,2.8,,,,,
Horvath et al. (2005),0,seminatural,1.1,1,,,"Vegetation
    period, whole day",AGM,3.3,,,,,
Horvath et al. (2005),0,seminatural,1.1,0.9,0,6.1,"
    Dormant season, daytime",AGM,4.1,,,,,
Horvath et al. (2005),0,seminatural,0.7,0.6,0,3.3,"
    Dormant season, nighttime",AGM,3.3,,,,,
Horvath et al. (2005),0,seminatural,0.9,0.8,,,"Dormant
    season, whole day",AGM,3.7,,,,,
Horvath et al. (2005),1,seminatural,1,,,,Annual mean,AGM
    ,3.5,,,,4,4
Meyers et al. (2006),1,agricultural,4.7,3.8,1,10,Summer,
    REA,2.8,1.4,1.4,5.2,1,1
Myles et al. (2007),1,agricultural,1.3,15.5,-35.2,31.2,
    Daytime mean,REA,1.6,0.2,,,1,1
Neirynck & Ceulemans (2008),1,mixed,3,4.6,,,Annual mean,
    AGM,4.1,6.5,,,4,4
Neirynck et al. (2007),0,mixed,3.2,4.8,,,Winter,AGM
    ,,,,,,
Neirynck et al. (2007),0,mixed,2.8,4.5,,,Summer,AGM
    ,,,,,,
Neirynck et al. (2007),0,mixed,3.4,,,,"Summer, daytime",
    AGM,4,,,,,
Neirynck et al. (2007),0,mixed,1.7,,,,"Summer, nighttime
    ",AGM,4.3,,,,,
Neirynck et al. (2007),0,mixed,3.6,,,,"Winter, daytime",
    AGM,1.5,,,,,
Neirynck et al. (2007),0,mixed,3,,,,"Winter, nighttime",
    AGM,1.6,,,,,
Neirynck et al. (2007),0,mixed,3,4.6,,,Annual mean,AGM
    ,3,5.6,0,102.5,4,4
Neirynck et al. (2005),0,mixed,3.5,5.1,,,Daytime,AGM
    ,4.2,5.4,,,,
Neirynck et al. (2005),0,mixed,2.4,3.9,,,Nighttime,AGM
    ,4,7.5,,,,
```

```
Neirynck et al. (2005),0,mixed,2.9,,,,High NH3 daytime,
    AGM,8.8,,,,,
Neirynck et al. (2005),0,mixed,1.5,,,,High NH3 nighttime
    ,AGM,11,,,,,
Neirynck et al. (2005),0,mixed,3.7,,,,Low NH3 daytime,
    AGM,2.7,,,,,
Neirynck et al. (2005),0,mixed,2.6,,,,Low NH3 nighttime,
    AGM,2.1,,,,,
Neirynck et al. (2005),0,mixed,3,4.6,,,Annual mean,AGM
    ,4.1,6.5,,,4,4
Nemitz et al. (2004),0,seminatural,0.6,,-2.8,3.1,"
    Daytime, dry",AGM,,,,,,
Nemitz et al. (2004),0,seminatural,0.7,,-0.3,4,"
    Nighttime, dry",AGM,,,,,,
Nemitz et al. (2004),0,seminatural,1.8,,-0.7,5,"Daytime,
     wet",AGM,,,,,,
Nemitz et al. (2004),0,seminatural,1.6,,-0.3,4.9,"
    Nighttime, wet",AGM,,,,,,
Nemitz et al. (2004),1,seminatural,1.2,,,,Spring mean,
    AGM,5.2,4.1,,,1,2
Pan et al. (2012),0,unspecified,,,0.4,2,"Annual mean, n
    =10",INF,,,0.2,54.9,,
Pan et al. (2012),1,unspecified,1.2,,,,center of range,
    INF,,,,,4,4
Endo et al. (2011),0,mixed,,,0.5,0.9,Range of ten sites,
    INF,,,0.3,0.9,,
Endo et al. (2011),0,seminatural,,,0.2,0.6,Range of ten
    sites,INF,,,,,,
Endo et al. (2011),1,mixed,0.7,,,,Center of range,INF
    ,,,,,4,4
Endo et al. (2011),1,seminatural,0.4,,,,Center of range,
    INF,,,,,4,4
Staelens et al. (2012),1,seminatural,1.4,,0.7,2.2,
    Literature research (n = 13),LIT,,,,,4,4
Staelens et al. (2012),1,deciduous,1.5,,0.8,2.2,
    Literature research (n = 4),LIT,,,,,4,4
Staelens et al. (2012),1,coniferous,2.9,,2,3.8,
    Literature research (n = 12),LIT,,,,,4,4
Zimmermann et al. (2006),1,coniferous,3.3,,2,6,Annual
    mean,INF,0.5,,,,4,4
Kirchner et al. (2005),0,seminatural,,,0.5,2.2,
    Literature research (n = 3),LIT,,,,,,
Kirchner et al. (2005),1,seminatural,1.4,,,,Center of
    range,LIT,,,,,4,4
```

```
Kirchner et al. (2005),0,coniferous,,,0.8,4.5,Literature
     research (n = 1),LIT,,,,,,
Kirchner et al. (2005),1,coniferous,2.2,,,,Center of
    range,LIT,,,,,4,4
Sommer et al. (2009),1,agricultural,0.5,,0.3,0.7,Fall,
    CTM + BIO,,,0,13,1,2
Yang et al. (2010),1,agricultural,0.2,,,,Annual mean,INF
    ,4.1,0.3,1.3,16.3,4,1
Yang et al. (2010),1,urban,0.1,,,,Annual mean,INF
    ,5.4,0.5,1.8,17.2,4,1
Baek et al. (2006),1,agricultural,6.3,4.5,,,summer
    average,AGM,,,,,1,1
Bajwa et al. (2008),0,seminatural,1,,,,"Summer, daytime
    ",CTM,,,,,,
Bajwa et al. (2008),0,seminatural,0.1,,,,"Summer,
    nighttime",CTM,,,,,,
Bajwa et al. (2008),0,seminatural,1.7,,,,"Spring,
    daytime",CTM,,,,,,
Bajwa et al. (2008),0,seminatural,0.1,,,,"Spring,
    nighttime",CTM,,,,,,
Bajwa et al. (2008),0,seminatural,0.8,,,,"Fall, daytime
    ",CTM,,,,,,
Bajwa et al. (2008),0,seminatural,0.1,,,,"Fall,
    nighttime",CTM,,,,,,
Bajwa et al. (2008),0,seminatural,0.5,,,,"Winter,
    daytime",CTM,,,,,,
Bajwa et al. (2008),0,seminatural,0.1,,,,"Winter,
    nighttime",CTM,,,,,,
Bajwa et al. (2008),1,seminatural,0.6,,,,Annual mean,CTM
    ,,,,,4,1
Benedict et al. (2013),0,seminatural,,,0.1,2.3,Annual
    range,INF,,,0.1,0.2,,
Benedict et al. (2013),1,seminatural,1.2,,,,Center of
    range,INF,,,,,4,4
Cui et al. (2011),1,agricultural,0.3,,0,0.5,Annual mean,
    INF,171.7,,17.5,473.1,4,4
Cui et al. (2011),1,agricultural,0.4,,,,Literature
    research (n = 3),INF,,,,,4,4
Fan et al. (2009),1,deciduous,0.3,,9.4,206.5,Annual mean
    ,INF,90.9,,,,4,4
Hayashi et al. (2012),0,agricultural,0.6,,,,"Winter,
    fallow, daytime",AGM,4.7,2,,,,
Hayashi et al. (2012),0,agricultural,0.2,,,,"Winter,
    fallow, nighttime",AGM,3.1,1.3,,,,
```

```
Hayashi et al. (2012),0,agricultural,0.2,,,,"Summer,
    crop period, daytime",AGM,2.2,1.5,,,,
Hayashi et al. (2012),0,agricultural,0.2,,,,"Summer,
    crop period, nighttime",AGM,1.8,0.8,,,,
Hayashi et al. (2012),1,agricultural,0.3,,,,Mean,AGM
    ,,,,,2,1
Poor et al. (2006),1,urban,1.1,,,,Annual mean,CTM
    ,1.7,,,,4,4
Smith et al. (2007),1,water,0.6,,0.1,1.1,Summer,INF
    ,0.3,,0,1.2,1,2
Myles et al. (2011),1,agricultural,7.1,9.8,,,Fall,AGM
    ,0.9,0.6,,,1,1
Myles et al. (2011),1,seminatural,1.8,,,,Literature
    research (n = 4),LIT,,,,,4,4
Myles et al. (2011),1,agricultural,2.2,,,,Literature
    research (n = 4),LIT,,,,,4,4
Trebs et al. (2006),1,seminatural,1,,0.1,2,Fall,INF
    ,0.8,,0.4,2,1,2
Zhang et al. (2009),1,mixed,0.4,0.1,,,Mean of three
    sites,INF,,,,,4,2
Zhang et al. (2009),1,coniferous,0.5,0.1,,,Mean of two
    sites,INF,,,,,3,2
Zhang et al. (2009),1,deciduous,0.3,0.1,,,Mean of two
    sites,INF,,,,,2,2
Zhang et al. (2009),1,agricultural,0.3,0.1,,,Annual mean
    ,INF,,,,,1,1
Jones et al. (2007),0,seminatural,,,0.4,0.6,Range during
     spring,CHA,,,0,100,,
Jones et al. (2007),1,seminatural,0.5,,,,Center of range
    ,CHA,,,,,1,1
Milford et al. (2009),1,seminatural,0.2,,,,summer,AGM
    ,3.2,2.1,0.3,15,1,1
Loubet et al. (2011),0,agricultural,,,0.1,0.6,Annual
    range,INF,,,,,,
Loubet et al. (2011),1,agricultural,0.4,,,,Center of
    range,INF,,,2,12,4,4
Mohr et al. (2005),1,coniferous,1.6,,,,Annual mean,INF
    ,4.5,,,,4,4
Builtjes et al. (2011),0,agricultural,1.2,,,,Annual mean
     at zR = 25 m,CTM,,,,,,
Builtjes et al. (2011),0,coniferous,1.6,,,,Annual mean
    at zR = 25 m,CTM,,,,,,
Builtjes et al. (2011),0,deciduous,1.4,,,,Annual mean at
     zR = 25 m,CTM,,,,,,
```

```
Builtjes et al. (2011),0,water,0.7,,,,Annual mean at zR
    = 25 m,CTM,,,,,,
Builtjes et al. (2011),0,urban,0.7,,,,Annual mean at zR
    = 25 m,CTM,,,,,,
Builtjes et al. (2011),0,agricultural,1.7,,,,Annual mean
     at zR = 2.5 m,CTM,,,,,,
Builtjes et al. (2011),0,coniferous,2.1,,,,Annual mean
    at zR = 2.5 m,CTM,,,,,,
Builtjes et al. (2011),0,deciduous,1.9,,,,Annual mean at
     zR = 2.5 m,CTM,,,,,,
Builtjes et al. (2011),0,water,1,,,,Annual mean at zR =
    2.5 m,CTM,,,,,,
Builtjes et al. (2011),0,urban,0.8,,,,Annual mean at zR
    = 2.5 m,CTM,,,,,,
Builtjes et al. (2011),0,agricultural,1.9,,,,Annual mean
     at zR = 1 m,CTM,,,,,,
Builtjes et al. (2011),0,coniferous,2.3,,,,Annual mean
    at zR = 1 m,CTM,,,,,,
Builtjes et al. (2011),0,deciduous,2.1,,,,Annual mean at
     zR = 1 m,CTM,,,,,,
Builtjes et al. (2011),0,water,1.1,,,,Annual mean at zR
    = 1 m,CTM,,,,,,
Builtjes et al. (2011),0,urban,0.9,,,,Annual mean at zR
    = 1 m,CTM,,,,,,
Builtjes et al. (2011),1,agricultural,1.6,,,,Mean over
    all zR,CTM,,,,,4,4
Builtjes et al. (2011),1,coniferous,2,,,,Mean over all
    zR,CTM,,,,,4,4
Builtjes et al. (2011),1,deciduous,1.8,,,,Mean over all
    zR,CTM,,,,,4,4
Builtjes et al. (2011),1,water,0.9,,,,Mean over all zR,
    CTM,,,,,4,4
Builtjes et al. (2011),1,urban,0.8,,,,Mean over all zR,
    CTM,,,,,4,4
```

A.3 IPYTHON CODE

Listing A.2: IPython Notebook for data analysis (converted to plain Python 2.7 for portability). Refer to the Supplementary Material of the published paper for the original .ipynb file.

```
#!/usr/bin/env python
# coding: utf-8

# # Schrader & Bruemmer (2014): Land use specific ammonia
    deposition velocities: A review of recent studies
    (2004-2013)
# ## Import and extract relevant data
# First import the data analysis library "pandas".
# In[1]:
import pandas as pd

# Import the csv data base to a data frame.
# In[2]:
df = pd.read_csv("vd_data.csv", header=0, index_col=None)

# Count the number of unique references.
# In[3]:
df["reference"].nunique()

# Only use $v_\mathrm{d}$ values that are listed in the "
    Mean" column of Tab. 2 and visually check if everything
    was imported correctly by printing a few rows.
# In[4]:
df_avg = df[df["use_for_averaging"] == 1]
df_avg.head(3)

# Drop unused columns.
# In[5]:
df_reduced = df_avg.ix[:, ["reference","land_use", "vd","
    w_seasons","w_coverage"]]
df_reduced.head(3)

# ## Calculate weighted averages and medians by land use
# Group $v_\mathrm{d}$ by land use categories.
# In[6]:
df_grouped = df_reduced.groupby("land_use")
df_grouped.head(1)
```

```
# Define the function for the weighted average according to
    Eq. (2) in the article:
#
# \begin{equation}
#       \overline{v_\mathrm{d}} = \frac{ \sum_{i=1}^{n} \
    left(w_{\mathrm{c},i} \cdot v_{\mathrm{d},i} + w_{\mathrm
    {s},i} \cdot v_{\mathrm{d},i} \right) }{ \sum_{i=1}^{n} \
    left(w_{\mathrm{c},i}+w_{\mathrm{s},i}\right) }
# \end{equation}
# In[7]:
def weighted_average(data):
    vd = data["vd"]
    w = data["w_seasons"] + data["w_coverage"]
    vd, w = vd.astype(float), w.astype(float)
    return (vd * w).sum() / w.sum()

# Calculate the median for each land use category.
# In[8]:
medians = df_grouped["vd"].apply(median)
medians.round(1)

# Calculate the weighted average for each land use category.
# In[9]:
wavgs = df_grouped.apply(weighted_average)
wavgs.round(1)

# If any questions arise, please do not hesitate to contact
    the author at frederik.schrader@thuenen.de.
```

B

SUPPLEMENT TO CHAPTER 3

B.1 LIST OF SYMBOLS

Table B.1: List of frequently used symbols. Note that in some cases appropriate unit conversions are used in the text.

SYMBOL	UNIT	DESCRIPTION
a	–	exponential decay parameter in the MNS non-stomatal resistance parameterization
AR	–	molar ratio of total acid to ammonia concentrations $((2[SO_2] + [HNO_3] + [HCl])/[NH_3])$
d	m	zero-plane displacement height
D_{NH_3}	$m^2\,s^{-1}$	molecular diffusivity of ammonia in air
F_t	$\mu g^{-2}\,m^{-2}\,s^{-1}$	total (stomatal + non-stomatal) net flux density
G_w	$m\,s^{-1}$	non-stomatal conductance ($= R_w^{-1}$)
H	$W\,m^{-2}$	sensible heat flux
h_c	m	canopy height
k	–	von Kármán constant (= 0.41)
L	m	Obukhov length
LAI	$m^2\,m^{-2}$	one-sided leaf area index
LE	$W\,m^{-2}$	latent heat flux
$R_a\{z-d\}$	$s\,m^{-1}$	aerodynamic resistance at the reference height
R_b	$s\,m^{-1}$	quasi-laminar boundary layer resistance
R_c	$s\,m^{-1}$	canopy resistance
R_s	$s\,m^{-1}$	stomatal resistance
R_w	$s\,m^{-1}$	non-stomatal resistance
$R_{w,eff.}$	$s\,m^{-1}$	effective non-stomatal resistance
$R_{w,min}$	$s\,m^{-1}$	minimum non-stomatal resistance in the MNS parameterization
$R_{w,MNS}$	$s\,m^{-1}$	modeled non-stomatal resistance after Massad et al. (2010a)
$R_{w,obs.}$	$s\,m^{-1}$	observed non-stomatal resistance
$R_{w.WK}$	$s\,m^{-1}$	modeled non-stomatal resistance after Wichink Kruit et al. (2010)

(Continued on next page)

SYMBOL	UNIT	DESCRIPTION
RH	%	relative humidity
SN	–	molar ratio of sulfur dioxide to ammonia concentrations ($[SO_2]/[NH_3]$)
T	°C	(air) temperature
u_*	$m\,s^{-1}$	friction velocity
$u\{z-d\}$	$m\,s^{-1}$	wind velocity at the reference height
$v_{d,max}\{z-d\}$	$m\,s^{-1}$	maximum deposition velocity allowed by turbulence
$v_d\{z-d\}$	$m\,s^{-1}$	deposition velocity at the reference height
z	m	measurement height above ground
z_0	m	roughness length
$z_0{}'$	m	notional height of trace gas exchange
$z-d$	m	reference height
β	$°C^{-1}$	temperature response parameter in the MNS non-stomatal resistance parameterization
Γ_g	–	ground-layer emission potential
Γ_s	–	stomatal emission potential
Γ_w	–	non-stomatal emission potential
ν_{air}	$m^2\,s^{-1}$	kinematic viscosity of air
$\chi_{a,(n\,d)MA}$	$\mu g\,m^{-3}$	backward-looking moving average of ambient concentration (with n-day moving window)
$\chi_a\{z-d\}$	$\mu g\,m^{-3}$	ambient concentration at the reference height
χ_c	$\mu g\,m^{-3}$	canopy compensation point
χ_s	$\mu g\,m^{-3}$	stomatal compensation point
χ_w	$\mu g\,m^{-3}$	non-stomatal compensation point
Ψ_H	–	integrated stability correction function for entrained scalars
Ψ_M	–	integrated stability correction function for momentum

C

SUPPLEMENT TO CHAPTER 5

C.1 ADDITIONAL CASE STUDIES

C.1.1 *Synthetic data*

Further evaluations of the correction scheme were carried out for synthetic (LOTOS-EUROS modelled) data from four different grid cells in southern Germany with varying NH_3 concentration levels (Table C.1), and for five different land-use types (solid lines in Figure C.1). Additionally, we tested splitting the 1-year records into half, using the first half of the year (January to June) to derive parameters for the correction and predicting fluxes for the second half of the year (July to December) as a simple means of validating the method (dashed lines in Figure C.1). Both variants lead to a strong improvement in the average accuracy of the predicted fluxes at most sites, with the exception of the Forst Rotenfels site with arable land. Note that $n \neq 12$ for some sites where the leaf area index is assumed to be zero during certain times of the year (e.g. for arable land).

The land-use scenarios shown here are not necessarily representative for a significant fraction of land-use classes present in the grid cells. They are simply used to illustrate the effects of (not) correcting monthly average fluxes under different conditions.

C.1.2 *Measured data*

A similar analysis was carried out for NH_3 concentrations measured at a moorland site in southern Scotland (Flechard and Fowler, 1998a) during the years 1995, 1996 and 1998. Mean temperature at the site was 9.1 °C averaged across the sampling periods, and the mean NH_3 concentration was 0.8 µg m^{-3}, with a maximum of 32.9 µg m^{-3}; 95 % of all samples were below 2.9 µg m^{-3}. Concentration measurements and meteorological data were available at a frequency of 30 minutes. The evaluation of the proposed

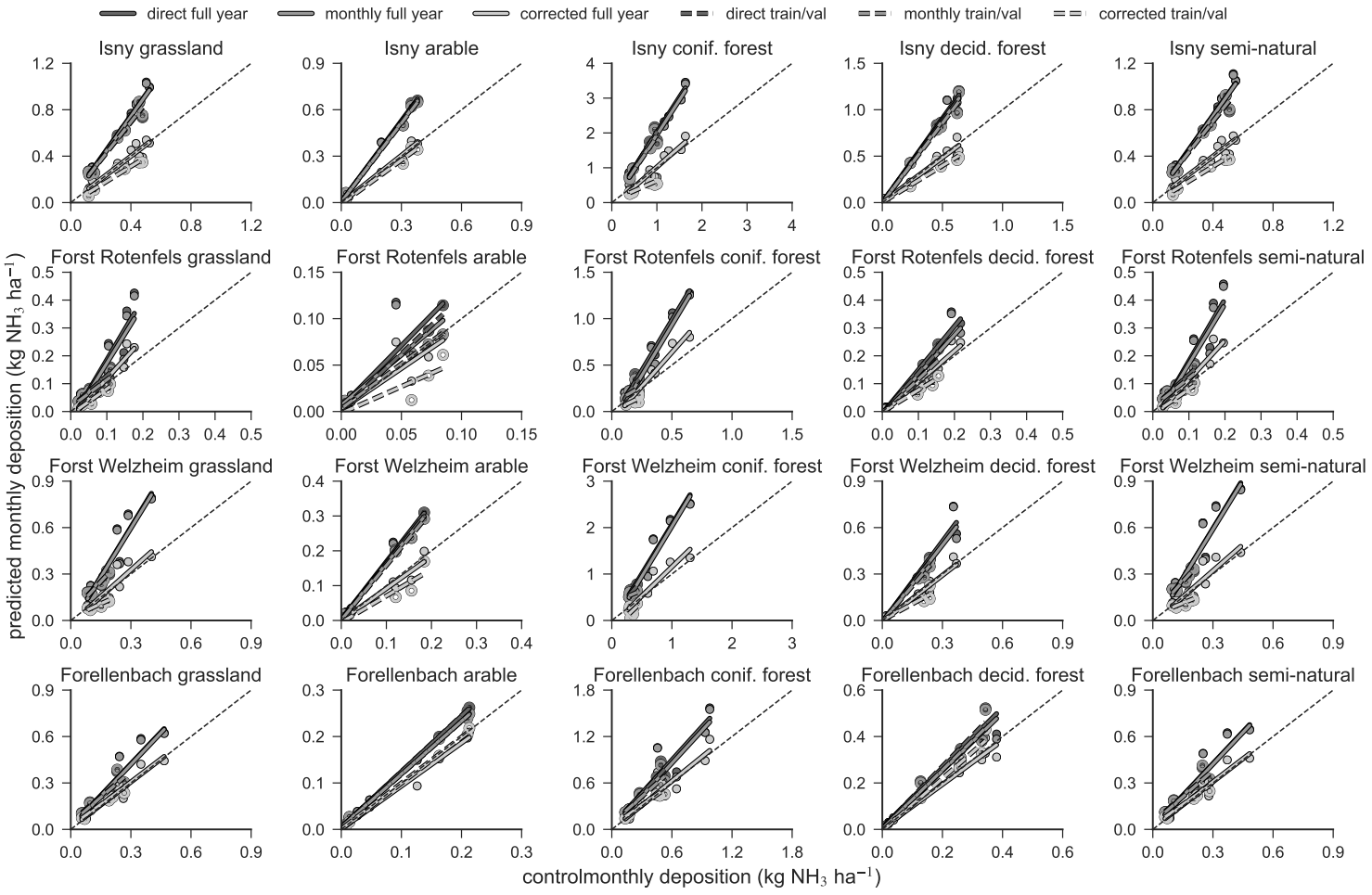

Figure C.1: Similar to Figure 5.3b,d, for four different sites and five different land-use types. Solid circles and regression lines use the whole modelled year 2016 for derivation of correction factors; hollow circles and dashed lines use the first half of the year for parameter estimation and the second half of the year for validation (data points and regression line only shown for second half). Confidence intervals for the regression are not shown to ensure visual clarity.

Table C.1: Site characteristics of the additionally tested four synthetic datasets in southern Germany. *Isny* corresponds to the synthetic dataset discussed in the main manuscript. Concentration and temperature values are annual averages ± standard deviations with min. and max. values in parentheses. ΣP is total annual precipitation.

SITE	LATITUDE	LONGITUDE	χ_a ($\mu g\,m^{-3}$)	T (°C)	ΣP (mm)
Isny	47°41′34.80″ N	10°2′6.00″ E	5.6 ± 5.1 (0.1–60.6)	8.1 ± 7.5 (−18.3–28.1)	1690
Forst Rotenfels	48°48′50.76″ N	8°23′47.40″ E	1.1 ± 1.3 (0.0–11.1)	10.1 ± 7.5 (−12.3–31.6)	986
Forst Welzheim	48°52′50.88″ N	9°34′47.64″ E	2.9 ± 2.8 (0.0–24.0)	9.7 ± 7.8 (−16.3–31.8)	990
Forellenbach	48°56′51.40″ N	13°25′14.05″ E	2.0 ± 2.3 (0.0–25.9)	6.0 ± 7.9 (−17.6–26.3)	1085

correction scheme was carried out using both the whole measurement period and only the year 1995 as the training dataset for the estimation of σ_{χ_a} and r_{v_{ex},χ_a}.

Results are shown in Figure C.2. Relative errors of up to 63 % in individual months could clearly be reduced using the proposed correction method with a maximum error of 38 % in one month of the *corrected* variant and below 20 % otherwise. In fact, total errors were reduced from 296.0 g ha^{-1} and 203.3 g ha^{-1} in the *direct* and *monthly* variants, respectively, to a mere 2.6 g ha^{-1} after correction (44.9 g ha^{-1} when only using data from 1995 for fitting the correction functions), at a total predicted *control* deposition of 1625.0 g ha^{-1}. Note that this prediction is very low compared to measured fluxes at this site (2.5 kg N ha^{-1} a^{-1} ≈ 3.0 kg ha^{-1} a^{-1}) (Flechard and Fowler, 1998b), likely due to a too high default minimum external leaf surface resistance in the model parameterisation we used (Massad et al., 2010a; Schrader et al., 2016). Nevertheless, we have no reason to assume that the performance of the correction scheme would be significantly different after calibrating the biosphere-atmosphere exchange scheme to site-specific conditions.

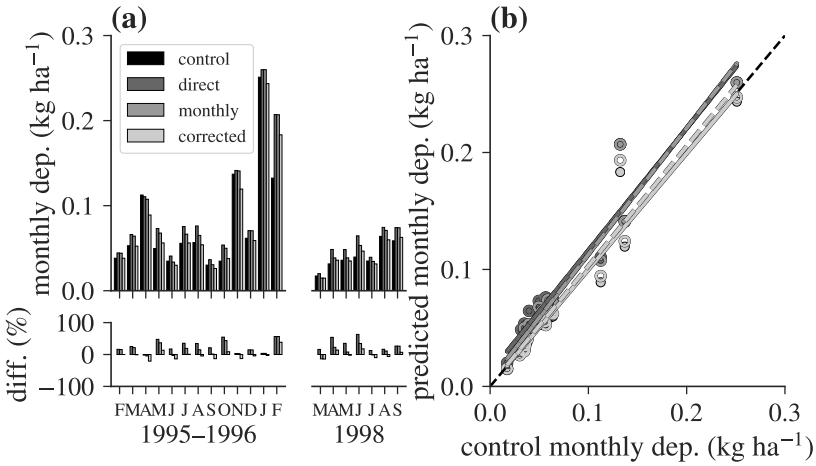

Figure C.2: Similar to Figure 5.3 for a Scottish moorland site. (a) Predicted cumulative monthly NH_3 deposition for the four scenarios *control*, *direct*, *monthly*, and *corrected*. Differences are given as percent deviation from *control*. (b) Predicted cumulative monthly NH_3 deposition of *direct*, *monthly*, and *corrected* variants against *control*. Solid circles and regression lines use the whole measurement period 1995–1998 for derivation of correction factors; hollow circles and dashed line use only the year 1995 for parameter estimation. Confidence intervals for the regression are not shown to ensure visual clarity.

C.2 SENSITIVITY TO THE SAMPLING RATE

Although many monitoring networks use a monthly sampling scheme (e.g., MAN in the Netherlands; Lolkema et al., 2015), it is nevertheless instructive to analyse the effect of modelling NH_3 fluxes using average concentration measurements in conjunction with high-frequency meteorological drivers at other temporal resolutions. For example, Hurkuck et al. (2014) and Dämmgen (2007) used weekly measurements obtained with KAPS denuders (Peake and Legge, 1987) to model atmospheric nitrogen deposition. We have therefore performed the same analysis as shown in Figure C.2 for averaging times between 1 hour and four weeks for the same dataset. We then evaluated the total relative difference from the *control* variant in two different ways: (i) as in the main manuscript, by upscaling average fluxes to total data coverage,

i.e., multiplying the daily average flux density with the averaging interval, and (ii) without upscaling, i.e., multiplying the daily average flux density with the (fractional) number of days with valid measurements within the averaging interval. The practical difference and reason for performing the analysis in both ways lies in the fact that with upscaling, the *control* total predicted flux is not equal between different averaging times as soon as there are gaps in the time series that are larger than the averaging interval, whereas without upscaling it is always equal.

As expected, the errors arising from both uncorrected variants (*direct* and *monthly*) are lowest at the smallest hypothetical sampling intervals (Figure C.3). At the same time, as fewer samples are used to determine $r_{v_{\mathrm{ex}},\chi_{\mathrm{a}}}$, noise increases and the effect of using the proposed correction scheme can actually be worse than not using a correction at all when the averaging period is small. However, this is quickly reversed as soon as concentrations are sampled at a temporal resolution of around half a week or less frequent. As averaging intervals become longer, *corrected* flux predictions fluctuate around *control* (i.e., zero relative error), with occasional outliers, whereas the errors in the uncorrected variants still increase. An interesting lesson to learn from this exercise is that the errors appear to slowly approach a plateau for this dataset. We expect this to be the case for other sites as well, as with increasing averaging time $\overline{\chi_{\mathrm{a}}}$ within each sampling interval converges to the *long-term average* NH_3 concentration at the site, therefore mitigating the effects of spreading out sampling times even longer. In other words, reducing the sampling frequency from, e.g,. monthly to quarterly will have less negative consequences than weekly to monthly.

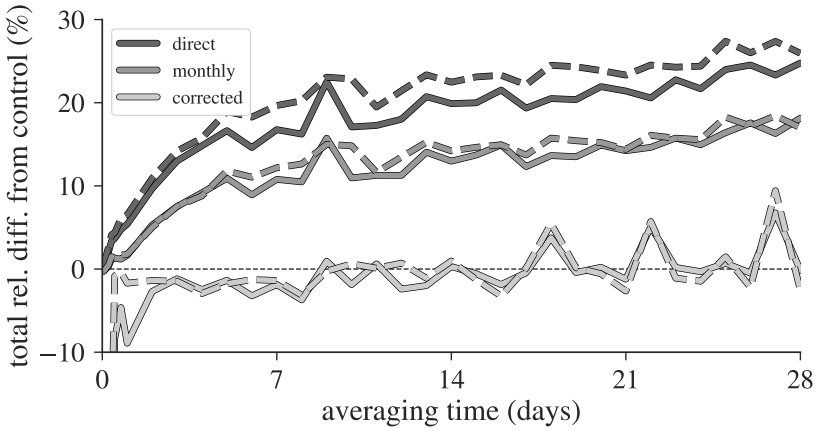

Figure C.3: Sensitivity of errors to an increasing sampling interval, exemplarily calculated for the Scottish moorland site previously shown in Figure C.2. Solid lines are with, dashed lines without upscaling to 100 % data coverage within the interval (refer to the text for detailed explanation). The errors are relative to the *control* total predicted flux over the whole measurement period 1995–1998.